Stony Brook University

The Roles of Nitric Oxide and Tuftsin during Experimental Autoimmune Encephalomyelitis (EAE)

A Dissertation Presented

by

Muzhou Wu

to

The Graduate School

in Partial Fulfillment of the

Requirements

for the Degree of

Doctor of Philosophy

in

Neuroscience

Stony Brook University

May 2009

Stony Brook University

The Graduate School

Muzhou Wu

We, the dissertation committee for the above candidate for the

Doctor of Philosophy degree,

hereby recommend acceptance of this dissertation.

Styliani-Anna Tsirka, PhD. - Dissertation Advisor
Professor, Department of Pharmacological Sciences

Holly Colognato, PhD. - Chairperson of Defense
Assistant Professor, Department of Pharmacological Sciences

William Van Nostrand, PhD.
Professor, Department of Medicine

Nicholas Carpino, PhD.
Assistant Professor, Department of Molecular Genetics and Microbiology

This dissertation is accepted by the Graduate School

Lawrence Martin
Dean of the Graduate School

Abstract of the Dissertation

The Roles of Nitric Oxide and Tuftsin during Experimental Autoimmune Encephalomyelitis (EAE)

by

Muzhou Wu

Doctor of Philosophy

in

Neuroscience

Stony Brook University

2009

Multiple sclerosis (MS) is a demyelinating autoimmune disease, which is characterized by infiltration and activation of T cells, and the accumulation of activated microglia and macrophages in the central nervous system. I have employed a mouse model of experimental autoimmune encephalomyelitis (EAE), to address questions related to the involvement of several factors in MS.

One of the major factors participating in the inflammation cascade of MS/EAE is nitric oxide (NO), which is produced by nitric oxide synthase (NOS). The role of NO during MS has been debated extensively. Using biochemical, cell culture, and in vivo techniques on genetically-modified mice, I identified contributions of individual NOS isoform-derived NO in the development of EAE. Specifically, I found that endothelial-NOS participates in mediating initial blood-brain barrier breakdown; neuronal-NOS

contributes to excitotoxicity; and inducible-NOS is responsible for the high output of NO during EAE lesions. Furthermore, NO has been found undertaking neurodegenerative or neuroprotective functions during different phases of EAE. These results suggested that modulation of NO production from their varied cellular sources and the timing of interference may have therapeutic potential in the management of MS.

The second part of my research was to study the role of tuftsin (TKRP), a microglial activator in the modulation of T cell phenotypes and thus the progression of EAE. Previously we found that tuftsin infusion through mini-osmotic pumps abrogated disease severity in EAE mice. My further studies revealed that both in vivo and in vitro, modulating microglial activity using tuftsin switched T cell phenotype from a Th1 dominant pro-inflammatory response to a Th2 dominant anti-inflammatory response, and also favored an expansion of regulatory T cells; moreover, adoptive transfer of tuftsin modulated T cells reversed clinical symptoms in established EAE mice, indicating that the interaction between microglia and T cells could be targeted therapeutically in MS.

Dedicated to my parents and everybody who has supported me in my life

Table of Contents

Table of Contents ……...vi

List of Figures ……..…x

List of Tables ……....…...xii

List of Charts……....xiii

List of Abbreviations ……..….xiv

Acknowledgements ……...xviii

Chapter I

General Introduction

Multiple sclerosis and experimental autoimmune encephalomyelitis ……...2

Microglia …….....……6

T cells…….……..…….……..9

Nitric oxide …….…….…….....11

Blood Brain Barrier …….....……...……15

Chapter II

General Methods and Materials

Animals …….……....20

MOG peptide ……..20

Induction of EAE with MOG35-55 peptide…….20

Evaluation of EAE symptoms…….....21

Time-controlled Drug Delivery……..…….....21

Eriochrome Cyanine stain……....22

FluoroMyelin stain…….22

Immunofluorescence……...23

TUNEL assays……..24

Western blotting…….25

BBB Breakdown assays…….....25

Measurement of nitrite levels……....27

BrdU-based proliferation assay…….…27

ELISA……..……...…….……28

Primary T cells culture from mouse spleen…….……....28

Mixed cortical cultures and Primary microglia culture …….…29

Primary Neuronal Cultures……..…….……....30

PCR arrays.……...……....30

Statistics ……..……...…….....31

Chapter III

Contributions of individual NOS isoform-derived NO in the development of experimental autoimmune encephalomyelitis (EAE), a mouse model of multiple sclerosis (MS)

Introduction ……...33

Results ……...36

Discussion ……50

Figures ……...57

Chapter IV

Identify the roles of nitric oxide on microglia and T cells properties in vitro

Introduction ……...92

Results ……...94

Discussion ……97

Figures ……...99

Chapter V

Tuftsin (TKPR) abrogates disease in experimental autoimmune encephalomyelitis (EAE): a switch to anti-inflammatory responses

Introduction ……...110

Results ……112

Discussion ……...…120

Figures …….124

Chapter VI

General Conclusions and Discussion

NO and MS/EAE…….....……147

The blood brain barrier ……..147

Excitotoxicity and MS/EAE…....……...……150

Protective autoimmunity and MS/EAE…….……..151

Neuropilin-1 and tuftsin……...…153

References ……...156

List of Figures

Chapter III

Figure III-1. eNOS$^{-/-}$ mice exhibit delayed EAE onset followed by exaggerated disease severity and limited recovery ……..57-58

Figure III-2. Delayed but ultimately more extensive BBB breakdown in eNOS-/- mice …..……...59-60

Figure III-3. Increased demyelination in eNOS$^{-/-}$ mice during EAE ……61-62

Figure III-4. Increased microglia/macrophage infiltration and activation in eNOS-/- mice ……..……63-64

Figure III-5. Recruitment of microglia/macrophages into regions of demyelination ……..65-68

Figure III-6. Therapeutic administration of an NO donor is beneficial in the recovery phase for eNOS$^{-/-}$ mice ……...….69-72

Figure III-7. iNOS$^{-/-}$ mice exhibit exaggerated disease severity and limited recovery ……..…73-74

Figure III-8. iNOS-/- mice showed altered pathological hallmarks during EAE …… ……....75-78

Figure III-9. Providing nitric oxide using an NO donor is beneficial for recovery in iNOS$^{-/-}$ mice …….……79-80

Figure III-10. nNOS$^{-/-}$ mice exhibit delayed EAE onset followed by exaggerated disease severity and limited recovery ……..…….81-82

Figure III-11. Blocking NO production using NMMA in wild-type mice exacerbated the progression of EAE ……..83-84

Figure III-12. Altered pathological hallmarks in the wild-type mice infused with NMMA during EAE ……..…...85-88

Chapter IV

Figure IV-1. The effect of NO on T cells proliferation……...…99-100

Figure IV-2. The effect of NO on T cells cytokines production ....…….....101-102

Figure IV-3. The effect of NO on apoprosis of T cells.....103-104

Figure IV-4. NO has no significant effect on microglia proliferation ……...105-106

Figure IV-5. The effect of NO on microglia cytokines production ….....107-108

Chapter V

Figure V-1. The direct effect of tuftsin on T cells cytokines production…….124-125

Figure V-2. Modulating microglia activity with tuftsin under excitotoxic conditions affected T cell cytokines production ……...126-127

Figure V-3. Tuftsin infusion induces type II T cells and Tregs …….….128-129

Figure V-4. Adoptive transfer of tuftsin modulated T cells prevents and reverses established EAE ……...130-131

Figure V-5. Attenuated demyelination pattern in EAE mice adoptively transferred with tuftsin-modulated T cells.…… ……...….132-135

Figure V-6. Reduced microglia/macrophage infiltration and activation in mice with adoptive tranfer ……136-137

Figure V-7. Increased Nrp-1 expression in tuftsin infused animals ……....138-139

List of Tables

Chapter III

Table III-1. Summery of clinical course and pathological markers in NOS deficient mice, NOS deficient mice infused with NOC-18, and wild-type mice infused with NMMA……..…89-90

Chapter V

Table V-1. PCR arrays on T cells reveal several responsible genes...……140-141

List of Charts

Chapter V

Chart V-1. An *in vitro* model to mimic the tuftsin infused EAE model *in vivo* ……...142-143

Chart V-2. Diagram of PCR array samples preparation…...…….....144-145

List of Abbreviations

AC	astrocyte
AG	aminoguanidine
APCs	antigen presenting cells
BBB	blood-brain-barrier
BCG	Bacille Calmette-Guérin
BH4	tetrahydrobipterin
BL	basal lamina
CFA	Freund's adjuvant
CNS	central nervous system
CSF	cerebral spinal fluid
DLAR	Stony Brook University animal facility
eNOS	endothelial NOS
eNOS-/-	eNOS-deficient
EAE	experimental autoimmune encephalomyelitis
EC	endothelial cell
ECAMs	endothelial cell adhesion molecules
EM	electron microscopy
GA	glatiramer acetate
HLA	human leukocyte antigen
HNO2	nitrous acid
iNOS	inducible NOS

iNOS-/-	iNOS-deficient
IACUC	Institute for Animal Care and Use Committee
ICAM-1	intercellular adhesion molecule-1
IFN-γ	interferon-γ
Ifnar1-/-	interferon alpha receptor 1 deficient
IL-1β	interleukin-1β
IL2RA	interlukin-2 receptor allele
IL-4	interlukin-4
IL-6	interlukin-6
IL7RA	interlukin-7 receptor allele
IL-10	interlukin-10
IL-13	interlukin-13
IL-17	interlukin-17
LPS	bacterial lipopolysaccharide
mtNOS	mitochondria NOS
MAGUK	membrane-associated guanylate kinase
MAPK	mitogen-activated protein kinases
MBP	myelin basic protein
MHC II	major histocompatibility complex type II proteins
MMP 12	Matrix metalloproteinase 12
MOG	myelin oligodendrocyte glycoprotein
MRI	magnetic resonance imaging

MS	multiple sclerosis
nNOS	neuronal NOS
nNOS-/-	nNOS-deficient
NMDA	N-methyl-D-aspartic acid
NMMA	N^g-Methyl-L-Arginine
NO	nitric oxide
NO-	nitroxyl
NO2	nitrogen dioxide
NOC-18	2,2'-(Hydroxynitroshydrazino)is-ethanamine
NOS	nitric oxide synthase
NPCs	neural precursor cells
ONOO-	peroxynitrite
ONOOH	peroxynitrous acid
OPCs	oligodendrocyte precursor cells
PC	pericytes
PCR	polymerase chain reaction
PECAM-1	platelet/endothelial cell adhesion molecule 1
PLP	proteolipid protein
PP-MS	primary progressive multiple sclerosis
PR-MS	progressive relapsing multiple sclerosis
PSD-95	post-synaptic density 95
RR-MS	relapsing-remitting multiple sclerosis

T1D	type 1 diabetes
Treg	regulatory T cell
TJ	tight junctions
TNF-α	tumor necrosis factor-alpha
tPA	tissue plasminogen activation
tPA-/-	tPA-deficient
VCAM-1	vascular cell adhesion molecule 1
VLA-4	very late Ag 4
wt/WT	wild-type

Acknowledgments

There have been many people in my life who have supported me in this path leading to science. My time here in the graduate program of neuroscience, and in Dr. Tsirka's lab is an incredible wealth for me. I will surely look back on this part of my life with best memories.

First I would like to thank my advisor Dr. Styliani-Anna Tsirka most sincerely, for all her advice and guidance. She gave me the freedom to explore the questions I want to answer, and she is always here for scientific discussion and good suggestions. Without her continuous encouragement and patience, I will not gain so much and become confident as a scientist. She is the best mentor one could ask for, and she is also a good friend who can share joys and tears. What I have learned from her will continue to benefit both my career and my life in the future.

I would also like to thank my committee members, Dr. Holly Colognato, Dr. William Van Nostrand, and Dr. Nicholas Carpino. I want to thank them for their guidance and support, with their valuable suggestions and encouragement during all my committee meetings, and their constructive criticism of my thesis proposal and dissertation.

A debt of gratitude is owed to Dr. Michael Frohman, for his great comments on my manuscripts. Mostly, I want to thank him for introducing me to Dr. Tsirka's lab, giving me the opportunity to gain this fantastic experience.

A big thanks goes to the current and former members of Tsirka lab, including Iordanis Gravanis and Madhuri Bhasin who were a tremendous help when I first joined this lab; Jack Sheehan, Susana Parathath-Fernandez, Westley Nolin and Martine Mirrione, who has provided exceptional advice and supporting for my research, and particularly for their friendship. I also have a big thanks to Haiyan Zhai, Jaime Emmetsberger, Noreen Bukhari, Yao Yao, Dorothy Konomos, George Georghiou, Kyungmin Ji, Zhen Gao, and Ari Abraham, with whom I shared wonderful memories through the years both in and outside the Tsirka-lab, including the parties, dinner at the greek restaurant, and also the unforgettable trip to neuroscience meeting. Particularly, I would like to thank Chun Zhou, who helped me a lot both in and outside the lab.

I would like to express my sincere appreciation to all the administrators of neuroscience program, especially coordinator Diane Godden, who has been a wonderful source of caring and support over the years, and I thank her especially for always lending a helping hand dealing with student issues. I also would like to thank pharmacology graduate program coordinator Beverly Campbell, who has adopted me over the years and helped me a lot with my questions.

Finally, I would like to thank my family. My mom and dad are the greatest parents, they always believe in me, and they always standing behind me with tremendous support no matter what. Their love has been encouraging me to accomplish more throughout my life. I also want to thank my boyfriend Hua Xu, who loves me unconditionally and stay with me during my ups and downs.

Chapter I

General Introduction

Multiple sclerosis (MS) and experimental autoimmune encephalomyelitis (EAE)

Multiple sclerosis (MS) is a chronic disabling autoimmune disease, in which the immune cells of the body, such as T cells, microglia and macrophages, mistakenly attack the myelin sheath that protects nerve fibers in both brain and spinal cord. The symptoms of MS range from blurry vision, loss of balance, muscle weakness, slurred speech, to mobility impairment (Steinman, 1996). MS afflicts an estimated 400,000 Americans and 2.5 million people in the world (National Multiple Sclerosis Society). MS usually occurs at young adulthood, be tween the ages of 20 and 50; and it strikes women twice as often as men.

The course of MS varies, as it presents in three forms. The most common one is "relapsing-remitting course" (RR-MS) which encompasses 80-90% of the cases. Patients having this form have attacks separated by periods of recovery. In 10-15% of patients, MS occurs with a "primary progressive course" (PP-MS), in which the patients have steadily progressive neurological deficits without acute relapse. The most rare form is called "progressive relapsing course" (PR-MS), which consists 5% of the cases. Patients with this form of MS develop progressive disease without periods of remission or recovery (Hemmer et al., 2006).

The prevalence of MS varies depending on the genetic background. MS is highly common in Caucasians, but rarely affect Asians or Africans (Compston, 1997). Moreover, the risk of developing the disease is significantly higher in family members of patients with MS (Ebers et al., 1995). These findings promoted a large number of studies to

identify disease loci and alleles. Human leukocyte antigen (HLA) class II alleles DR15/DQw6, which code for molecules that participate in antigen recognition by T lymphocytes, have been identified associated with MS (Olerup and Hillert, 1991). Most recently, two groups reported that alleles of IL2RA and IL7RA and those in the HLA locus are heritable risk factors for multiple sclerosis (Hafler et al., 2007). In addition, environmental and viral components play important roles in the MS. MS is often associated with common viral infections (Sibley et al., 1985), and migration from high-risk to low-risk areas reduces the risk of developing MS (Gale and Martyn, 1995). Although the etiology of MS is unknown, combinations of genetic, environmental and viral influences are thought to cause the disease (Steinman, 1996).

The immunological attacks in MS damage the brain and spinal cord in several ways. The most prominent and important are demyelination and lack of remyelination. Myelin is a fatty sheath that wraps around the axons in the nervous system; it acts as an insulator and is important for signal transduction and transmission along the nerve fibers. Myelin is produced by oligodendrocytes in the CNS. During MS, the process of destruction of the endogenous myelin sheaths by cells of the immune system is called demyelination. Oligodendrocytes express myelin component proteins that may be the target of autoimmune attack thus decreasing the number of cells or factors that can re-myelinate (Franklin, 2002). Remyelination may also fail because of the lack of oligodendrocyte precursor cells (OPCs), which differentiate into mature myelinating oligodendrocytes and contribute to remyelination. An insufficient recruitment of OPC or their failure to differentiate into remyelinating oligodendrocytes may also contribute to lack of

remyelination (Franklin, 2002; Raivich and Banati, 2004). Secondly, the inflammatory damage caused by activated T cells, brain resident microglia and infiltrating macrophages interferes with the propagation of electrical impulses along the nerve fibers, which can lead to their degeneration (Hemmer et al., 2006; Steinman, 2003;). Finally, gliosis is also a prominent feature of MS, characterized by increased astrocyte proliferation, enhanced glial fibrillary acidic protein expression and hypertrophy (Dinter et al., 1997). This gliosis leads to difficulty in conducting electrical signals down the nerve fibers (Dinter et al., 1997).

Most treatments for MS aim at inhibiting the immunological attacks. The initial induction of MS requires migration and activation of T cells in the CNS. The migration of encephalitogenic T cells to the CNS is dependent on the interaction of adhesion molecules, such as very late Ag 4 (VLA-4) on T cells, with vascular cell adhesion molecule 1 (VCAM-1) expressed by vascular endothelial cells. As a cosequence, one treatment for MS involves interfering with the adhesive molecules. Blocking $\alpha 4$ integrin, which is an adhesion molecule expressed by the attacking immune cells, has been found to reverse the disease in a model of MS called experimental autoimmune encephalomyelitis (EAE) (Yednock et al., 1992). Another strategy is to block the immune activity of the immunological cells, such as inhibiting production of pro-inflammatory cytokines, chemokines and oxygen reactive species (Steinman, 2001). A recently developed approach is to utilize neural precursor cells (NPCs) (Pluchino et al., 2003). It has been reported that the multipotent NPCs can move to the lesion areas once injected

into the blood. These NPCs can differentiate into myelinating cells (oligodendrocytes) and also generate new neurons (Pluchino et al., 2003).

EAE is an experimentally induced autoimmune disease and used as one animal model for studying MS disease. EAE can be actively induced by injection of a protein component of myelin, such as myelin oligodendrocyte glycoprotein (MOG), myelin basic protein (MBP), or proteolipid protein (PLP). These proteins are recognized as non-self and immune attack is stimulated. The similarity of the injected proteins to self myelin, aided by other injected antigens which assault the integrity of the blood-brain-barrier (BBB), results in an autoimmune response on myelin, thus mimicking the symptoms of MS. Another method to induce EAE is by adoptive transfer. Primed T cells isolated from spleen and lymph nodes of immunized animals can transfer EAE to naïve recipients. EAE can be induced in various animal models such as rats, mice, monkeys and guinea pigs. However, the disease course and severity are strain dependent (Hjelmstrom et al., 1998). EAE is a good model for MS in that it mimics the demyelination hallmarks seen in human patients. EAE is a simple animal model with an acute version of the disease with no remission or relapse, which is not the case in human patients. So it is important to acknowledge that EAE is a limited, simple model of a very complex human disease.

The animal model I have been using is MOG_{35-55} peptide induced EAE. Myelin oligodendrocyte glycoprotein (MOG) is a membrane protein found primarily on the extracellular surface of oligodendrocytes in the outermost lamellae of the myelin sheath. It is present in low amounts in myelin and constitutes only 0.05% of total myelin proteins, but it has high immunogenic potential. MOG has been used to induce EAE in C57BL6

mice and transgenic animals with C57BL6 background. MOG-induced EAE in these mice is characterized by an acute attack followed by progressive recovery. This model mimics the inflammation and demyelination events which occur in MS patients (Hjelmstrom et al., 1998).

Microglia

The cells of the central nervous system (CNS) parenchyma are collectively divided into neurons and glial cells. The common characteristic of neurons is their excitability, which is coupled with their ability to communicate with each other via electrical or chemical synapses and results in the formation of sophisticated networks. The glial cells are the supporting cells that are attributed with many essential functions, such as trophic support, secretion of neurotrophic factors, disposal of deleterious factors, insulation of neuronal connections, and regulation of neurotransmission (Baumann and Pham-Dinh, 2001; Jessen, 2004; Kreutzberg, 1996; Verkhratsky and Toescu, 2006).

In the CNS there are three types of glial cells: microglia (which function as immune cells), astrocytes (supporting and neuron-modulating cells) and oligodendrocytes (myelinating cells), all of which have been shown to play important roles in MS. My work during this Thesis has focused on the roles and modulatory functions of microglia, and therefore I will describe these cells further.

Microglia were first described in 1932 by del Rio-Hortega as a distinct class of glial cells, which play critical roles in innate and adaptive immune responses of the CNS. Microglia are derived from leptomeningeal mesenchymal cells, which enter the brain during development and transform into microglia (Bechmann et al., 2007). Microglia are the resident immune cells in CNS, which comprise 10-20% of the total glial cells and about 7% of all the CNS cells. In a normal brain, they exist in a resting (ramified) form, characterized of small cell bodies and long, thin processes. They are described to use these processes to sense their environment and respond to it (van Rossum and Hanisch 2004). Based on the expression of major histocompatibility complex type II proteins (MHC II) and cell surface markers, resting microglia represent immature antigen presenting cells (Adachi et al., 1997).

When microglia sense injury to the brain, they migrate to the lesion site and undergo a process called activation: as characterized by changes in proliferation, gene expression and morphology (Kreutzberg, 1996b). Microglia proliferate locally, and their morphology changes from the resting state to an activated state with enlarged cell bodies and extensive branches. In the fully activated state they acquire an ameboid shape. Microglia secrete cytokines, chemokines and reactive oxygen species, which aid in the inflammatory response. They also upregulate MHC and adhesion molecules on their surface, which promote the recruitment of other inflammatory cells, such as neutrophils, lymphocytes and monocytes, into the injury site (Hanisch, 2002).

Microglia have been implicated in the pathogenesis of many neurodegenerative diseases including MS (Carson, 2002), Alzheimer's disease (Eikelenboom et al., 2002),

and AIDS (Garden, 2002). However, microglia may play dual roles in these diseases: they have been reported to mediate the inflammatory response and to also undertake neuroprotective functions (please see below).

During MS/EAE it remains a matter of debate whether microglial activation is neurotoxic or neuroprotective. Most likely, microglia can be both protective and neurodegenerative; the timing and strength of their activity determine which of these effects is expressed. As antigen-presenting cells, microglia secrete chemokines and adhesion molecules, such as intercellular adhesion molecule-1 (ICAM-1) and CD40, which cause activation and recruitment of T cells (Cannella and Raine, 1995). Tumor necrosis factor-alpha (TNF-α) and nitric oxide (NO) produced by microglia cause damage to oligodendrocytes and myelin, thus contributing to demyelination (Chao et al., 1992). However, the effect of microglia is not only deleterious, as they can produce anti-inflammatory cytokines that are associated with inhibition or prevention of EAE, such as transforming growth factor beta (TGF-β) and interleukin-10 (IL-10). IL-10 has been reported to suppress EAE (Rott et al., 1994), while TGF-β has been shown to inhibit TNF-α production and EAE progression (Stevens et al., 1994). In addition, TGF-β is thought to reduce astrocytic scar formation, thus promoting tissue repair (Kreutzberg, 1996). Early activation of microglia has been shown to cross-talk with the immune response and potentially induce ‘protective autoimmunity’. In a model of optic nerve crush injury, earlier activation of microglia results in resistance to injury and increased neuronal survival (Shaked et al., 2004), and this is due to the fact that the early activation

of microglia can interact and modulate the adaptive immune response and thus promote the secretion of neurotrophic factors from T cells.

During MS/EAE, following the compromise of the blood-brain barrier (BBB), the blood-derived macrophages infiltrate the CNS and become activated in a similar manner as microglia (Hickey 1991). Because both microglia and blood-derived macrophages are derived from the same lineage and they express a lot of the same surface receptors, it is difficult to dissect out the individual contributions of these two cell types.

T cells

T cells belong to a group of white blood cells known as lymphocytes, and play a central role in cell-mediated immunity. T cells consist of different subsets: T helper cells, cytotoxic T cells, memory T cells, regulatory T cells and natural killer T cells. Depending on the cytokine milieu present at the time of the initial engagement of their T-cell receptor, naïve T cells can differentiate into different sub-categories. My study focuses on T helper cells and regulatory T cells. T helper cells are also known as effector T cells, which constitutively express the surface protein CD4; they play an important role in establishing and maximizing the capabilities of the immune system. There are three subsets of T helper cells, Th1, Th2 (Mosmann and Coffman, 1989) and the recently described Th17 cells (Langrish et al., 2005). In the presence of interferon-γ (IFN-γ), naïve T helper cells differentiate into Th1 cells and produce pro-inflammatory cytokines,

such as TNFα and IFN-γ, and participate in the clearance of intracellular pathogens; in presence of IL4, naïve T helper cells differentiate into Th2 cells, and produce anti-inflammatory cytokines, such as interleukin-10 (IL-10), interleukin-4 (IL-4), interleukin-13 (IL-13), and orchestrate the clearance of extracellular pathogens. Both TGF and IL6 can induce naïve T helper cells to differentiate into Th17 cells, which produce interleukin-17 (IL17), and have recently been found to play a pathogenic role in inducing autoimmune tissue inflammation (Lock et al., 2002; Lohr et al., 2006; Wilson et al., 2007). However, in the presence of TGF-β alone, naive T cells convert into Foxp3-expressing induced Treg cells, which express high levels of CD25 and play a role suppressing activation of the immune system (Kohm et al., 2002; McGeachy et al., 2005; Liu et al., 2006; Lohr et al., 2006; Olivares-Villagomez et al., 1998). It should be noticed that Th17 cells, once thought to only act as pathogenic effectors, have been shown to have regulatory properties as well, with co-production of the anti-inflammatory cytokine IL-10 by a subset now referred to as regulatory Th17 cells (Nikoopour et al. 2008).

MS/EAE is a CD4 T helper cell-mediated autoimmune disease. During MS/EAE, T helper precursor cells can recognize crossreactive antigens presented by antigen presenting cells (APCs), and differentiate into anti-myelin specific Th1 cells. These T cells then cross the BBB and enter the CNS, where the myelin antigens are presented to T cells by microglia; T cells get activated and initiate an inflammatory cascade, during which the T cells proliferate, produce both pro- and anti- inflammatory cytokines, chemokines which cause damage to the CNS; in addition, T cells can activate microglia, and cause further recuitment of macrophages to the CNS.

Nitric oxide

In the late 1980s nitric oxide (NO) has been reported to play several important physiological roles in biological systems; a lot of studies have focused on the roles of NO in many neurodegenerative diseases. The chemistry of NO is complex, and poorly understood *in vivo*, particularly in inflamed tissues. Because NO is a reactive molecule, it does not only exist as a free radical, but also gives rise to several related compounds. *In vivo*, the inflamed tissue contains a lot of factors that could affect the chemistry of NO in different ways (pH, or oxygen tension), and NO could exist in one or several forms of compounds, including nitroxyl (NO-) ion, nitrous acid (HNO2), the nitrogen dioxide (NO2) radical, peroxynitrite (ONOO-) (a product of the combination of superoxide and nitric oxide) and peroxynitrous acid (ONOOH) (Beckman et al., 1994; Beckman et al., 1996). Thus the forms that NO take at sites of inflammation are not known with much certainty (Smith and Lassmann 2002).

Nitric oxide is produced by nitric oxide synthases (NOS). NOS consume L-arginine, nicotinamide adenine dinucleotide phosphate-oxidase (NADPH) and O2, and produce equal amount of NO, nicotinamide adenine dinucleotide phosphate (NADP) and citrulline (Alderton et al., 2001). This process requires calmodulin and tetrahydrobipterin (BH4) as cofactors (Nathan and Xie, 1994). There are four types of NOS isoforms. They are named after the cell types they were originally described to produce them: inducible NOS (iNOS), endothelial NOS (eNOS), neuronal NOS (nNOS) (Dawson et al., 1991; Lamas et al., 1992; Stuehr et al., 1989) and more recently mitochondria NOS (mtNOS), which is

localized in the mitochondria (Ghafourifar and Cadenas, 2005; Kobzik et al., 1995). Both nNOS and eNOS isoforms are constitutively expressed and produce low concentrations of NO in a calcium-dependent manner. NO produced by these NOSes contribute to the regulation of blood flow and participate in some synaptic transmission. iNOS isoform is not present in normal conditions, but its expression is up-regulated during inflammatory conditions. In this case, it produces high levels of NO in a calcium-independent manner, and contributes to inflammatory process.

All the NOS isoforms are present in the CNS and the level of NO has been to be up-regulated during neurodegenerative diseases such as ischemia, stroke and MS (Endoh et al., 1994; Murphy, 2000; Nomura and Kitamura, 1993; Zhang et al., 1995). The specific roles of NOSes still remain unclear, but it's believed that nitric oxide generated from different cellular sources can be either neurodegenerative or neuroprotective during disease (Samadani et al., 1997). During inflammatory conditions, glial cells such as microglia and astrocytes produce large amount of NO through the induction of iNOS (Bal-Price and Brown, 2001). Generally, iNOS is considered to be responsible for the high output of NO seen in various pathological states of CNS that involve inflammation (Chao et al., 1992). In a model of focal ischemia, activation of eNOS contributes to neuroprotection, while activation of nNOS exhibits neurotoxic effects (Samadani et al., 1997).

It has been well addressed that the production of NO is significantly upregulated within MS lesions. Since much of the NO produced within the body is ultimately converted to nitrite and nitrate, several studies have examined the concentrations of these

ions in the cerebral spinal fluid (CSF), blood, and urine of MS patients. High levels of nitrite and nitrate were detected, indicating important disregulation of NO metabolism in MS. NO may be involved in the development of several pathological features of MS, and the induction and control of the inflammatory process. As a vasodilator, NO can provoke the vasodilatation of the cerebral vasculature. In pathological conditions, NO-mediated vasodilation can decrease the velocity of blood flow, and facilitate the migration of leukocytes through the vasculature, and thereby promotes inflammation. Vasodilation can also cause a disturbance of the blood-brain barrier, which will promote the passage of inflammatory cells and mediators into the CNS parenchyma (Brian et al., 1996). It has been found that the nitrite and nitrate concentrations in CSF of MS patients are correlated with BBB breakdown, as measured by the leakage of albumin (Giovannoni, 1998). Although it has been showed that NO can disturb BBB permeability in both *in vivo* and *in vitro* settings, the precise mechanism is complex and poorly understood. With their cell bodies wrapping around the capillary lumen and the ends of the cells sealed by tight junctions, endothelial cells are well-positioned to regulate BBB integrity by controlling the entry of cells into the CNS. Moreover, eNOS expression is up-regulated in endothelial cells during EAE (Zhao et al., 1996). It has been reported that in a model of kainite- induced hippocampal excitotoxicity, eNOS-derived NO mediates breakdown of the BBB (Parathath et al., 2006).

A potential role for NO is to cause damage of oligodendrocytes. *In vitro*, it has been shown that oligodendrocytes are much more sensitive to NO-mediated toxicity than microglia and astrocytes (Mitrovic et al., 1994). Some of the effects of NO on

oligodendrocytes may be mediated by promotion of DNA strand breaks (Mitrovic et al., 1994). *In vivo*, NO causes direct damage to oligodendrocytes, which results in demyelination. NO has also been found to block the axon conduction by affecting sodium and calcium channels in axon terminals (Ahern et al., 2000; Kurenny et al., 1994).

Despite the detrimental roles of NO in MS, it has also been reported that NO can mediate protective effects by interfering with the T cell mediated inflammatory cascade. NO can cause inhibition of T cell proliferation and activation, thus inhibiting T cell mediated inflammation (Albina et al., 1991); NO can also down-regulate the expression of adhesion molecules, which would inhibit further recruitment of inflammatory cells (Kubes et al., 1991); NO can promote apoptosis of T cells, contributing to the termination of inflammation response (Zettl et al., 1997). Some contradictory results were obtained by several NOS/iNOS inhibitor treatment study reports for EAE (Okuda et al., 1998; Zhao et al., 1996): in some cases the inhibitors ameliorated the disease symptoms, whereas in others, more severe symptoms were provoked, possibly because the treatments were delivered or were effective at different times in the disease course. Aminoguanidine (AG), a selective inhibitor for iNOS, has been reported to have different effects on EAE in the induction and progression phase. Administration of AG during the induction phase showed partial preventive effects, while administration during the progression phase had a harmful effect with more severe disease and higher mortality (Okuda et al., 1998). Both *in vitro* and *in vivo* experiments provide evidences that NO play both aggravating and protective roles in MS/EAE.

Blood Brain Barrier

In the early 1900s, Lewandowsky found that some intravenously administered pharmacological drugs such as bile acids or ferrocyanide had no effect in the CNS (Lewandowsky 1900); this might be due to that a physical barrier existing between the CNS and the rest of the body. The failure of the intravenously administered trypan blue dye to stain the brain and spinal cord tissue confirmed this view. This physical barrier was thus referred to as the blood brain barrier (BBB).

Electron microscopy (EM) studies showed that the BBB is localized at the level of tight junctions (TJ) between adjacent brain endothelial cells, which normally inhibit the free exchanges of solutes between brain and blood (Reese and Karnovsky, 1967). In healthy conditions, BBB prevents the entry of blood cells, leukocytes and plasma components into the CNS. In neurodegenerative conditions, such as intracerebral hemorrhage, ischemia and multiple sclerosis, the BBB is compromised, and these blood components can cross the BBB, enter the CNS, and generate neurotoxic factors which can cause further damage to disease (Hawkins and Davis, 2005). However, small lipid-soluble molecules (molecular weight lower than 400 Da) with fewer than nine hydrogen bonds, can cross the BBB through lipid-mediated diffusion (Pardridge, 2007). Therefore, all drugs in clinical use now for CNS therapy are small molecules with these characteristics.

The basic structure of BBB is comprised of several cell types. One of the major cell types is the endothelial cell. A single endothelial cell wraps around the capillary lumen,

and their end-feet are connected by tight junction. The second major cell type is the pericytes, which are attached to the abluminal surface of the endothelial cells. These two cell types are surrounded by the basal lamina (BL), which is contiguous with the plasma membranes of astrocytic end-feet and endothelial cells. Endothelial cells maintain the BBB integrity through the function of tight junctions. Pericytes play a role in maintaining the integrity of the BBB, as well as in regulating homeostatisis (Balabanov and Dore-Duffy, 1998; Shepro and Morel, 1993) . The final major cell type of BBB is the astrocytes. Astrocytes play a role in the BBB formation by increasing the tight junction protein expression in endothelial cells junctions (Janzer and Raff, 1987; Tao-Cheng et al., 1987). They also enhance BBB properties of endothelial cells and thus enhance BBB integrity (Abbott et al., 2006; Gaillard et al., 2000; Hayashi et al., 1997).

Tight junctions seal the end-feet of endothelial cells, and restrict the influx of molecules into CNS. Tight junctions consist of various components. Occludin was the first integral membrane protein discovered within the tight junction of endothelial cells. Deleting the N terminus of occludin had a dramatic effect on the tight junction integrity, indicating an important role of N terminus of occludin in maintaining BBB function (Bamforth et al., 1999). In addition to the function as a tight junction protein, occludin has some other important physiological roles, such as regulation of epithelial cell differentiation (Schulzke et al., 2005) and control of cell apoptosis through inhibition of mitogen-activated protein kinases (MAPK) and Akt signaling pathways (Murata et al., 2005). Recent study showed that occludin dephosphorylation was observed prior to the change of BBB permeability and the development of clinical symptoms in a mouse

model of EAE (Morgan et al., 2007). This suggested a role of occludin in regulating BBB integrity in response to inflammation in MS. Claudins are a multigene family of more than 20 members that form another component of the tight junctions. They form tight junctions through homophilic claudin-claudin interactions. Claudin-5, -3, and -12 are localized at the BBB (Nitta et al., 2003), whereas the presence of claudin-1 is controversial (Lee et al., 2003). Each claudin regulates the diffusion of a group of molecules of a certain size (Nitta et al., 2003). The peripheral membrane-associated guanylate kinase (MAGUK) family contains some cytoplasmic multidomain scaffolding proteins such as ZO-1, ZO-2, and ZO-3 (Hawkins and Davis, 2005). These proteins act as a cytoskeletal anchorage for the transmembrane tight junction proteins. In MS lesions, a reduced ZO-1 expression was related to a tight junction abnormality (Kirk et al., 2003).

Failure of the BBB is a critical event in the development and progression of several diseases that affect the CNS. Increased BBB permeability is a consequence of some diseases such as ischemia (Ilzecka, 1996) and brain trauma (Morganti-Kossmann et al., 1999). Compromisation of BBB could also be a cause of the diseases, such as multiple sclerosis (Floris et al., 2004). While in other conditions, such as Alzheimer's disease, the relationship between BBB breakdown and pathology is not clear (Wardlaw et al., 2003).

In normal conditions, few leukocytes are present in the CNS. During some pathological conditions such as MS, once the BBB is compromised, the leukocytes can cross the BBB and enter the CNS; about 80% of these leukocytes are T cells. The infiltrating T cells can trigger an inflammatory cascade, during which a lot of inflammatory cells release Th1 cytokines, including active T cells,

microglia/macrophages, and astrocytes. The major Th1 cytokines involved in pathogenesis of relapses of MS are IFN-γ, TNF-α, interleukin-1-β (IL-1β), and IL-6. These Th1 cytokines can activate endothelial cells, which modulate the BBB phenotype by induction of several inflammatory genes. Cytokines can also induce the expression of endothelial cell adhesion molecules (ECAMs), including ICAM-1, VCAM-1, E-selectin, and platelet/endothelial cell adhesion molecule 1 (PECAM-1) (Dore-Duffy et al., 1993; Losy et al., 1999). Elevated levels of ICAM-1 have been described in MS during relapses and are associated with enhancing lesions on MRI (Giovannoni et al., 1997; Hartung et al., 1995; Rieckmann et al., 1997). Similarly, soluble forms of ECAMs are also increased in MS CSF and correlate with disease activity (Elovaara et al., 1998; Losy et al., 1999; Rieckmann et al., 1994). Endothelial cells exposed to Th1 cytokines, particularly IFN-γ, can alter the architectural organization of the tight and adherens junctions.

Chapter II

General Methods and Materials

Animals

C57BL6 (wild-type, wt), eNOS deficient ($eNOS^{-/-}$) (Shesely et al. 1996), nNOS deficient ($nNOS^{-/-}$) (Huang et al. 1993) and iNOS deficient ($iNOS^{-/-}$) (Laubach et al. 1995) mice were bred in-house under specific pathogen-free conditions [Division of Laboratory Animal Resources at the State University of New York (SUNY) Stony Brook], controlled for temperature (21°C), and maintained under a 12-hour light/dark cycle. Access to food and water was *ad libitum*. All transgenic mice used have been backcrossed for more than 12 generations into the C57/BL6 background. Adult (6- to 8-week-old) female mice were used in all experiments and were routinely genotyped to confirm the NOS isoform deficiency.

MOG peptide

MOG35-55 peptide (MEVGWYRSPFSRVVHLYRNGK) was synthesized by Quality Controlled Biochemicals and purified using reverse-phase (C18) HPLC.

Induction of EAE with MOG_{35-55} peptide

EAE was induced as described previously (Bernard et al. 1997; Bhasin et al. 2007; Lu et al. 2002) by subcutaneous injection into the mouse flank on day 0 with 300 μg of MOG_{35-55} peptide thoroughly emulsified in complete Freund's adjuvant (CFA) containing 500 μg of heat-inactivated Mycobacterium tuberculosis (Difco, Detroit, MI). One week

later (day 7), the mice were boosted with 300 µg of MOG_{35-55} peptide subcutaneously in the other flank. 500 ng Pertussis toxin (List Biologicals, Campbell, CA) in 200 µl of PBS was injected intraperitoneally on days 0 and 2.

Evaluation of EAE symptoms

After immunization with MOG, mice were observed and weighed daily. Symptom severity was scored on a scale of 0 to 5 with graduations of 0.5 for intermediate symptoms. The score is designed as follows (Hjelmstrom et al. 1998): 0, no detectable symptoms; 1, loss of tail tone; 2, hindlimb weakness or abnormal gait; 3, complete paralysis of the hindlimbs; 4, complete hindlimb paralysis with forelimb weakness or paralysis; 5, moribund or death.

Time-controlled Drug Delivery

Alzet miniosmotic pumps (Durect, Cupertino, CA) were used to ensure time-controlled drug delivery. 14-day pumps (rate of infusion 0.25 µl/hr, 100 µl total volume) were filled with PBS, 1mM NO donor 2,2'-(Hydroxynitroshydrazino)is-ethanamine [NOC-18 (Calbiochem; San Diego, CA)], 1mM N^g-Methyl-L-Arginine [NMMA (Sigma, Saint Louis, MO)] or 500µM Tuftsin (American Peptide Company, Sunnyvale, CA), and incubated at 37˚C overnight before implantation.

Adult mice (6-10 weeks old) were deeply anesthetized using atropine (0.6mg/kg body weight) and 2.5% avertin (0.02ml/g body weight). The pumps were implanted subcutaneously in the back of the mice. The pumps were replaced with fresh pumps after 14 days delivery.

Eriochrome Cyanine stain

Eriochrome cyanine staining was used to visualize myelin. In brief, spinal cord sections previously stored at -80˚C were air-dried for 1 hour at room temperature and a second hour at 37˚C in a dry incubator. After incubation with acetone for 5 minutes, the slides were air-dried for 30 minutes and then stained in eriochrome cyanine solution (0.2% eriochrome cyanine RS (Sigma), 0.5% H_2SO_4 (Sigma), 10% iron alum (Sigma) in distilled water) for 30 minutes, differentiated in 5% iron album (Sigma) for 10 minutes, and placed in borax-ferricyanide solution (1% borax (Sigma), 1.25% potassium ferricyanide (Sigma), in distilled water) for 5 minutes. The slides were then dehydrated through graded ethanol solutions and coverslipped using Permount (Fisher Scientific, NJ, USA).

FluoroMyelin stain

FluoroMyelin fluorescent myelin stain was also used to visualize myelin. Experiments were performed following the manufacturer's instructions. In brief, slides previously stored at -80˚C were rehydrated in PBS or PBS-T for 20 minutes, incubated in

staining solution (300-fold dilution of stock solution in PBS) for 20 minutes at room temperature, washed 3 times for 10 minutes each with PBS, and then mounted with Fluoromount-G (Southern Biotech, AL, USA). Myelin profiles were quantified based on the fluorescent intensity of Fluoromyelin staining. Briefly, the mean fluorescent intensity in spinal cord white matter was calculated by the total fluorescent intensity in spinal cord white matter/areas selected. The mean fluorescent intensity in spinal cord grey matter was also calculated and used as background. The myelin signal was calculated using the mean fluorescent intensity in spinal cord white matter subtracts the mean fluorescent intensity in spinal cord grey matter (background). Quantifications were performed on five sections per mouse for three different mice in three separate EAE experiments.

To co-image Iba1, after the wash step above the slides were blocked with 5% goat serum and processed using standard immunostaining with anti-Iba1 antibodies (please see below).

Immunofluorescence

Mice were transcardiacally perfused using 4% paraformaldehyde/PBS and the spinal cords removed and post-fixed in 4% paraformaldehyde/PBS for 1 hour at room temperature followed by 30% sucrose dehydration at 4ºC overnight. The spinal cords were embedded in Tissue-Tek (Miles, Elkhart, IN) optimal cutting temperature compound, frozen on dry ice, and stored at -80°C until use. Cross sections (20 µm) were cut on a cryostat (Leica, Nussloch, Germany) at -20°C.

Spinal cord sections were blocked in serum of the host of the secondary antibody [5% serum in PBS-T (0.5% TritionX-100 in PBS)], and then incubated overnight at 4°C in rabbit anti-mouse Iba1 (Wako, Japan) at a 1:500 dilution in PBS to detect both resting and activated microglia/macrophages. After washing in PBS, sections were incubated with fluorescence-conjugated (FITC or Texas Red) goat anti-rabbit secondary antibody for 1 hour at room temperature, washed 3 times 10 minutes each with PBS, and mounted using Fluoromount-G (Southern Biotech, AL, USA).

The stained sections were photographed using a SPOT RT camera with a Nikon Eclipse E1600W microscope.

TUNEL assays

TUNEL assays were performed according to manufacturer's guide (Roche). Briefly, T cells were fixed with 4% paraformaldehyde and incubate on ice for 30 min. T cells then were washed with PBS three times. Ice cold 70% Ethanol was added to cells for additional fixation, and incubated on ice for 30 min. The cells were incubated with the TUNEL reaction mixture containing TdT and fluoresceindUTP. Apoptosis cells were indentified using a SPOT RT camera with a Nikon Eclipse E1600W microscope.

Western blotting

Mice were sacrificed and the spinal cords isolated and homogenized in 0.25% Triton X-100 in PBS. Debris was removed by centrifugation, and the supernatant protein concentration measured using the Bio-Rad Bradford detergent-compatible (DC) assay. Protein (20 mg) was separated by SDS-PAGE and transferred to a polyvinylidene difluoride membrane. Membranes were blocked using 5% nonfat dry milk in PBS containing 0.05% Tween 20, and then incubated with rabbit anti-mouse Iba1 antibody (1:1000, Wako, Japan), rabbit anti-mouse actin antibody (1:2500, Sigma), rat anti-mouse IL4 antibody (1:1000, BD Pharmingen), rat anti-mouse IL10 antibody (1:1000, BD Pharmingen), rabbit anti-mouse phospho-STAT1 (1:1000, Cell Signaling), rabbit anti-mouse pan-STAT1 (1:2500, BD Transduction), rat anti-mouse Foxp3 (1:1000, eBioscience), rabbit anti-mouse neuropilin-1 (1:1000, Abcam), overnight at 4°C. Horseradish peroxidase (HRP)-conjugated secondary antibody (Jackson Immunoresearch) was used at appropriate dilutions and detected using the LumiGLO Chemiluminescent Substrate System (KPL).

BBB Breakdown assays

BBB breakdown was assessed both by the disruption of occludin immunostaining, as well as by Evans Blue diffusion, as described before (Parathath et al. 2006; Yepes et al. 2003). For the Evans Blue diffusion method, in brief, $eNOS^{-/-}$ and wild-type mice were injected intravenously with a solution of 2% Evans blue (Sigma). After 24 hours, the

mice were sacrificed by transcardiac perfusion with saline, and the spinal cords removed, weighed, and homogenized in 0.5% TritonX-100 in PBS, and centrifuged at 21,000xg for 30min. The amount of Evans blue in the supernatant was quantified at 620nm, subtracted from the background, and divided by the wet weight of the tissue. Values are presented as a percent of the total signal and represent average values for a minimum of three mice per experimental group.

I also used occludin immunostaining as an indicator of BBB integrity (Parathath et al. 2006; Parathath et al. 2007). Briefly, mice were transcardiacally perfused using PBS and the spinal cords were removed and dehydrated in 30% sucrose at 4ºC overnight. The spinal cords were embedded in Tissue-Tek (Miles, Elkhart, IN) optimal cutting temperature compound, frozen on dry ice, and stored at -80°C until use. Cross sections (20 μm) were cut on a cryostat (Leica, Nussloch, Germany) at -20°C. Spinal cord sections (20μm) were fixed in 95% ethanol for 30min at 4°C followed by an additional 3min incubation with acetone. After blocking in serum [5% serum in PBS-T (0.5% TritonX-100 in PBS)], sections were incubated with 3μg/mL mouse anti-occludin (Zymed; San Francisco, CA) overnight at 4°C. After a 10min wash in PBS, FITC-goat anti-mouse secondary antibody was added for 1hr at room temperature. Sections were washed 3 times for 10min in PBS and mounted using Fluoromount-G. The stained sections were photographed using a SPOT RT camera with a Nikon Eclipse E1600W microscope.

Measurement of nitrite levels

Measurement of nitrite levels was based on the reaction of nitrates/nitrites with 2,3-diaminonaphthalene (DAN) under acidic conditions, which results in the formation of the fluorescent product 2,3-naphthyltriazole. In brief, 100 μl of sample or standard ($NaNO_2$) were loaded in each well of a black 96-well plate with a clear bottom. 20 μl freshly prepared DAN (0.05 mg/ml in 0.62 M HCl) was added to each well. The reaction was allowed to proceed at RT for 20 min and then terminated by the addition of 100 μl 0.28 M NaOH. After 10 min incubation at RT, fluorescence was measured on a Titertek Fluoroscan II fluorescence plate reader using an excitation 355 nm and an emission 460 nm filter pair.

BrdU-based proliferation assay

The BrdU-based cell proliferation assay (Roche) was performed to assess the proliferation of T cells and microglia. Briefly, 10 μl of the BrdU labeling solution was added to each well of a 96-well plate and the cells were left to incorporate the BrdU for 16 h. Cells were fixed with 200 μl/well of FixDenat solution for 30 min at RT. Anti-BrdU-POD was then added to each well and was incubated for 2 h at 37 ^{o}C. After three washes, 100 μl of substrate was added to each well and incubated for 30 min. Reaction was stopped by H_2SO_4. Absorbance was read at 370 nm on a SpectraMax microplate reader using the Softmax Pro software.

ELISA

To measure levels of TNFα/IL10/IL4 in the culture medium, the OptEIA Set Mouse TNF/IL10/IL4 kit from BD Biosciences were used according to manufacturer's instructions. Briefly, Nunc MaxiSorp 96-well plate was coated with capturing antibody in coating buffer (0.2 M sodium phosphate buffer pH 6.5) overnight. The plate was washed three times with PBS-T (0.05% Tween-20/PBS) and blocked with Assay Diluent for 1 hour at RT. Following three washes with PBS-T, 100 μl of cytokine standard and experimental samples were added to the wells and incubated for 2 hours at RT. After 5 washes with PBS-T, 100 μl of Assay Diluent containing biotin-conjugated detection antibody and Avidin-HRP reagent were added and incubated for 1 hour at RT. Following 7 washes with PBS-T, 100 μl of Substrate Solution was added to each well. After 30 min incubation in the dark, 50 μl of Stop Solution (2 N H2SO4) were added and absorbance was read at 450 nm using a SpectraMax microplate reader.

Primary T cells culture from mouse spleen

T cell negative isolation kit (Invitrogen) was used to isolate primary T cells from mouse spleen. Briefly, a mixture of monoclonal antibodies against unwanted cells was added to spleen cells. T cells were isolated by depleting the antibody-labeled cells using mouse depletion dynabeads and a dynal MPC. T cells were resuspended in RPMI medium supplemented with 10% FBS.

Mixed cortical cultures and Primary microglia culture

Tissue culture plates used for plating mixed cortical cultures were coated with 5 μg/ml poly-D-lysine (PDL, Sigma) overnight at 4 ^{o}C. Newborn (d 0-d 2) pups of wild-type mice were euthanized, and the heads were removed and briefly immersed in 70% ethanol and then transferred to Hank's Balanced Salt Solution (HBSS). The brains were removed, and the cortices were freed from meninges, hippocampi and basal ganglia and kept in HBSS on ice.

The cortical tissue was digested in 0.25% Trypsin/EDTA (Sigma) at 37 ^{o}C for 20 min and trypsin was inactivated by addition of full medium (DMEM, 10% FBS, 40 μg/ml Gentamycin). The tissue was triturated and filtered through a 40 μm cell strainer. The cell suspension was plated at desired density.

The medium was changed 3 days after plating. Microglial cells were harvested 10 days after plating. Briefly, lidocaine was added directly to the culture medium at a final concentration of 1mM and the culture was left at RT for 15 min. The medium containing the floating microglia was collected, and 5 mM EDTA was added to the microglial suspension. Cell suspension was centrifuged at 500g for 5 min, then resuspended in microglia medium (DMEM, 1% FBS) and counted using a hemocytometer. Cells were plated at the desired density and left to rest for 2 days before treatment.

Primary Neuronal Cultures

Tissue culture plates used for plating neuronal cultures were coated with 5 μg/ml poly-D-lysine (PDL, Sigma) overnight at 4 ^{o}C. Primary neuronal cultures were prepared from embryonic day 17-19 mice as previously described (Rogove and Tsirka, 1998; Siao and Tsirka, 2002). Briefly, mouse cortices were dissected and put in Hanks solution (HBSS), and gently trypsinized (0.25% trypsin in HBSS) at 37°C for 20 minutes and then triturated to form single cell suspensions. The cells were plated at a density of 100,000 cells/cm^2 in Neurobasal medium with B27 supplements, 25 μM glutamate, 0.5 mM L-glutamine and 10 g/L gentamycin sulfate. The medium was changed 4 hours after the initial plating and the glutamate removed after four days in culture. Neurons were used after 7 days after plating.

PCR arrays

Mouse inflammatory cytokines and receptors arrays (SABioscience) were used on RNA samples isolated from T cells. Briefly, RNA was isolated from T cells after different treatment. cDNA was prepared from RNA samples using RT2 First Strand Kit (SABioscience). cDNA and RT-PCR master mix were added to 96-well PCR array plate. Thermal cycling was performed. Data was analyzed using PCR Array Data Analysis Web Portal provided by SABiosciences.

Statistics

Statistical analysis was performed using one-way ANOVA followed by a Bonferroni-Dunn test for multiple comparisons within a group, or a two-tailed t-test for comparisons between groups as indicated by the figure legends; $p < 0.05$ was considered significant and is marked by an (*) or ($^{\#}$); $p < 0.01$ and $p < 0.001$ were considered very significant and are marked by two (**) or ($^{\#\#}$); and three (***) or ($^{\#\#\#}$) respectively. All results are represented as average with error bars indicating the standard error of the mean. In all experiments, n refers to the number of animals used for each genotype or condition.

Chapter III

Contributions of individual NOS isoform-derived NO in the development of experimental autoimmune encephalomyelitis (EAE), a mouse model of multiple sclerosis (MS)

Introduction

Multiple sclerosis is a demyelinating autoimmune disease resulting from immune attack on myelin, leading to neurodegeneration. A widely used MS animal model is experimental autoimmune encephalomyelitis (EAE), which mimics histopathological hallmarks of human MS. During EAE, T cells, which are normally excluded from CNS, infiltrate the CNS through a compromised blood-brain barrier (BBB). T cells recruit and activate microglia and macrophages (Boje and Lakhman 2000; Steinman 1996) that release cytokines and chemokines and affect disease progression (Kreutzberg 1996; Raivich and Banati 2004; Rott et al. 1994; Stevens et al. 1994) by promoting either neurodegeneration or neuroprotection.

Activated microglia produce nitric oxide (NO), which can modulate demyelination and inflammation (Farias et al. 2007; Mitrovic et al. 1994). NO can aggravate CNS inflammation, but studies using NO synthase (NOS) inhibitors to treat MS produced confusing results (Kahl et al. 2003; Okuda et al. 1997; Okuda et al. 1998). NO was suggested to have opposing roles as a proinflammatory factor, promoting cytotoxicity, and as an anti-inflammatory factor, suppressing the immune response (Cowden et al. 1998; O'Brien et al. 1999; Okuda et al. 1997).

There are three major NOS isoforms: neuronal (nNOS), endothelial (eNOS), and inducible (iNOS) (Dawson et al. 1991; Lamas et al. 1992; Stuehr et al. 1989). Because the three NOS isoforms are expressed primarily by distinct cell types, part of the complexity of NO effects appears to result from different location of the isoforms and

kinetics of NO production. Neuronal NO produced by nNOS has toxic consequences in focal ischemia animal models, whereas endothelial NO produced by eNOS confers neuroprotection (Samdani et al. 1997). iNOS, expressed primarily by glia (Bal-Price and Brown 2001; Marques et al. 2008; Tran et al. 1997), is responsible for the high NO output seen in pathological states of CNS inflammation (Calabrese et al. 2002; Chao et al. 1992; Farias et al. 2007; Shin et al. 2000). iNOS mRNA (Koprowski et al. 1993) and protein (Cross et al. 1997; Van Dam et al. 1995) expression within the inflammatory lesions of EAE animals, coincides temporally and quantitatively with the severity of clinical symptoms. Extensive literature exists investigating the role of iNOS in MS/EAE (Dalton and Wittmer 2005; Kahl et al. 2004; Kahl et al. 2003; Zehntner et al. 2004), but the other two NOS isoforms have not been evaluated.

BBB disruption is associated with several CNS diseases including MS. In pathological conditions, exaggerated NO-mediated vasodilation increases BBB permeability so that inflammatory cells can infiltrate the CNS (Hurst and Fritz 1996; Shukla et al. 1996; Thiel and Audus 2001) in conditions like stroke (Mayhan and Didion 1996) and hypertension (Mayhan 1995). We showed previously that mice deficient in individual NOS isoforms respond differently to excitotoxicity, and that BBB integrity is differentially affected by the loss of each isoform (Parathath et al. 2007; Parathath et al. 2006). However, it's not known which NOS isoform produces the NO that mediates BBB breakdown in EAE (Thiel and Audus 2001).

In this chapter, I indentified contributions of individual NOS isoform-derived NO in the development of EAE. First, I determined which NOS isoform-derived NO is

responsible in mediating BBB breakdown in EAE. BBB is composed primarily of endothelial cells that express eNOS (Reese and Karnovsky 1967). The endothelial cells their cell bodies wrap around the capillary lumen and their end-feet are sealed by tight junction proteins, which are important in maintaining BBB integrity, so endothelial cells are well-positioned to influence BBB permeability. Activation of eNOS and NO production by endothelial cells would be ideally situated to mediate a powerful local effect on BBB integrity. To investigate the role of NO and eNOS in MS, I applied the myelin oligodendrocyte glycoprotein (MOG)-induced EAE model to eNOS-deficient ($eNOS^{-/-}$) mice and examined disease progression. Our results indicate that lack of eNOS affects the onset, severity and recovery from EAE in a complex manner: decreased eNOS-produced NO protects the BBB, but enhances the severity and persistence of the autoimmune response. The late pathology was largely rescued by delivering an NO donor, suggesting that a useful approach to this disease might be through the judicious use of both NOS inhibitors and NO agonists at different phases of the process.

Second, I also determined the contribution of iNOS/nNOS-derived NO in development of MOG-induced EAE. Our results showed that iNOS-deficient ($iNOS^{-/-}$) mice exhibited a similar disease onset as the wild-type mice, but with much more severe symptoms and limited recovery, while delivery of NO donor was beneficial for the late pathology. nNOS-deficient ($nNOS^{-/-}$) mice, showed severe and sustained symptoms similar to both eNOS and iNOS-deficient mice, however, they exhibited more delayed disease onset, indicating a role of nNOS during the early events of EAE.

Furthermore, I blocked general NO production by delivery of the global NOS inhibitor NMMA in the wild-type mice with MOG-induced EAE. NMMA infusion resulted in exaggerated symptoms and limited recovery, suggesting a protective role of NO during the late phase of EAE.

The results from this chapter will help us to characterize the role of individual NOS in the development of MS/EAE, thus modulation of NO production from their varied cellular sources may have therapeutic potential in the management of MS.

Results

eNOS-deficient mice reveal dual roles for nitric oxide during EAE

Altered progression of EAE in eNOS$^{-/-}$ mice

To evaluate the role of eNOS in EAE, the clinical course of MOG-induced EAE was assessed in wild-type (wt) and eNOS$^{-/-}$mice (Fig. III-1A). Wt mice exhibited signs of disease on average at day 7 (7.2±0.4) after immunization, in contrast to the eNOS$^{-/-}$ mice, which showed a significant delayed disease onset (day 11.9±0.3). However, the eNOS$^{-/-}$ mice exhibited a dramatic exacerbation of signs on about day 15 (score 2.36±0.12). Symptoms worsened faster than those of the wt mice, which had a more gradual onset of disease severity (score 1.36±0.23 on day 15). Disease severity also peaked at different levels for the eNOS$^{-/-}$ mice and wt mice. In wt mice, the peak of disease severity was

around days 20 - 22, with a maximum score of 2.25±0.14. In contrast, the disease peak in eNOS$^{-/-}$ mice started on day 17 and persisted until day 22 with a maximum score of 2.75±0.25. All of the eNOS$^{-/-}$ mice exhibited paralysis of one or both hindlimbs, which was not the case for the wt mice. Following the peak of disease, wild-type mice showed a progressive recovery; by day 50, the clinical score observed for wt mice was 0.85±0.23 (loss of tail tone) and they exhibited no other motor dysfunction. In contrast, the eNOS$^{-/-}$ mice exhibited sustained symptoms with a slow and limited recovery (score 2.18±0.11 on day 50), and their neurological and motor dysfunction was persistent.

An alternate approach to characterize EAE severity is to weigh the mice daily, since mice become sick and lose weight as a consequence of the disease process. Wild-type mice exhibited weight loss as disease progressed, with the biggest drop seen between days 18 to 22 (Fig. III-1B). The mice then re-gained weight as the recovery began. The eNOS$^{-/-}$ mice similarly showed significant weight loss with biggest drop between days 18 to 22. However, the eNOS$^{-/-}$ mice only slowly re-gained weight during the recovery period, paralleling the slow symptomatic recovery seen in Fig. III-1A.

Taken together, the delayed onset of disease and the prolonged recovery period suggested that eNOS-generated NO plays both an early damaging role and a late protective role in MOG-induced EAE.

eNOS$^{-/-}$ mice exhibit delayed BBB breakdown

The delay in onset of EAE in eNOS$^{-/-}$ mice indicates that the NO produced by eNOS contributes to the induction of disease. Since eNOS is primarily expressed by endothelial cells and by astrocytes (Lin et al. 2007), cells that are the main constituents of the BBB, and T cell infiltration through a compromised BBB is a requisite early event in the disease, this raised the possibility that the role of the NO generated in this setting might be to affect BBB permeability.

We evaluated BBB integrity by assessing the diffusion of Evans Blue dye in the spinal cord at different time points after immunization with MOG; the presence of Evans Blue after perfusion would indicate breakdown of the BBB. On day 0, WT and eNOS$^{-/-}$ mice displayed very low levels of Evans Blue dye in the spinal cord (0.46±0.01 and 0.46±0.02, respectively), which was indicative of BBB integrity (Fig. III-2A). Increased levels of Evans Blue dye were detected on day 8 in WT mice (1.18±0.06), but no increase was observed for the eNOS$^{-/-}$ mice until day 12 (0.96±0.06), which correlated with the delayed disease onset observed in Fig. 1. The extent of BBB breakdown as reflected by the level of Evans Blue dye increased progressively in WT mice with the maximal level seen on day 22 (3.01±0.16). In contrast, eNOS$^{-/-}$ mice showed a dramatic increase on day 15 (2.97±0.09) that went beyond that seen in the WT mice and that peaked on day 18 (4.5±0.18). Recovery of BBB integrity was observed for both genotypes; however, the eNOS-/- mice lagged substantially behind the WT mice.

Breakdown of the BBB was also investigated by immunofluorescence using an anti-occludin antibody, since occludin localizes exclusively to tight junctions which are important for maintaining BBB integrity (Hirase et al. 1997). In the cerebellum of untreated wt and eNOS$^{-/-}$ mice on day 0, occludin showed strong and typical staining of the endothelial layer at contact points between cells (Fig. III-2B). By day 8, WT mice began to exhibit a diffuse staining pattern, indicating significant BBB breakdown. This pattern persisted, peaking on day 22 and then resolving by day 30. In contrast, the eNOS$^{-/-}$ mice showed a normal-looking staining pattern until day 15, at which point a marked and much more diffuse occludin staining was observed that progressed until day 22, suggesting almost complete breakdown of the BBB. The diffuse staining pattern improved subsequently but still remained incompletely resolved at day 40.

The results from these experiments suggested that the considerable difference in the clinical course of EAE between eNOS$^{-/-}$ and wild-type mice correlates with the differences in extent of BBB breakdown. To determine whether there was a general correlation between BBB permeability and disease severity, the quantification of the levels of Evans Blue dye in the spinal cord from different time points were plotted against the clinical score on that day (Fig. III-2C). A close linear correlation was evident ($r^2 = 0.884$ for wild-type mice, and r2 = 0.936 for eNOS-/- mice).

Altered demyelination pattern during disease progression in eNOS$^{-/-}$ mice

Inflammation and demyelination are two well-defined characteristics of EAE. Eriochrome cyanine (EC) staining was used to detect myelin profiles in mouse spinal cord. On day 0, both wild-type and eNOS$^{-/-}$ mice showed compact myelin staining in the white matter of spinal cord (Fig. III-3A). In contrast, severe demyelination was detected in eNOS$^{-/-}$ mice on day 15, as characterized by a large area devoid of EC staining (asterisks), whereas only minimal demyelination was observed in WT mice. By day 22, WT mice showed large areas lacking EC staining, and eNOS$^{-/-}$ mice exhibited almost 50% demyelination of the white matter. Recovery (remyelination) was apparent by day 30 and complete by day 40 for the WT mice. In contrast, although partial remyelination was seen in the eNOS-/- mice, large areas of demyelination still remained at days 30 and 40.

Demyelination was also evaluated by FluoroMyelin, a fluorescent myelin stain, for which similar results were obtained (Fig. III-3B). Quantification of the fluorescence intensities (Fig. III-3C) revealed that the extent of demyelination was significantly different from day 15 through the end of the experiment at day 40.

eNOS$^{-/-}$ mice exhibit increased microglial infiltration and activation

During EAE, infiltrating T cells attack the endogenous myelin. Activated microglia are then recruited to the demyelinated area and through their phagocytotic activity

remove cellular debris (Benveniste 1997; Diemel 1998). We evaluated the levels of microglia/macrophage activation at different time-points (Day 15, 22, 30, and 40) during EAE, using the Iba1 antibody which detects resting microglia/macrophages and becomes upregulated during activation (Fig. III-4A, B). Iba1 staining in WT and eNOS$^{-/-}$ mice on day 0 revealed resting microglia/macrophages, as defined by a ramified morphology with long thin cell bodies (arrows). On day 15 in WT mice, the microglia/macrophages observed still appeared to be largely in the resting state, whereas in eNOS$^{-/-}$ mice, dramatic numbers of activated microglia/macrophage were visible in the white matter of spinal cord, as defined by an ameboid shape and extensive branching. This accumulation of activated microglia/macrophages continued in eNOS$^{-/-}$ mice through day 40. WT mice, on the other hand, where characterized by activated microglia/macrophage on day 22 to day 30, but a return to the resting state and a decrease in the total number of Iba1-positive cells was apparent by day 40.

Spinal cord extracts were prepared at different time points during EAE and western blotting performed to determine Iba1 expression as a quantitative measure of the extent of microglia/macrophage recruitment and activation (Fig. III-4C). In both WT and eNOS$^{-/-}$ spinal cord extracts, the levels of Iba1 increased as disease progressed. eNOS$^{-/-}$ spinal cords showed early upregulation of Iba1 starting on day 15, whereas no increase was observed in WT spinal cords. By day 22, increased Iba1 was seen for both genotypes, but the levels of expression were much higher in the eNOS$^{-/-}$ spinal cords. The eNOS$^{-/-}$ spinal cord levels of expression remained elevated at day 30, whereas the levels of expression in WT spinal cords had begun to decrease. These results correlate with the extent of

microglia/macrophage activation described in panels A and B, and with the clinical symptoms described earlier.

Microglia recruits in the demyelinated area and perform phagocytotic activity

Previous studies reported that in the early stages of EAE there is extensive axonal damage, which results in recruitment and activation of microglia (Carson, 2002). Activated microglia phagocytose the myelin debris and hasten the loss of myelin progression. To investigate the role of microglia during demyelination, we stained spinal cord with FluoroMyelin fluorescent myelin stains and Iba1 antibody for microglia/macrophage. As shown in Fig. III-5A, on sections of wild-type mice spinal cords on day 15, the white matter showed compact FluoroMyelin stain, and Iba1 stained microglia/macrophage with resting morphology and long thin cell bodies. In Fig. III-5B, in day 22 wild-type mice, FluoroMyelin stain showed demyelinated area, and double staining with Iba1 revealed activated microglia/macrophage accumulating especially in the demyelinated areas. In sections from $eNOS^{-/-}$ mice on day 22, more severe demyelination was evident and activated microglia/macrophage were evident over all the FluoroMyelin-negative area (Fig. III-5C). These findings suggested that during EAE microglia/macrophage are recruited into the demyelinated area.

Higher magnification revealed that in the demyelinated area activated microglia/macrophages are recruited from the surrounding area potentially to phagocytose cell debris. Fig. III-5D shows that in the demyelinated area a large number

of activated microglia/macrophage were present, while in the compact myelin area, there were only a few microglia/macrophage present.

Providing nitric oxide using an NO donor does not affect the onset and severity of disease, but is beneficial for recovery in eNOS$^{-/-}$ mice

As shown above, eNOS$^{-/-}$ mice exhibit a delayed but then worsened clinical course, pattern of demyelination and extent of microglial infiltration in comparison to WT mice. To determine whether it is the lack of eNOS gene or the lack of nitric oxide produced during disease that caused these differences, we provided nitric oxide using the NO donor 2,2'-(Hydroxynitroshydrazino)is-ethanamine (NOC-18) by delivery through mini-osmotic pumps into the eNOS$^{-/-}$ mice. 14-day pumps (rate of infusion 0.25 μl/hr, 100 μl total volume) filled with PBS or 1mM NOC-18 in PBS were implanted in the back of the mice on day 1 after MOG immunization, and replaced with fresh pumps on days 15 and 29. As shown in Fig. III-6A, the eNOS$^{-/-}$ mice infused with NOC-18 showed delayed disease onset with symptoms starting around day 12, similar to the mice infused just with PBS. The rapid exacerbation of disease symptoms started on day 15 with a maximal severity score of 2.67±0.24 on day 18. However, in contrast to the limited recovery seen in eNOS$^{-/-}$ mice, the mice infused with NOC-18 recovered faster, with the clinical score on days 30 and 40 indistinguishable from that seen for WT mice, and EC staining (Fig. III-6B) that showed a remyelination pattern like that of WT mice. The extent of

infiltration and activation of microglia also altered during the recovery period in eNOS$^{-/-}$ mice infused with NOC-18: fewer activated microglia were recruited on day 30 to the spinal cord (Fig. III-6C). On day 40, most Iba1-positive microglia were in a resting state, correlating with the better remyelination at this timepoint.

BBB breakdown in NOC-18-infused eNOS$^{-/-}$ mice was investigated using occluding immunofluorescence (Fig. III-6D). More diffused occludin staining was observed in the animals starting on day 15, progressed to day 22, and resolved by day 30. The early BBB breakdown in these mice is consistent with the rapid exacerbation of disease symptoms, which resembled that of eNOS$^{-/-}$ mice. However, these mice showed an almost complete BBB restoration during the recovery period, comparable to the wt mice, suggesting that the NO provided by NOC-18 plays a beneficial role.

To determine whether NOC-18 was effective in providing nitric oxide during the 14-day period of pump implantation, we measured nitrite production in the spinal cords during EAE. Nitrite production was measured at different time points in WT mice, eNOS$^{-/-}$ mice and eNOS$^{-/-}$ mice infused with NOC-18, and we found that the NOC-18 as delivered only partially restored the nitrite levels towards normal levels seen in WT mice (Fig. III-6E). Interesting, the overall level of nitrites decreased in correlation with the severity of the EAE symptoms in all mice examined; the basis for this is not presently understood.

These experiments suggested that providing even modest amounts of NO using NOC-18 are beneficial during the recovery phase for mice lacking eNOS, and that higher levels

of NOC-18 delivery might succeed in reversing the altered onset and disease progression during the early stages of EAE.

Characterization of EAE in iNOS-deficient mice

iNOS$^{-/-}$ mice show altered disease progression of EAE

I applied MOG-induced EAE to wild-type (wt) and iNOS$^{-/-}$ mice, clinical course and weight score were assessed. iNOS$^{-/-}$ mice showed similar disease onset as that of the wild-type mice around day 7 (7.3±0.5 for wild-type mice and 7.35±0.5 for iNOS$^{-/-}$ mice). However, iNOS$^{-/-}$ mice had a more dramatic exacerbation of symptoms during the progression phase, with score 2.54±0.3 on day 15, while wild-type mice had a progressively increased symptoms, with score 1.6±0.25 on day 15. Disease was much more severe in iNOS$^{-/-}$ mice, peaking around day 18 (18.05±0.21) with score 2.95±0.15; in contrast, in wild-type mice it reached peak around day 20 with score 2.35±0.12. Following the peak of disease, wild-type mice showed a nice recovery and only scored 0.5±0.1 on day 50, however, the iNOS$^{-/-}$ mice scored 2.03±0.1 on day 50; symptoms sustained and only minimal recovery was observed (Fig. III-7A). The weight course showed the similar trend as the clinical course (Fig. III-7B).

Previous literature showed that iNOS$^{-/-}$ mice display exaggerated symptoms in response to EAE induction (Dalton and Wittmer, 2005). Our experiments of iNOS$^{-/-}$ mice showed consistent results with previous findings.

iNOS$^{-/-}$ mice show altered pathological hallmarks during EAE

I examined the demyelination pattern using eriochrome cyanine (EC) staining in both wild-type and iNOS$^{-/-}$ mice (Fig. III-8A). iNOS$^{-/-}$ mice showed severe demyelination starting from day 15, and peaking around day 22, compared to wild-type mice which exhibited less severe demyelination. During the recovery phase, large areas of demyelination were still observed in iNOS$^{-/-}$ mice, only minimal remyelination occurred. However, in wild-type mice remyelination was apparent from day 30, and recovery was almost complete by day 40.

Increased microglia/macrophage infiltration and activation is another pathological hallmark of EAE, so I evaluated the levels of microglia/macrophage activation at different time-points (Day 15, 22, 30, and 40) during EAE, using the Iba1 antibody (Fig. III-8B). iNOS$^{-/-}$ mice showed an early recruitment and activation of microglia/macrophage starting from day 15, with more dramatic numbers of activated microglia/macrophage on day 22, and this activated pattern continued until day 40. In contrast, in wild-type mice, the numbers of activated microglia/macrophage peaked on day 22, and reduced during the recovery phase. By day 40, most of the cells re-assumed their resting morphology.

The patterns of demyelination and microglia/macrophage infiltration and activation correlated with the clinical symptoms described earlier.

Providing nitric oxide using an NO donor is beneficial for recovery in iNOS$^{-/-}$ mice

Previously I showed that providing nitric oxide using an NO donor promoted the recovery in eNOS$^{-/-}$ mice (Fig. III-6). I wanted to examine if this also is the case in iNOS$^{-/-}$ mice. Using the same method (as described early), I provided nitric oxide using the NO donor NOC-18 by delivery through mini-osmotic pumps into the iNOS$^{-/-}$ mice. 14-day pumps filled with PBS or 1mM NOC-18 in PBS were implanted in the back of the mice on day 1 after MOG immunization, and replaced with fresh pumps on days 15 and 29. The iNOS$^{-/-}$ mice infused with NOC-18 showed disease onset starting around day 7, and a rapid exacerbation of disease symptoms starting on day 15, similar to the mice infused just with PBS. However, NOC-18 infused animals showed less severe symptoms during the peak of disease, with score 2.45±0.13 on day 18, compared to PBS infused iNOS$^{-/-}$ mice which scored 2.95±0.15 on day 18. In contrast to the limited recovery seen in iNOS$^{-/-}$ mice, the mice infused with NOC-18 recovered faster, with the clinical score reassembled that seen for WT mice (Fig. III-9A). iNOS$^{-/-}$ mice infused with PBS exhibited comparable clinical symptoms as iNOS$^{-/-}$ mice carrying no pumps, indicating that the difference caused by NOC-18 was not an effect of the infusion process or pump placement.

Both the remyelination pattern and the extent of infiltration and activation of microglia/macrophages were altered in the NOC-18 infused iNOS$^{-/-}$ mice (Fig. III-9B, C): remyelination was promoted during the recovery period; fewer activated microglia were recruited and most of the cells were in their resting state by day 40.

nNOS-deficient mice exhibit altered disease progression of EAE

MOG-induced EAE was applied to wild-type (wt) and $nNOS^{-/-}$ mice and the clinical score was recorded each day after the induction (Fig. III-10). Wt mice exhibited signs of symptoms around day 7 (7.3±0.4) after immunization, in contrast to the $nNOS^{-/-}$ mice which showed a more significantly delayed onset (day 14.5±0.5). More interestingly, same as that of $eNOS^{-/-}$ and $iNOS^{-/-}$ mice, the $nNOS^{-/-}$ mice also exhibited a dramatic exacerbation of symptoms, which worsened faster than that of the wt mice. Disease was much more severe in the $nNOS^{-/-}$ mice, peaking around day 21 (21.5±0.5) with score 2.83±0.23, while wild-type mice peaked around day 21 with score 2.35±0.25. Same as both $eNOS^{-/-}$ and $iNOS^{-/-}$ mice, the $nNOS^{-/-}$ mice showed sustained symptoms with minimal recovery until day 50.

These results together with our findings in both $eNOS^{-/-}$ and $iNOS^{-/-}$ mice suggested that NO may have protective roles during the recovery period of EAE by exerting an immunosuppressive effect, and that this effect is independent on the cellular source of NO production.

Blocking NO production in wild-type mice exacerbated the progression of EAE

Blocking NO production alters the clinical course in the wild-type mice

Our previous results showed that individual NOS isoform-derived NO may contribute differently during EAE, especially in the early progression phase; however, all three NOS

isoform-deficient mice showed sustained clinical symptoms during the recovery period. To determine if the cellular source-independent NO production is beneficial for the recovery of EAE, I blocked the general NO production by delivery of the global NOS inhibitor NMMA in the wild-type mice, and applied MOG-induced EAE in these mice. The NMMA infused wild-type mice showed comparable clinical course as the PBS infused controls during the progression period of disease (Fig. III-11A). However, they reached much more severe peak of disease around day 21 - day 22 with score 2.88±0.18, while the PBS infused controls peaked around day 20 - day 21 with score 2.35±0.12. In the NMMA infused wild-type mice, the symptoms sustained until day 50 (score 2.14±0.15), with minimal recovery, while the PBS infused controls scored 0.53±0.1 on day 50 (loss of tail tone with no other motor dysfunction). The weight score showed the same trend as the clinical course (Fig. III-11B).

Blocking NO production results in altered pathological hallmarks in the wild-type mice during EAE

Demyelination pattern was assessed using eriochrome cyanine (EC) staining in wild-type mice infused with NMMA and PBS (Fig. III-12A). NMMA infused animals showed comparable demyelination pattern as PBS-infused controls on day 15 (when they both got minimal demyelination) and day 22 (when they had large areas of demyelination), however, the severe demyelination continued until day 40 with limited remyelination in

the NMMA infused mice, while the PBS infused controls showed almost compact myelin staining on day 40. The demyelination pattern in the NMMA infused mice was consistent with the impaired recovery shown in the clinical course.

I next examined the levels of microglia/macrophage activation at different time-points (Day 15, 22, 30, and 40) during EAE, using the Iba1 antibody (Fig. III-12B). Both NMMA and PBS infused mice showed large numbers of activated microglia/macrophages in the spinal cord white matter on day 22 (the peak of disease), however, they showed different pattern during the recovery period: NMMA infused mice had recruitment of activated microglia/macrophages until day 40, while in the PBS infused controls most cells returned to their resting morphology.

These results suggested that blocking general NO production in wt mice worsened disease symptoms, impaired remyelination and caused sustained recruitment and activation of inflammatory cells during EAE. We therefore conclude, that the cellular source-independent NO has protective roles during the recovery period of EAE. The mechanism underlying needs to be further investigated.

Discussion

The cellular source from which NO is produced has been proposed to be responsible in part for determining whether NO has toxic or protective effects during many neurological diseases. In this chapter, in an effort to determine NOS isoform-specific

effects, we used individual NOS isoform-deficient animals and analyzed the development and pathological hallmarks of EAE. We identified that the individual NOS isoform-derived NO contributes specifically the progression phase of EAE.

Initial BBB breakdown is crucial for the induction of EAE. It has been reported that NO can disturb BBB permeability in both in vivo and in vitro settings, however, the precise mechanism is poorly understood. With their cell bodies wrapping around the capillary lumen and the ends of the cells sealed by tight junctions, endothelial cells are well-positioned to regulate BBB integrity by controlling the entry of cells into the CNS. eNOS expression is up-regulated in endothelial cells during EAE (Zhao et al. 1996). In the model of kainate hippocampal excitotoxicity, eNOS-derived NO mediates breakdown of the BBB (Parathath et al. 2006), and we report a similar finding here in the EAE model of MS (Fig. III-2). Accordingly, developing methods to preventing eNOS-derived NO production might succeed in delaying or preventing initiation of new MS (EAE) events.

The nNOS isoform is physically and functionally linked to the NMDA receptor via interaction with the scaffolding protein post-synaptic density 95 (PSD-95) (Brenman et al. 1996; Sattler et al. 1999). This interaction places nNOS in close proximity to the calcium entering the cell through the NMDA receptor upon its activation (Sattler and Tymianski 2000). Since nNOS requires increased calcium levels to produce NO, the opening of the NMDA receptor is functionally coupled to the production of NO. It has demonstrated that the pharmacological or genetic disruption of nNOS function results in neuroprotection after NMDA treatment (Ayata et al. 1997). Previous work in our lab showed that nNOS was a mediator of neurodegeneration and $nNOS^{-/-}$ mice resisted excitotoxicity (Parathath

et al. 2007). In our model, nNOS$^{-/-}$ mice showed delayed disease onset of EAE (Fig. III-10). One explanation is that the nNOS-deficient mice were resistant to excitotoxicity, and there was no neuronal death in the CNS, so microglia/macrophages cannot be activated and thus were not be able to recruit the other cell types into the CNS. Since all the events that were required to trigger BBB breakdown were inhibited, so BBB breakdown was slowly occurred and disease onset was delayed. Another possibility is that the nNOS-derived NO may directly participate in mediating BBB breakdown, thereby caused delayed disease onset. There is evidence that like eNOS, nNOS can regulate cerebral blood flow (Montecot et al. 1997). nNOS may mediate BBB permeability independently from eNOS through indirect signaling events from neurons to BBB.

We report here that all three NOS isoform-deficient mice showed (1) increased severity and limited recovery of neurological and motor dysfunction; (2) early severe demyelination around day 15 which persists through day 40; and (3) an altered pattern of microglia infiltration and activation that occurs early and is similarly persistent. These results suggest that general NO production has a protective role by promoting innate immunosuppression during EAE symptom progression and recovery. Delivery of global NOS inhibitor NMMA in the wild-type mice showed impaired recovery, which further confirmed this finding (Fig. III-11, 12).

The literatures showed that NO secreted by iNOS plays a crucial role in EAE. iNOS activity significantly increases during EAE in correlation with the clinical course, and the NO produced by iNOS is thought to mediate protective effects, since EAE symptoms are exacerbated in mice lacking this isoform (Fenyk-Melody et al. 1998). Mechanistically,

iNOS-generated NO may function to increase T-helper 1 responses (Kahl et al. 2003) or to eliminate inflammatory cells from the CNS by promoting their apoptosis (Okuda et al. 1997). Our results of $iNOS^{-/-}$ mice were consistent with previous findings. Moreover, results of both $eNOS^{-/-}$ and $nNOS^{-/-}$ mice showed persistent recruitment and activation of microglia/macrophages in the spinal cord, indicating a similar role, directly or indirectly, for eNOS and nNOS. The immunosuppressive effects of NO might be functioning through any of several mechanisms including inhibition of T cell proliferation or down-regulation of adhesion molecules, both of which would inhibit further recruitment of inflammatory cells.

These NOS findings shed light on contradictory results obtained by several NOS/iNOS inhibitor treatment study reports for EAE (Okuda et al. 1998; Zhao et al. 1996): in some cases the inhibitors ameliorated disease, whereas in others, more severe symptoms were provoked, possibly because the treatments were delivered or were effective at different times in the disease course. Aminoguanidine (AG), a selective inhibitor for iNOS, has been reported to have different effects on EAE in the induction and progression phase. Administration of AG during the induction phase showed partial preventive effects, while administration during the progression phase had a harmful effect with more severe disease and higher mortality (Okuda et al. 1998). These studies, along with our study, suggest that the timing or route of drug administration must be considered as an important factor.

Here we indentified the roles of different NOS isoform-derived NO during the development of MOG-induced EAE. Several studies have been done to investigate the

role of NO in neurotoxicant-induced demyelination model (Arnett et al. 2002; Linares et al. 2006). This model features demyelination hallmarks, but with a less prominent immunologic component. In a cuprizone-induced demyelination model, iNOS-/- mice exhibited more severe demyelination in the corpus callosum compared to wild-type mice, however they displayed less extent of activation of microglia and macrophages. The severe demyelination may be attributed with a greater depletion of the mature oligodendrocytes. The $eNOS^{-/-}$ mice mice showed a similar extent of demyelination as the wild-type mice, but with a slightly delayed remyelination. Moreover, the demyelination was greatly inhibited in the $nNOS^{-/-}$ mice, which was associated with a dramatic increase in mature oligodendrocyte survival. These findings suggested that NO has protective roles in the neurotoxicant-induced demyelination model. Different NOS isoform-derived NO exhibit individual pathological effect.

Early studies reported that total NOS activity is increased in the CSF from MS patients (Calabrese et al. 2002), but more recent studies have complicated the story: Total NOS activity in the spinal cord has also been reported to remain unchanged or to decrease during EAE (Kahl et al. 2003), and calcium-dependent NOS (eNOS and nNOS) activity in the brain have been reported to decrease concomitantly with iNOS upregulation (Teixeira et al. 2002). The different outcomes reported might be explained by the use of different models for EAE induction, or the different tissue examined (brain, spinal cord or CSF). However, since the NOS activity represents the combined activity of all three NOS isoforms, it is conceivable that each isoform could play a different role in EAE. In this chapter, we describe the finding that nitrite levels in the spinal cord are

about 20% lower in eNOS$^{-/-}$ mice than in WT mice, and that the nitrite levels fall in parallel for both strains during EAE progression and then rise again during recovery (Fig. III-6C). We also observe benefit in recovery for the eNOS$^{-/-}$ mice when nitrite levels are partially restored through administration of the NO donor NOC-18 (Fig. III-6A, B). Although not tested, this now raises the possibility that administration of NOC-18 to elevate the falling levels of nitrite in WT animals during the course of EAE could have a beneficial outcome for them as well.

It is intriguing that NO appears to play both aggravating and protective roles in EAE in different contexts. Although both could be mediated directly by NO, it is also possible that the negative outcomes triggered by NO production could ensue from its conversion to the toxic metabolite peroxynitrite ($ONOO^-$) through reaction with superoxide. $ONOO^-$, a highly reactive oxidant, modifies proteins through the formation of nitrotyrosine adducts and when present at sufficiently high levels, induces excitotoxicity, DNA damage, and apoptosis (Brown and Bal-Price 2003; Crow and Beckman 1996; Kroncke et al. 2001). Contrasting roles for NO and $ONOO^-$ have been reported. *In vitro*, peroxynitrite induces lipid peroxidation in myelin preparations, whereas NO inhibits it (Hooper et al. 2000), and human adult CNS-derived oligodendrocytes are relatively resistant to NO-mediated damage but highly susceptible to peroxynitrite-mediated injury (Beckman et al. 1994). We hypothesize that NO may be a protective molecule in the recovery phase of EAE, whereas its toxic metabolite peroxynitrite triggers BBB breakdown. Future studies will focus on the effects of peroxynitrite in EAE.

Finally, in our attempt to complement eNOS deficiency by administering a synthetic NO donor (NOC-18), we noted that no effect was observed in the phase where NOS-generated NO is harmful, i.e. BBB breakdown, since no change in the timing of EAE was observed, but beneficial outcomes were obtained in the recovery phase (Fig. III-6A). This could reflect the fact that the NO provision only partially restored the deficiency triggered by eNOS deficiency (Fig. III-6C), and that lower levels of nitrite are required for immunosuppression than for BBB breakdown. Alternately, it could indicate that diffuse provision of nitrate suffices to confer immunosuppression in this setting, whereas BBB breakdown requires local production by the endothelial cells that can not be mimicked by diffuse exogenous provision. Regardless of the mechanism, this outcome is potentially useful and suggests that a combination therapy based on an eNOS inhibitor and NOC-18 supplementation could simultaneously delay or prevent new MS episodes by preventing BBB breakdown while enhancing immunosuppression/recovery for ones in progression.

Figure III-1: eNOS$^{-/-}$ mice exhibit delayed EAE onset followed by exaggerated disease severity and limited recovery.

(A). Clinical course of EAE. Wild-type (WT) and eNOS$^{-/-}$ mice were injected with MOG_{35-55} peptide in CFA and pertussis toxin to induce EAE. The disease severity was scored on a clinical scale from 0 to 5 as described in Experimental Procedure. (B). Weight score of WT and eNOS$^{-/-}$ mice during EAE (Experiment has been repeated three times. Cumulative data was provided; total number of animals tested, n=25/genotype).

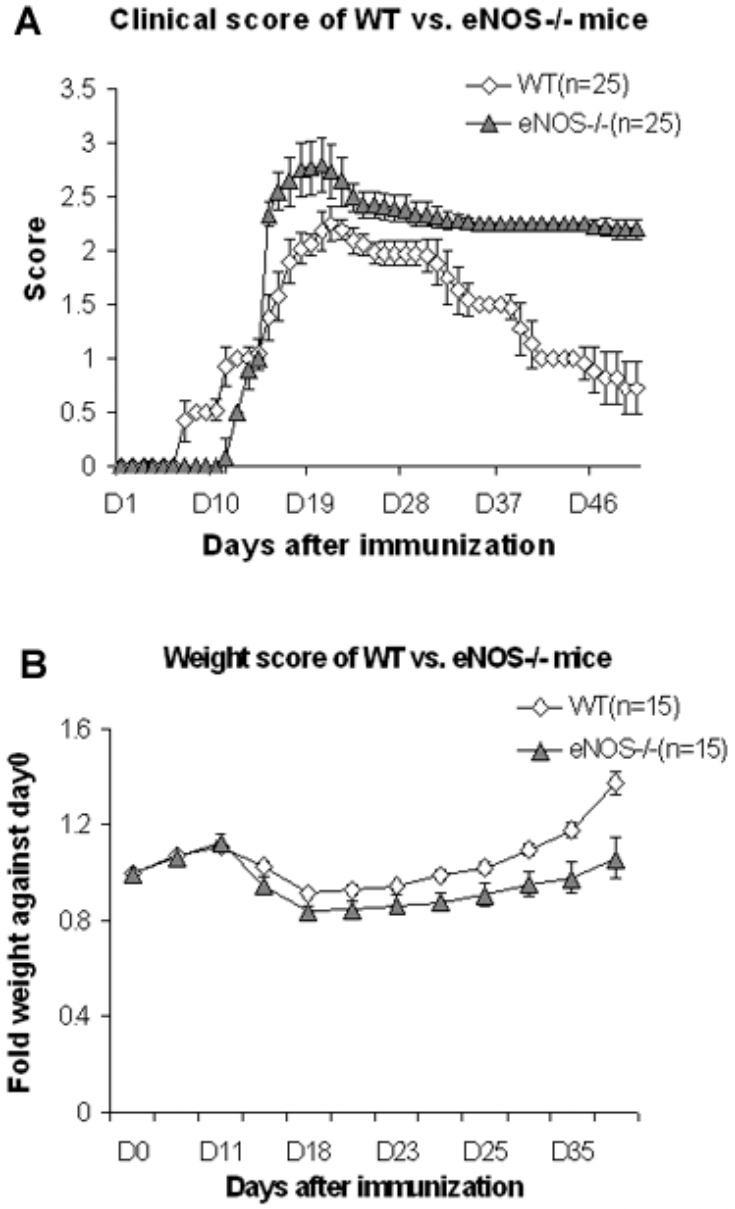
A
Clinical score of WT vs. eNOS-/- mice
WT(n=25)
eNOS-/-(n=25)
Score
3.5
3
2.5
2
1.5
1
0.5
0
D1
D10
D19
D28
D37
D46
Days after immunization
B
Weight score of WT vs. eNOS-/- mice
WT(n=15)
eNOS-/-(n=15)
Fold weight against day0
1.6
1.2
0.8
0.4
0
D0
D11
D18
D23
D25
D35
Days after immunization

Figure III-2: Delayed but ultimately more extensive BBB breakdown in eNOS$^{-/-}$ mice.

(A). WT and eNOS$^{-/-}$ mice were injected with 2% Evans Blue intravenously at different time points after MOG immunization. 24 hours later, the mice were perfused with 4% PFA and the spinal cords removed, weighed, and homogenized. The extent of BBB breakdown was assessed as the amount of Evans Blue (quantified using absorbance at 620 nm) that leaked into the spinal cord normalized to the wet weight. Values are presented as a percent of the total amount of Evans Blue Dye and represent the average of a minimum of three mice per experimental group. A two-tailed *t* test was performed to analyze the difference of BBB breakdown between wild-type and eNOS$^{-/-}$ mice for each timepoint (***, $p<0.001$; **, $p<0.01$). (B). BBB breakdown in the cerebellum was assessed by immunofluorescent staining of the tight junction protein occludin, which in the non-disease setting visually presents as spatially-restricted puncta (e.g. day 0). When BBB breakdown occurs, the pattern of localization becomes more diffuse (e.g. day 22). (C). Correlation between BBB permeability and disease severity.

A.

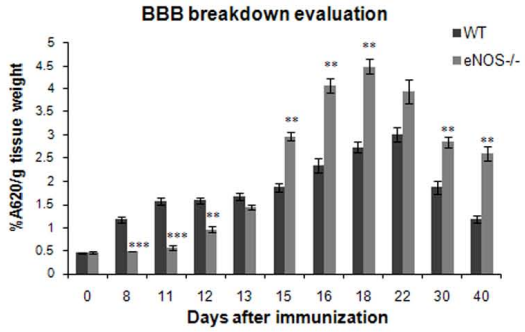
BBB breakdown evaluation
WT
eNOS-/-
%A620/g tissue weight
Days after immunization
0
8
11
12
13
15
16
18
22
30
40

B.

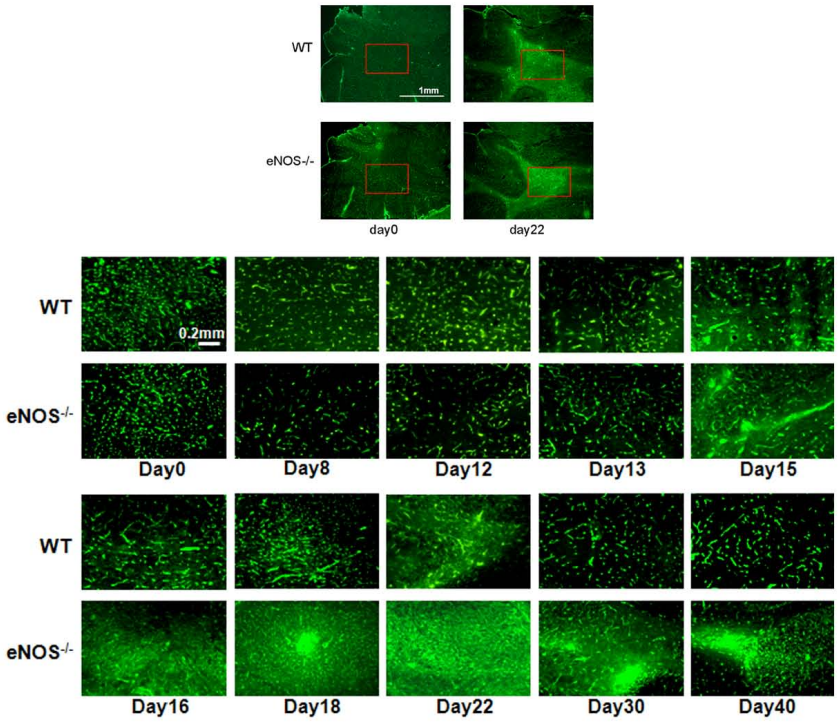
WT
eNOS-/-
day0
day22
1mm
0.2mm
Day0
Day8
Day12
Day13
Day15
Day16
Day18
Day22
Day30
Day40

C.

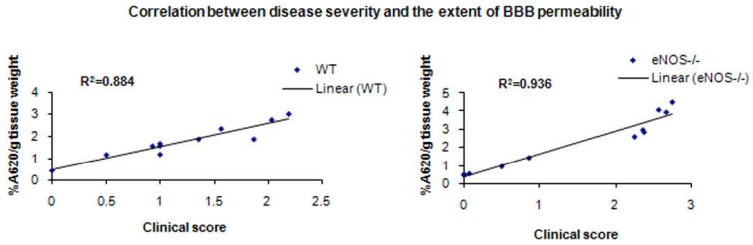
Correlation between disease severity and the extent of BBB permeability
R²=0.884
WT
Linear (WT)
%A620/g tissue weight
Clinical score
R²=0.936
eNOS-/-
Linear (eNOS-/-)
%A620/g tissue weight
Clinical score

Figure III-3: Increased demyelination in eNOS$^{-/-}$ mice during EAE.

(A). Frozen cross-sections of spinal cords isolated from WT and eNOS$^{-/-}$ mice at different time points during the EAE course were stained with Eriochrome cyanine (EC), which visualizes myeline (blue). Sites of demyelination are indicated by asterisks (e.g. eNOS$^{-/-}$ mice at day 15). (B, C). Use of FluoroMyelin to fluorescently and quantitatively image myelin. (Quantifications were performed on five sections per mouse for three different mice in three separate EAE experiments; results are presented as an average with error bars indicating the standard error of the mean. A two-tailed *t* test was performed to analyze the significance of the difference of FluoroMyelin staining intensity between WT and eNOS$^{-/-}$ mice at each timepoint (*** $p<0.001$; **$p<0.01$).

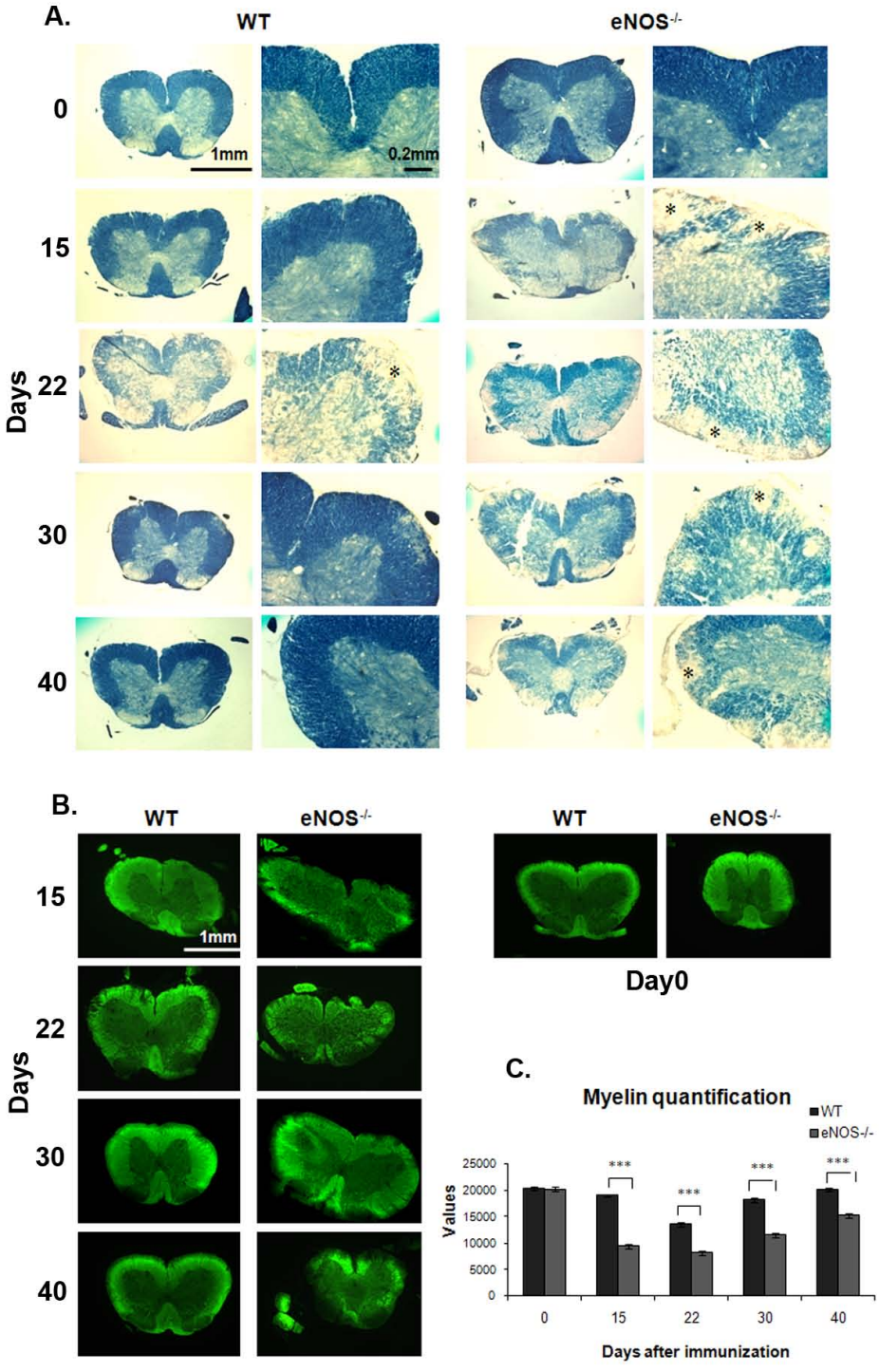
A.
WT
eNOS-/-
0
15
22
30
40
Days
1mm
0.2mm
B.
WT
eNOS-/-
Day0
C.
Myelin quantification
WT
eNOS-/-
Values
Days after immunization
***

Figure III-4: Increased microglia/macrophage infiltration and activation in eNOS$^{-/-}$ mice.

(A). Frozen cross-sections of spinal cords from WT and eNOS$^{-/-}$ mice at different time points in EAE were stained with anti-Iba1 to detect microglia. Iba1 is expressed on both resting and activated microglia, which can be distinguished by their morphological appearance. Arrows (e.g. as seen in Day 0 panel) indicate resting microglia, characterized by long, thin cell bodies. Arrowheads (e.g. as seen in Day 22 and 30 panels) indicate activated microglia that are characterized by thicker, rounded cell bodies and multi-branched cellular protrusions. (Experiment has been repeated three times. In total five mice were assessed for immunostaining each timepoint per genotype, representative data were provided.) (B). Higher magnification (boxed areas in panel A) shows morphology of resting state (day 0) and activated state (day 22) microglia/macrophages. (C). Protein extracts from WT and eNOS$^{-/-}$ mice spinal cords were collected at different timepoints in EAE and analyzed using western blotting to quantitate levels of Iba1. Equal loading of protein was confirmed by anti-actin blotting. (Western blot was repeated three times on mouse spinal cord samples from three separate EAE experiments.)

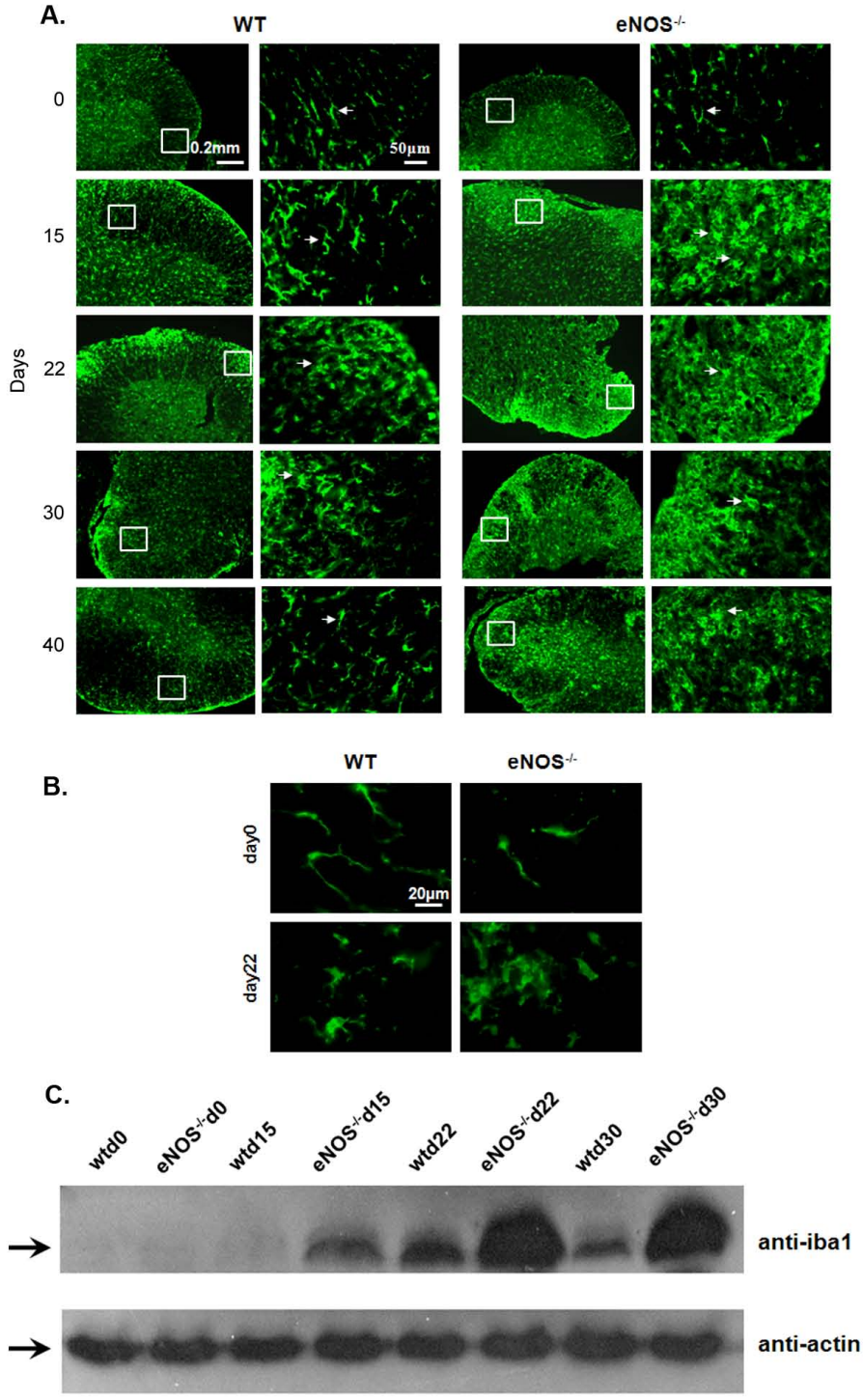
A.
WT
eNOS-/-
0
15
22
30
40
Days
0.2mm
50μm
B.
WT
eNOS-/-
day0
day22
20μm
C.
wtd0
eNOS-/-d0
wtd15
eNOS-/-d15
wtd22
eNOS-/-d22
wtd30
eNOS-/-d30
anti-iba1
anti-actin

Figure III-5A-C: Recruitment of microglia/macrophages into regions of demyelination.

Double staining with FluoroMyelin and anti-Iba1 to image regions of demyelination and microglia/macrophage localization. (A). WT day 15 section, low and high magnification. (B). WT day 22 section. (C). $eNOS^{-/-}$ day 22 section.

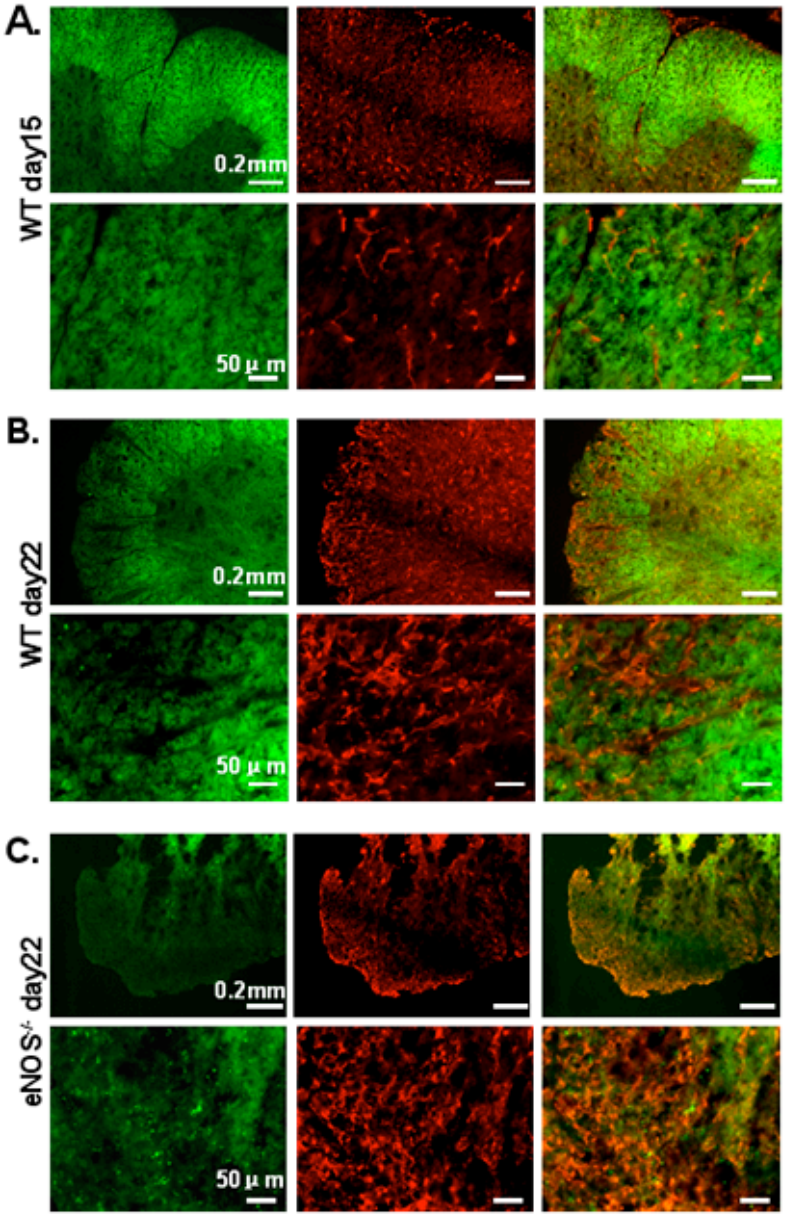
A.
WT day15
0.2mm
50 μ m
B.
WT day22
0.2mm
50 μ m
C.
eNOS-/- day22
0.2mm
50 μ m

Figure III-5D: Recruitment of microglia/macrophages into regions of demyelination. (D). Higher magnification revealed that in the demyelinated area, activated microglia/macrophage recruited from the surrounding area potentially to phagocytose (Sites of demyelination are indicated by asterisks, arrows point to activated microglia surrounding demyelinated areas).

D.

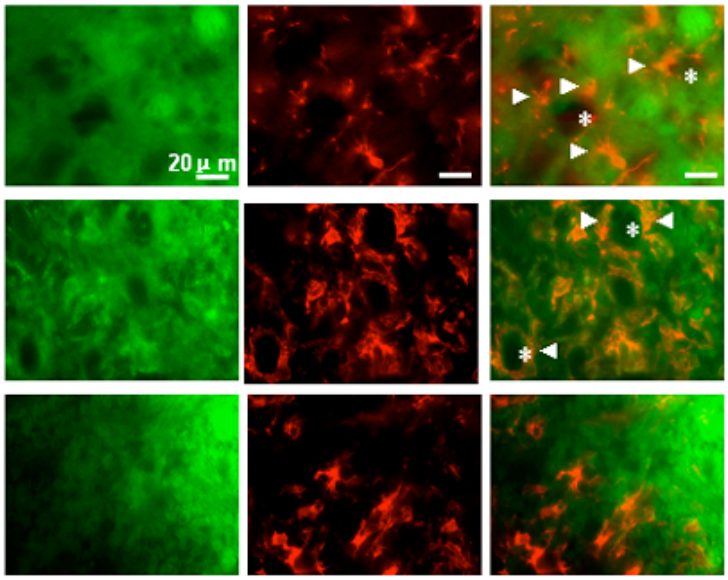

Figure III-6A-C: Therapeutic administration of an NO donor is beneficial in the recovery phase for eNOS$^{-/-}$ mice.

(A). Clinical course and weight score in eNOS$^{-/-}$ mice infused with NOC-18 pumps. (Experiment has been repeated three times. Cumulative data was provided; total number of animals tested: n=19/WT, n=19/eNOS$^{-/-}$, n=21/eNOS$^{-/-}$ infused with NOC-18.) (B). Eriochrome cyanine (EC) staining to assess demyelination in spinal cords of eNOS$^{-/-}$ mice supplemented with NOC-18. (C). Anti-Iba1 staining to show extent of microglia/macrophage infiltration and activation in eNOS$^{-/-}$ mice supplemented with NOC-18. (At least four mice were assessed each timepoint per genotype for both EC staining and Iba-1 staining; representative data were provided.) Quantitative data was provided as the relative microglia/macrophages intensity.

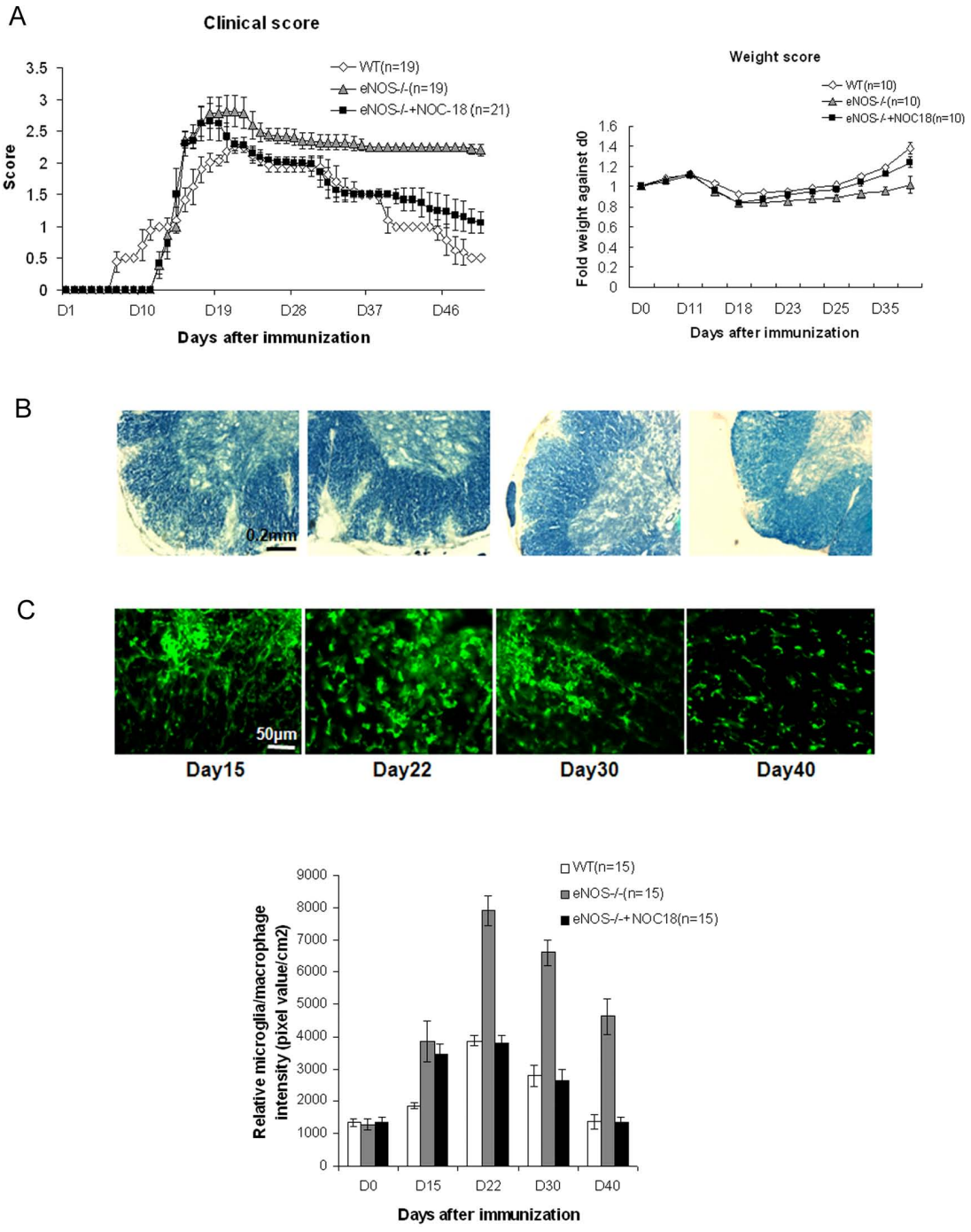
A
Clinical score
WT(n=19)
eNOS-/-(n=19)
eNOS-/-+NOC-18 (n=21)
Score
Days after immunization
Weight score
WT(n=10)
eNOS-/-(n=10)
eNOS-/-+NOC18(n=10)
Fold weight against d0
Days after immunization
B
0.2mm
C
50μm
Day15
Day22
Day30
Day40
WT(n=15)
eNOS-/-(n=15)
eNOS-/-+NOC18(n=15)
Relative microglia/macrophage intensity (pixel value/cm2)
Days after immunization

Figure III-6D-E: Therapeutic administration of an NO donor is beneficial in the recovery phase for eNOS$^{-/-}$ mice.

(D). BBB breakdown was assessed by immunofluorescent staining of the tight junction protein occludin in eNOS$^{-/-}$ mice supplemented with NOC-18. These mice showed diffused occludin staining from day 15 through day 22, but with almost complete BBB restoration by day 30. (E). Nitrite production during EAE, measured as described in Methods. Statistical analysis was performed using one-way ANOVA followed by a Bonferroni-Dunn test for multiple comparisons within each timepoint. *$p < 0.05$ indicates significant difference in nitrite production, **$p < 0.01$ and ***$p < 0.001$ indicates very significant difference in nitrite production. Within each genotype or treatment (i.e. WT mice, eNOS$^{-/-}$ mice and eNOS$^{-/-}$ mice infused with NOC-18), one-way ANOVA was conducted and followed by a Bonferroni-Dunn test for multiple comparisons for all timepoints versus control (day 0). $^{\#}p < 0.05$ indicates significant difference in nitrite production, $^{\#\#}p < 0.01$ and $^{\#\#\#}p < 0.001$ indicates very significant difference in nitrite production.

D

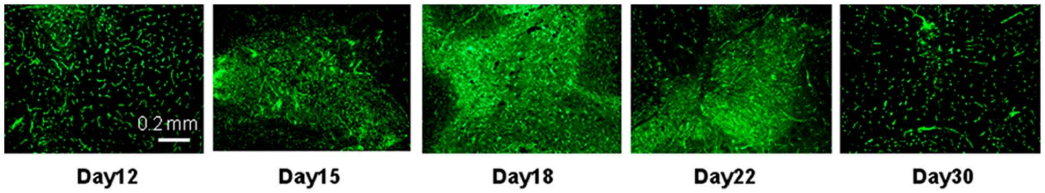
0.2 mm
Day12
Day15
Day18
Day22
Day30

E

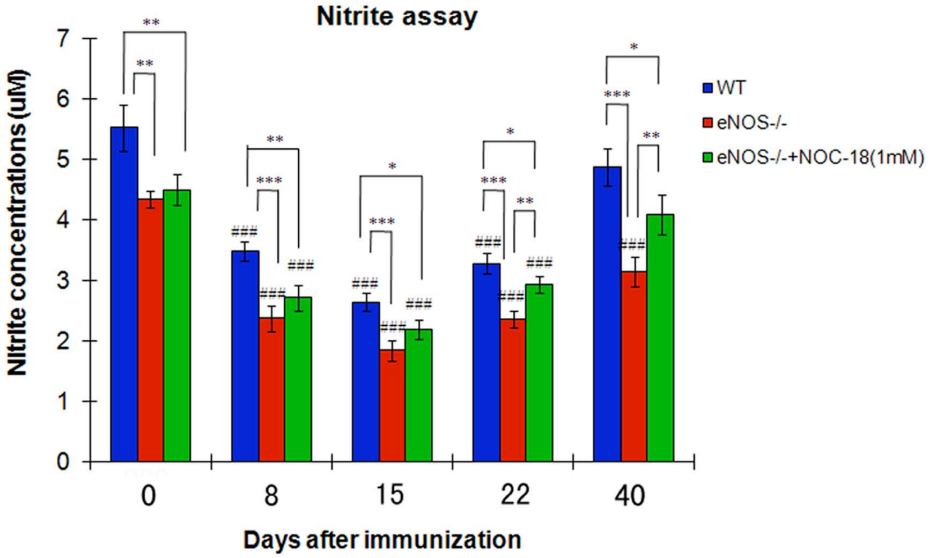
Nitrite assay
Nitrite concentrations (uM)
Days after immunization
0
8
15
22
40
WT
eNOS-/-
eNOS-/-+NOC-18(1mM)

Figure III-7: iNOS$^{-/-}$ mice exhibit exaggerated disease severity and limited recovery.

(A). Clinical course of EAE. Wild-type (WT) and iNOS$^{-/-}$ mice were injected with MOG_{35-55} peptide in CFA and pertussis toxin to induce EAE. The disease severity was scored on a clinical scale from 0 to 5 as described in Experimental Procedure. (B). Weight score of WT and iNOS$^{-/-}$ mice during EAE (Experiment has been repeated three times. Cumulative data was provided; total number of animals tested, n=20/genotype).

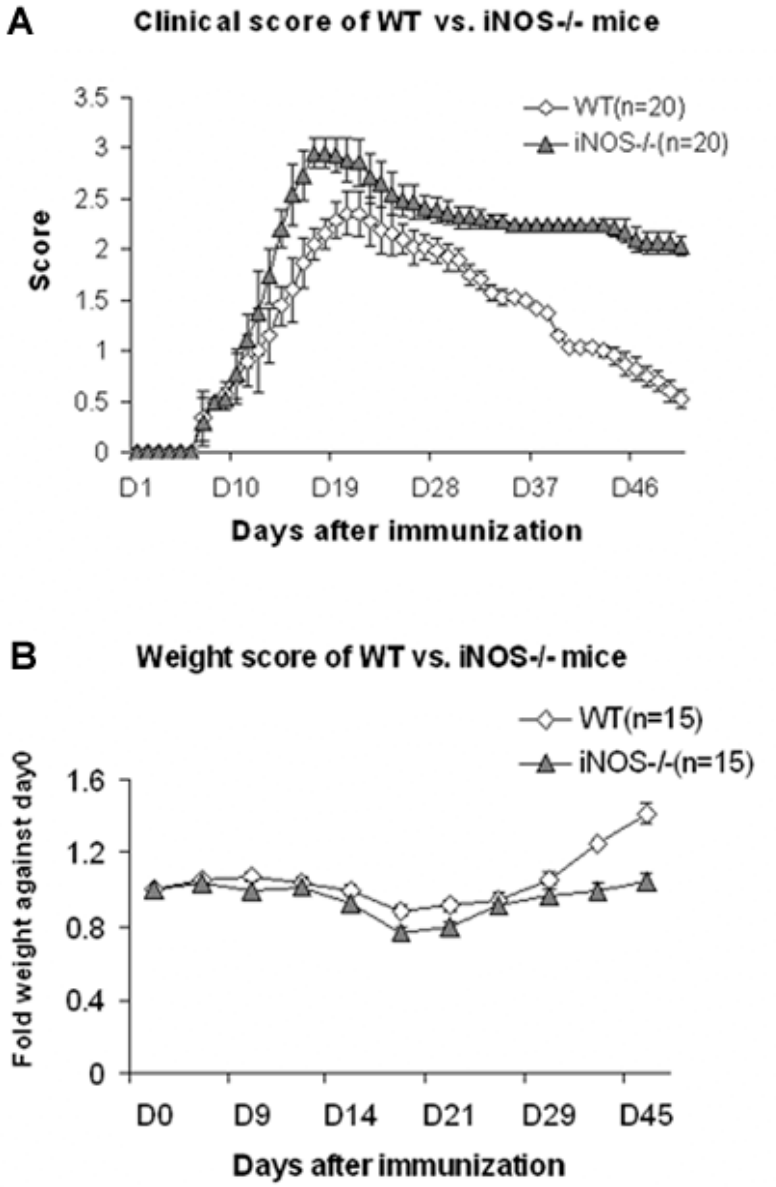
A
Clinical score of WT vs. iNOS-/- mice
WT(n=20)
iNOS-/-(n=20)
Score
3.5
3
2.5
2
1.5
1
0.5
0
D1
D10
D19
D28
D37
D46
Days after immunization
B
Weight score of WT vs. iNOS-/- mice
WT(n=15)
iNOS-/-(n=15)
Fold weight against day0
1.6
1.2
0.8
0.4
0
D0
D9
D14
D21
D29
D45
Days after immunization

Figure III-8A: iNOS$^{-/-}$ mice showed altered pathological hallmarks during EAE.

(A). Frozen cross-sections of spinal cords isolated from WT and iNOS$^{-/-}$ mice at different time points during the EAE course were stained with Eriochrome cyanine (EC) to assess demyelination pattern. (Experiment has been repeated three times**.** In total five mice were assessed for immunostaining each timepoint per genotype, representative data were provided.)

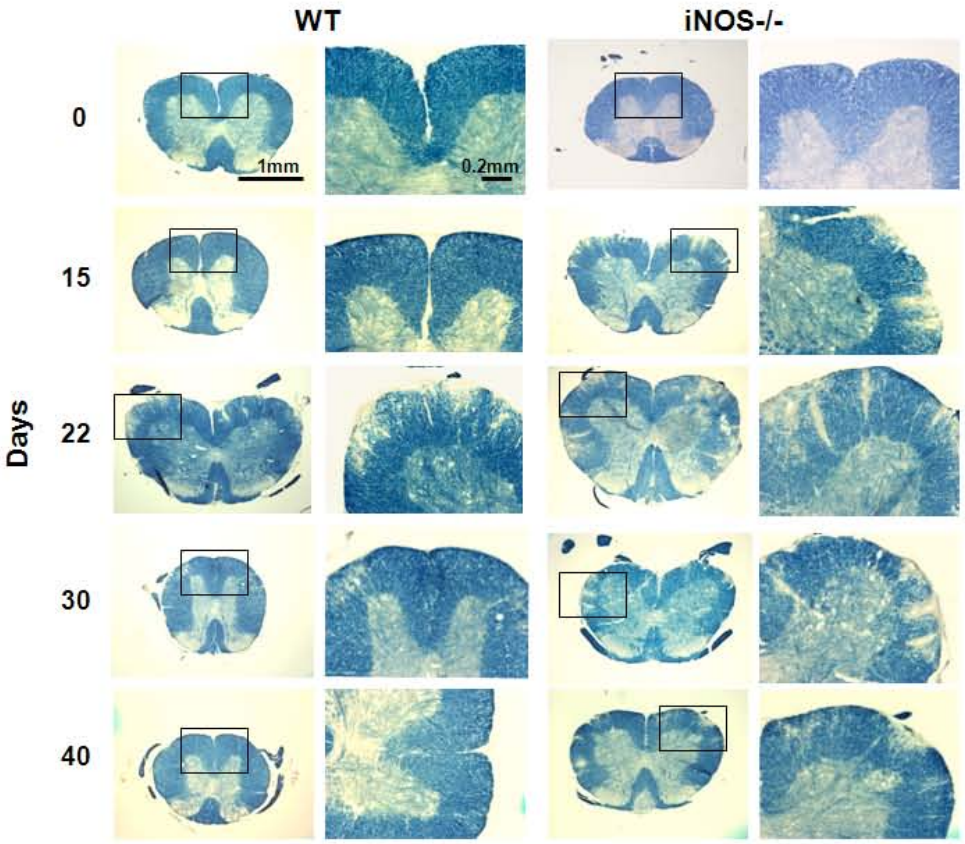
WT
iNOS-/-
Days
0
15
22
30
40
1mm
0.2mm

Figure III-8B: iNOS$^{-/-}$ mice showed altered pathological hallmarks during EAE.

(B). Spinal cord sections were stained with anti-Iba1 to detect microglia/macrophages. Iba1 is expressed on both resting and activated microglia, which can be distinguished by their morphological appearance. Resting microglia (e.g. as seen in Day 0 panel), are characterized by long, thin cell bodies. Activated microglia (e.g. as seen in Day 22 and 30 panels) are characterized by thicker, rounded cell bodies and multi-branched cellular protrusions. (Experiment has been repeated three times**.** In total five mice were assessed for immunostaining each timepoint per genotype, representative data were provided.)

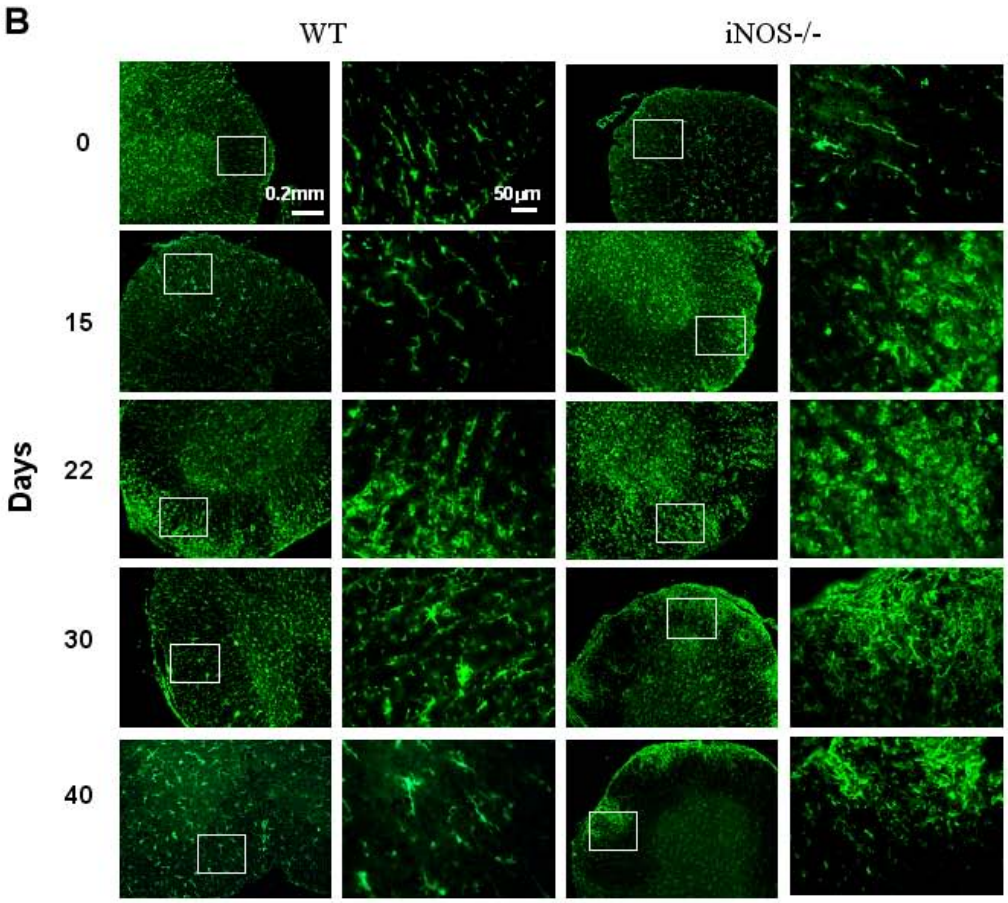
B
WT
iNOS-/-
Days
0
15
22
30
40
0.2mm
50μm

Figure III-9: Providing nitric oxide using an NO donor is beneficial for recovery in iNOS$^{-/-}$ mice.

(A). Clinical course and weight score in iNOS$^{-/-}$ mice infused with NOC-18 pumps. (Experiment has been repeated three times. Cumulative data was provided; total number of animals tested: n=20/wild-type mice infused with PBS, n=20/iNOS$^{-/-}$ mice infused with PBS, n=20/iNOS$^{-/-}$ mice infused with NOC-18) (B). Eriochrome cyanine (EC) staining to assess demyelination in spinal cords of iNOS$^{-/-}$ mice supplemented with NOC-18. (C). Anti-Iba1 staining to show extent of microglia/macrophage infiltration and activation in iNOS$^{-/-}$ mice supplemented with NOC-18. (At least four mice were assessed each timepoint per genotype for both EC staining and Iba-1 staining; representative data were provided.)

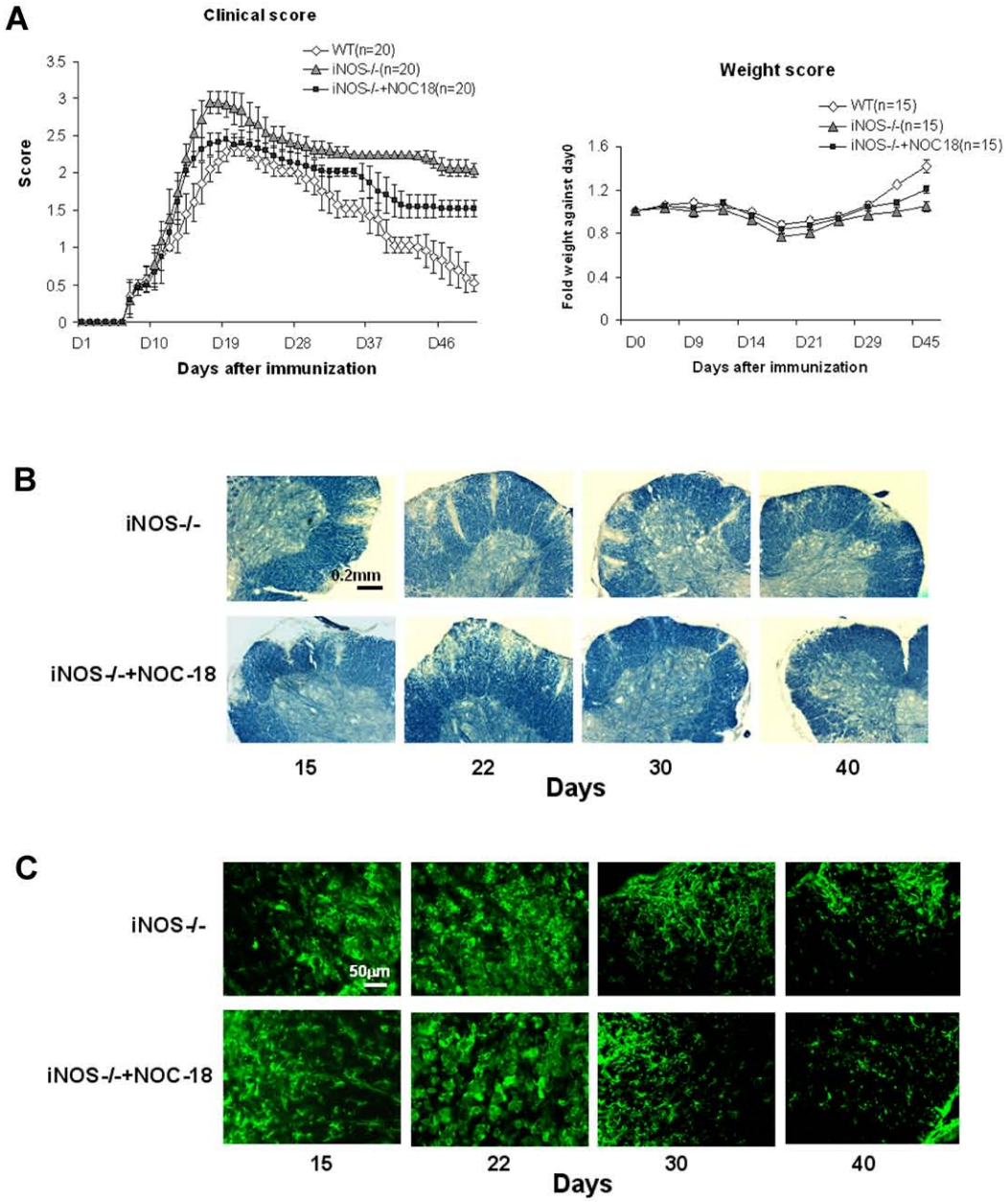
A
Clinical score
WT(n=20)
iNOS-/-(n=20)
iNOS-/-+NOC18(n=20)
Score
Days after immunization
Weight score
WT(n=15)
iNOS-/-(n=15)
iNOS-/-+NOC18(n=15)
Fold weight against day0
Days after immunization
B
iNOS-/-
iNOS-/-+NOC-18
0.2mm
15
22
30
40
Days
C
iNOS-/-
iNOS-/-+NOC-18
50μm
15
22
30
40
Days

Figure III-10: nNOS$^{-/-}$ mice exhibit delayed EAE onset followed by exaggerated disease severity and limited recovery.

Wild-type (WT) and nNOS$^{-/-}$ mice were injected with MOG_{35-55} peptide in CFA and pertussis toxin to induce EAE. The disease severity was scored on a clinical scale from 0 to 5 as described in Experimental Procedure. (Experiment has been repeated twice. Cumulative data was provided; total number of animals tested, n=10/genotype)

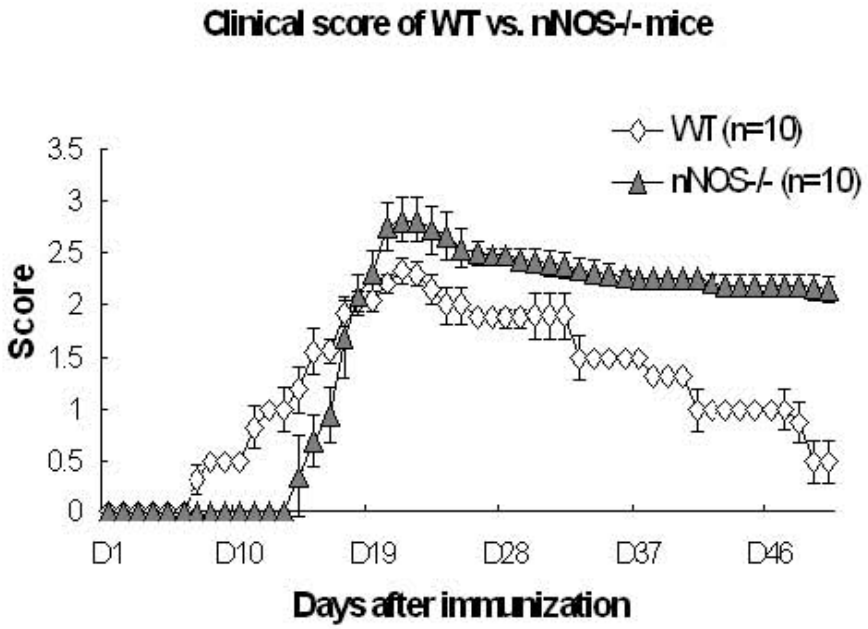
Clinical score of WT vs. nNOS-/- mice
WT (n=10)
nNOS-/- (n=10)
Score
3.5
3
2.5
2
1.5
1
0.5
0
D1
D10
D19
D28
D37
D46
Days after immunization

Figure III-11: Blocking NO production using NMMA in wild-type mice exacerbated the progression of EAE.

(A). Clinical course of EAE. Wild-type (WT) were infused with global NO production inhibitor NMMA and PBS on day 1 after MOG immunization. The disease severity was scored on a clinical scale from 0 to 5 as described in Experimental Procedure. (B). Weight score of EAE. (Experiment has been repeated three times. Cumulative data was provided; total number of animals tested, n=20/PBS infused wild-type mice, n=18/NMMA infused wild-type mice).

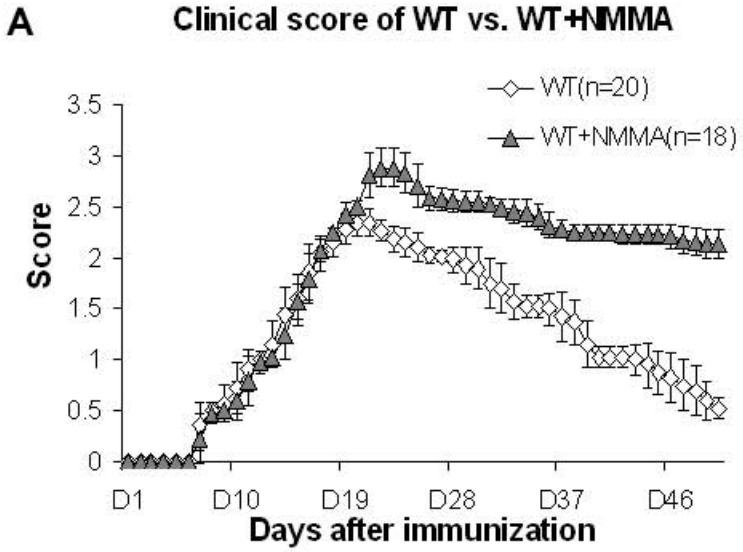
A
Clinical score of WT vs. WT+NMMA
WT(n=20)
WT+NMMA(n=18)
Score
3.5
3
2.5
2
1.5
1
0.5
0
D1
D10
D19
D28
D37
D46
Days after immunization

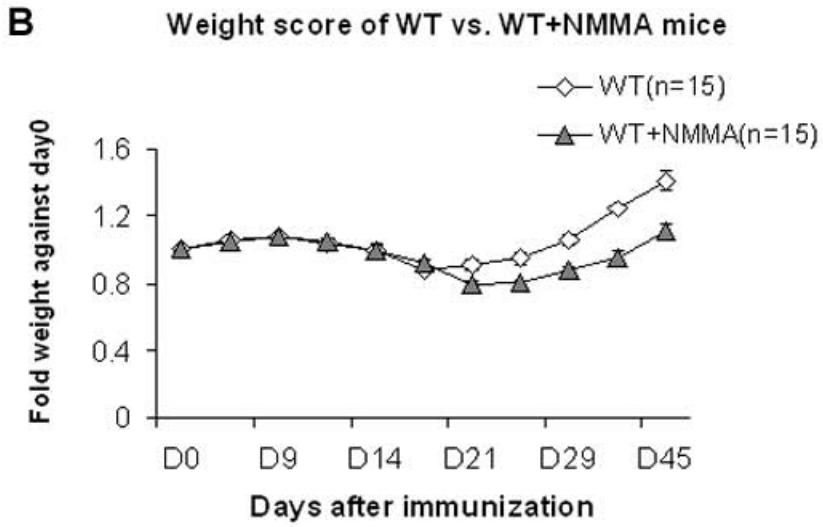
B
Weight score of WT vs. WT+NMMA mice
WT(n=15)
WT+NMMA(n=15)
Fold weight against day0
1.6
1.2
0.8
0.4
0
D0
D9
D14
D21
D29
D45
Days after immunization

Figure III-12A: Altered pathological hallmarks in the wild-type mice infused with NMMA during EAE.

(A). Frozen cross-sections of spinal cords isolated from NMMA and PBS infused wild-type mice at different time points during the EAE course were stained with Eriochrome cyanine (EC) to assess demyelination pattern. (Experiment has been repeated three times**.** In total five mice were assessed for immunostaining each timepoint per genotype, representative data were provided.)

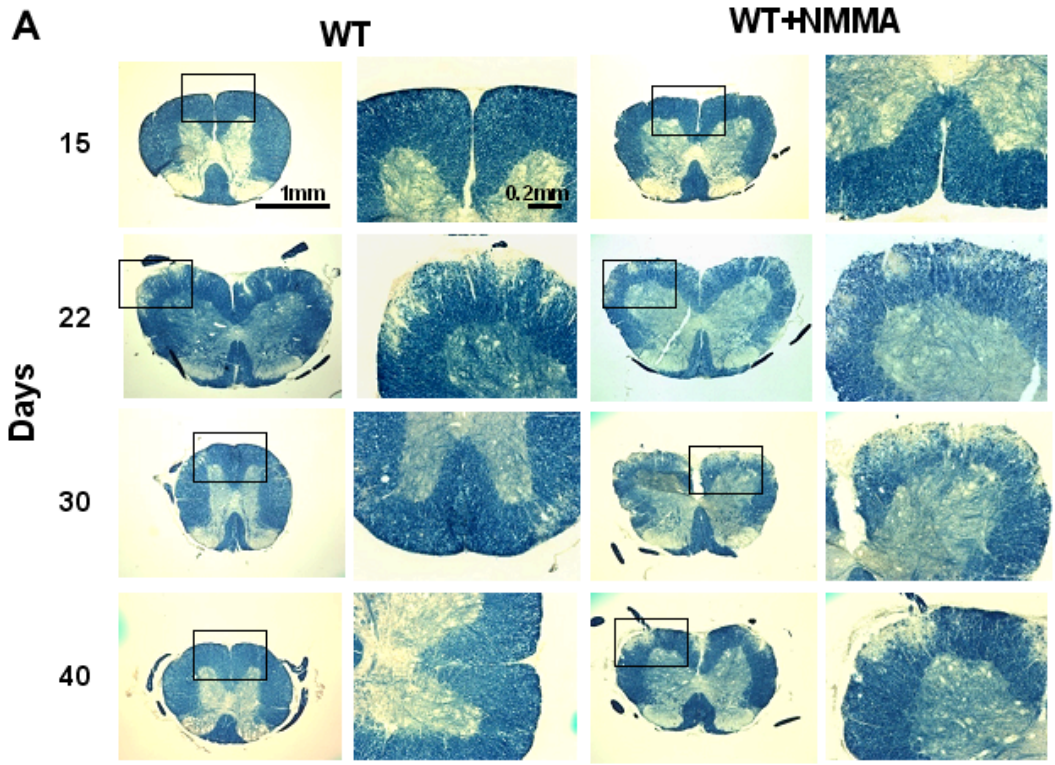
A
WT
WT+NMMA
Days
15
22
30
40
1mm
0.2mm

Figure III-12B: Altered pathological hallmarks in the wild-type mice infused with NMMA during EAE.

(B). Spinal cord sections were stained with anti-Iba1 to detect microglia/macrophages. Iba1 is expressed on both resting and activated microglia, which can be distinguished by their morphological appearance. Resting microglia (e.g. as seen in Day 0 panel), are characterized by long, thin cell bodies. Activated microglia (e.g. as seen in Day 22 panel) are characterized by thicker, rounded cell bodies and multi-branched cellular protrusions. (Experiment has been repeated three times**.** In total five mice were assessed for immunostaining each timepoint per genotype, representative data were provided.)

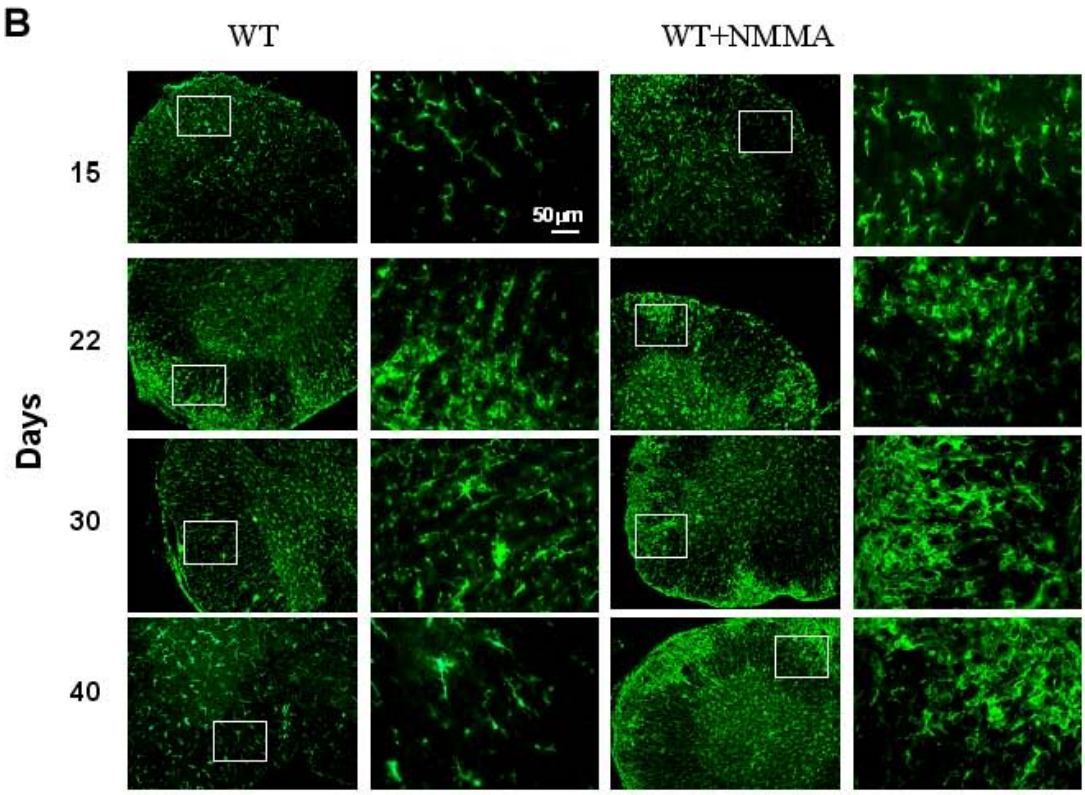
B
WT
WT+NMMA
15
22
30
40
Days
50μm

Table III-1. Summery of clinical course and pathological markers in NOS deficient mice, NOS deficient mice infused with NOC-18, and wild-type mice infused with NMMA.

Behavior/timing/ pathology / Genotype	Clinical score			Pathological markers	
	Onset	*Peak*	*Recovery*	*Demyelination pattern (EC staining)*	*Infiltration and activation of microglia (iba1 immunosteining)*
Wild-type	Day 7	Day 21	Around day 40	Progressive DM with almost complete RM	Peak day 21, then decrease
Wild-type + NMMA			Chronic disease, limited recovery	Severe DM, minimal RM	extensive, sustained
eNOS$^{-/-}$	Day 12 (delayed)	Day 19	Chronic disease, limited recovery	Early and severe DM, minimal RM	Early, extensive, sustained
eNOS$^{-/-}$ + NOC-18			Enhanced recovery	Enhanced RM	Decreased
iNOS$^{-/-}$	Day 7	Day 19	Chronic disease, limited recovery	Early and severe DM, minimal RM	Early, extensive, sustained
iNOS$^{-/-}$ + NOC-18			Enhanced recovery	Enhanced RM	Decreased
nNOS$^{-/-}$	Day 15 (delayed)	Day 19	Chronic disease, limited recovery	Early and severe DM, minimal RM	Early, extensive, sustained

Chapter IV

The effects of nitric oxide on microglia and T cell properties *in vitro*

Introduction

MS/EAE is a T helper 1 (Th1) cell-mediated autoimmune disease. Th1 cells can infiltrate the compromised BBB and enter the CNS, where they encounter the myelin antigens presented by microglia and become activated. The activated T cells then initiate an inflammatory cascade, during which they proliferate, produce both pro- and anti-inflammatory cytokines and chemokines which can affect the CNS; in addition, T cells can activate microglia, and cause recruitment of macrophages to the CNS.

Microglia/macrophages are the major inflammatory cells during MS/EAE; they become activated and are recruited to the lesion site. However, it has not been clear whether microglial activation contributes to neurotoxicity or neuroprotection. Most likely, microglia can be both protective and neurodegenerative; the timing and strength of their activity determine which of these effects is expressed. As antigen-presenting cells, microglia secrete chemokines and adhesion molecules, and further recruit T cells (Cannella and Raine, 1995). Microglia can produce pro-inflammatory cytokines (i.e. TNFα) and oxygen reactive species (i.e. NO), which can damage the oligodendrocytes and myelin sheath. Microglia can also produce anti-inflammatory cytokines, such as IL10 and TGFβ, which suppress EAE (Rott et al., 1994) and promote tissue repair (Kreutzberg, 1996).

There are three subtypes of Th cells (Th1, Th2 and Th17 cells) that participate during MS/EAE. Th1 cells produce proinflammatory cytokines such as TNFα, IFN-γ, and IL6, which contribute to the development of inflammatory response, while Th2 cells secrete

anti-inflammatory cytokines such as IL4, IL10 and TGFβ, which play a role suppressing activation of the immune system. Th17 cells primarily secrete the cytokine IL17. The balance between the Th1 and Th2 response determines the status of the immune system, thus either promoting or preventing the development of MS/EAE.

In the previous chapter I presented results that NO can play deleterious and protective roles during the development and progression of EAE. In this chapter, I investigate the effects of NO on microglia and T cells, which are the major effector cell types during MS/EAE. Previous literature showed that NO plays a role in nerve repair and recovery from injury by modulating accumulation of microglia in the lesion areas (Chen et al., 2000). In the studies presented here, I cultured primary microglia from wild-type mouse brain and evaluated the proliferation rate and cytokine profiles of microglia after NO treatment. NO has been found to interfere with the T cell mediated inflammatory cascade: NO can influence T cell proliferation, modulate the expression of adhesion molecules, affect T cell apoptosis, and change the balance between Th1 and Th2 cytokine production. I isolated primary T cells from wild-type mouse spleen, and measured T cell properties in response to NO donor (NOC-18) treatment. I proposed that by modulating the properties of microglia and T cells, NO can affect the outcome of the immune response during EAE. These findings will provide further insights into the underlying mechanisms of the NO effect during MS/EAE.

Results

Effects of NO on T cell properties

NO affects T cell proliferation rate in a dose-dependent manner

Primary T cells from wild-type mouse spleen were cultured, as described in Methods. Anti-CD3 antibody was used to coat the tissue culture plate to activate the T cells, and NOC-18 in a gradient of concentrations was added to the culture. BrdU assay was performed to measure the T cell proliferation rate after 72 hours incubation. Fig. IV-1 shows that NOC-18 affects T cell proliferation in a dose-dependent manner. CD3 alone activates T cells and promotes T cell proliferation. Low levels of NOC-18 further increase the proliferation rate of T cells (T cells incubated with 100 μM NOC-18 proliferate 1.3 fold more than CD3-treated controls; T cells treated with 200 μM NOC-18 proliferate approximately 1.8 fold more than the control group). In contrast, high levels of NOC-18 (500 μM) decreased the T cell proliferation rate by 20% of that of the control group.

NO modulates T cell cytokine profiles

The next question addressed was whether NO modified the T cell cytokine profiles by affecting the production of Th1 and Th2 cytokines. T cells were incubated with multiple concentrations of NOC-18 for 72 hours. ELISA assays were performed to evaluate the

levels of Th2 cytokines IL4 and IL-10, and Th1 cytokine TNFα (Fig. IV-2). CD3 alone activates T cells and elevates the production of all three cytokines compared to the untreated group. Providing NO (with NOC-18) did not have significant effect on TNFα production, however, the levels of both IL-4 and IL-10 increased after treatment with 100μM and 200μM NOC-18 (they increased 2 fold with 200μM NOC-18 treatment). The levels of IL-4 and IL-10 decreased after treatment with 500μM NOC-18. These results suggested that low levels of NO can induce an up-regulated Th2-response.

NO promotes apoptosis of T cells

Previous reports suggested that NO may act as an anti-inflammatory factor by promoting apoptosis of T cells. T cell apoptosis was measured using TUNEL assay (Fig. IV-3A). Both untreated and only CD3 antibody-treated cultures showed minimal numbers of apoptotic T cells. However, the number of TUNEL-positive cells increased in cultures that had been treated with NOC-18. High levels of NOC-18 treatment resulted in increased numbers of apoptotic T cells.

Effects of NO on the properties of microglia

NO exerts no significant effect on microglial proliferation

Primary microglia were isolated from wild-type mouse brain, as described in Methods. 100ng/ml lipopolysaccharide (LPS) was added in the culture to activate microglia, and a gradient of concentrations of NOC-18 were added to the culture. After 10 hours incubation, BrdU assay was performed to measure the microglial proliferation rate (Fig. IV-4). LPS alone activated microglia and promoted the microglial proliferation rate compared to untreated group, in agreement with the literature. However, adding NOC-18 had no additional effect on the microglial proliferation rate; they showed comparable proliferation rate as the LPS alone treated group.

NO does not affect microglial cytokine profiles

Next we asked whether NOC-18 can modulate microglial cytokines profiles. 100ng/ml LPS and multiple concentrations of NOC-18 were added to the primary microglial culture. After 10 hours incubation, ELISA assays were performed to quantify the production of Th2 cytokine IL-10, and Th1 cytokine TNFα secreted by microglia (Fig. IV-5). LPS treatment activated microglia and caused an upregulation of the production of both IL10 and TNFα. However, the addition of NOC-18 has no significant effect on either cytokine production.

Discussion

Both microglia and T cells play important roles during the inflammatory cascade in MS/EAE. In the previous chapter, I showed that NO has protective effect during the recovery period of EAE, and early damaging roles in a cellular-source dependent manner. In an effort to determine the underlying mechanism of NO functions during EAE, I proposed that NO may affect the properties of immune cells such as microglia and T cells, which further modulate the outcome of MS/EAE. In this chapter, I examined the roles of NO on microglia and T cells in culture. The results showed that NO affected the T cell properties in a dose-dependent manner. Low levels of NO (100 μM, 200 μM) increased T cell proliferation, and caused up-regulation of anti-inflammatory cytokines IL10, IL4 production; while high levels of NO (500 μM) decreased T cell proliferation rate, and inhibited the production of IL10 and IL4. The results suggested that low levels NO promoted the anti-inflammatory properties of T cells, and potentially favored Th2 cell development. Under the treatment of low doses of NO, T cells are driven to the Th2 cell fate, and in the mean time, low levels of NO can increase T cell proliferation, thus boosting the Th2 response. High levels of NO treatment, however, inhibit the anti-inflammatory properties of T cells, suggesting a dominant Th1 response. Adding high doses of NO decreased the T cell proliferation rate, potentially confining the pro-inflammatory response. Taken together, both low and high levels of NO are potentially protective during MS/EAE, by modulating T cell properties, either to promote anti-inflammatory responses or to contain pro-inflammatory responses.

Next I determined the role of NO in affecting T cell apoptosis. The results showed that NO promoted T cell apoptosis in a dose-dependent manner. I also examined the effects of NO on primary microglia. The results showed that NO had no significant effect on microglia proliferation or cytokine production. Then I asked, whether NO could affect microglia apoptosis. In Fig. III-4A and Fig. III-8B, NOS deficient mice ($eNOS^{-/-}$ and $iNOS^{-/-}$ mice) showed accumulation of activated microglia/macrophages in spinal cord white matter on day 22 (peak of disease), which continued until day 40 (recovery period). This activation pattern of microglia/macrophages was consistent with the sustained symptoms in these mice. It has been reported that NO can eliminate the inflammatory cells by promoting their apoptosis. We then hypothesized that it might be because of the lack of NO in the NOS deficient mice, which caused deficiency in clearing the inflammatory cells out of the lesion site, such as microglia/macrophages. Further studies may focus on the role of NO on microglia apoptosis both in culture and *in vivo*.

Figure IV-1: The effect of NO on T cells proliferation.

BrdU-based cell proliferation assays were performed to evaluate the proliferation of T cells. n = 4, a two-tailed t-test was used for comparisons between experimental groups and CD3 alone treated group. *, $p<0.05$.

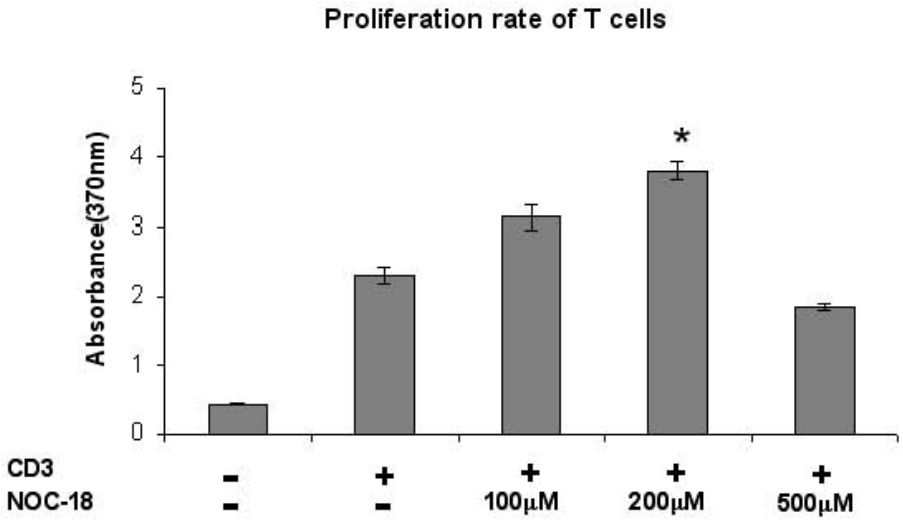
Proliferation rate of T cells
Absorbance(370nm)
5
4
3
2
1
0
*
CD3
NOC-18
-
-
+
-
+
100μM
+
200μM
+
500μM

Figure IV-2: The effect of NO on T cells cytokines production.

ELISA assays were performed to evaluate the proinflammatory cytokine TNFα (A), anti-inflammatory cytokine IL-10 (B) and IL4 (C) produced by T cells. n = 4, a two-tailed t-test was used for comparisons between experimental groups and CD3 alone treated group. *, $p<0.05$; **, $p<0.01$.

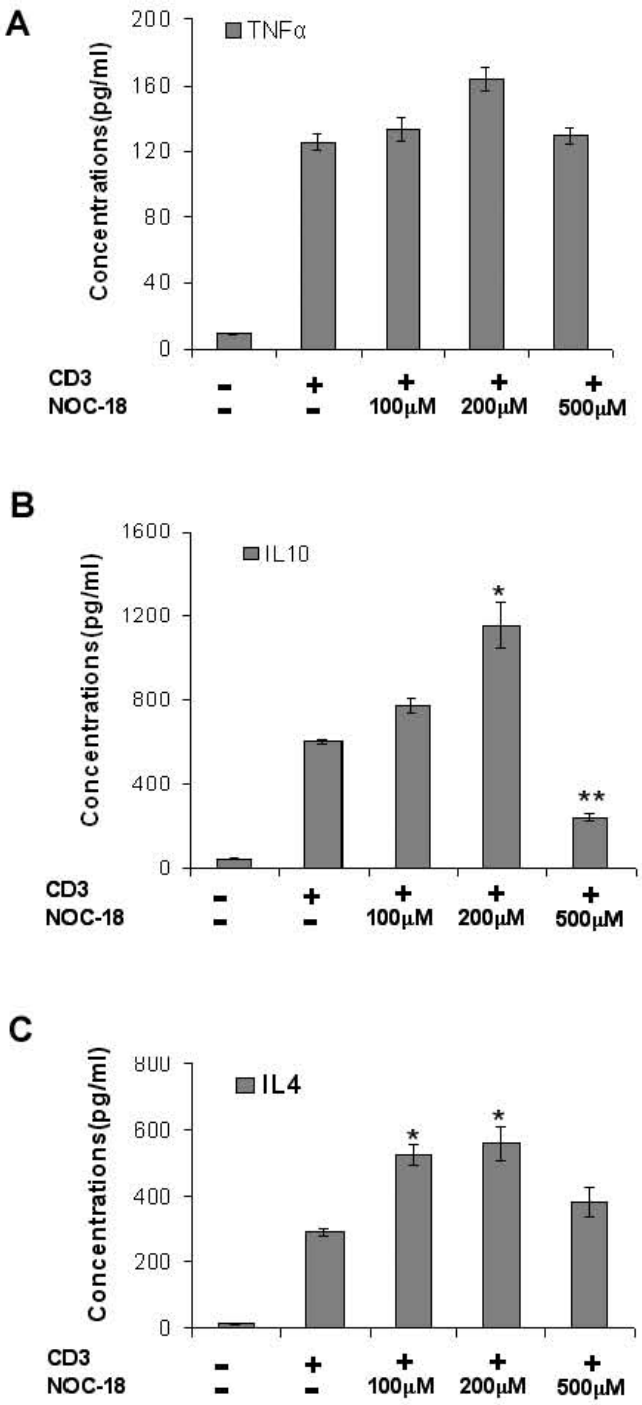
A
TNFα
Concentrations(pg/ml)
200
160
120
80
40
0
CD3
NOC-18
-
-
+
-
+
-
+
100μM
+
200μM
+
500μM
B
IL10
Concentrations(pg/ml)
1600
1200
800
400
0
*
**
CD3
NOC-18
C
IL4
Concentrations(pg/ml)
800
600
400
200
0
*
*
CD3
NOC-18

Figure IV-3: The effect of NO on apoptosis of T cells.

(A), T cell apoptosis was measured using TUNEL assay. (B), Quantification of the percentage of TUNEL-positive T cells out of CD3-positive cells. *, $p<0.05$; **, $p<0.01$.

A

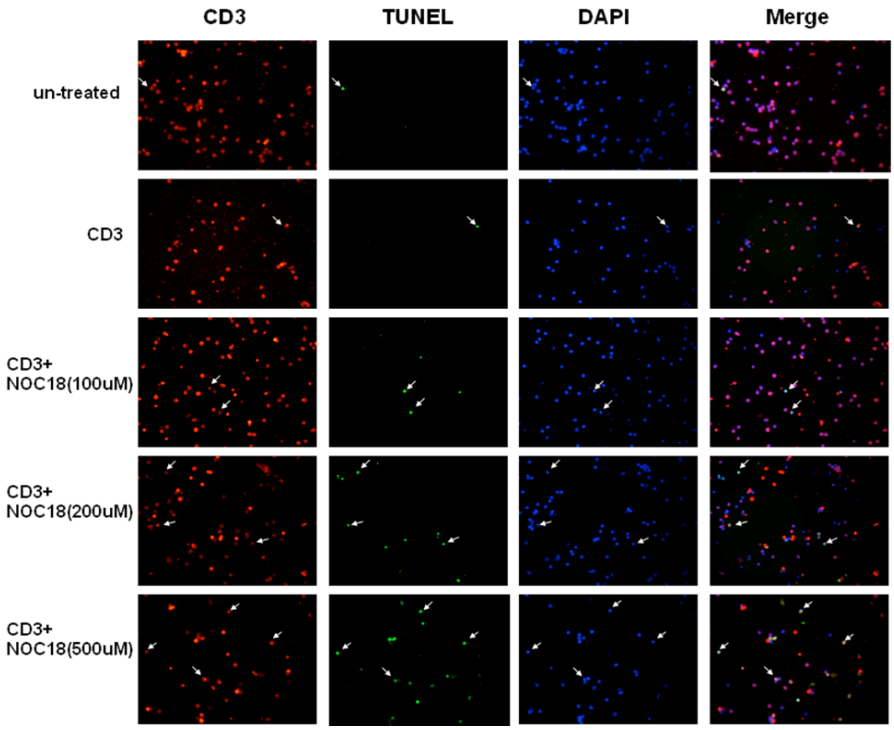
CD3
TUNEL
DAPI
Merge
un-treated
CD3
CD3+ NOC18(100uM)
CD3+ NOC18(200uM)
CD3+ NOC18(500uM)

B

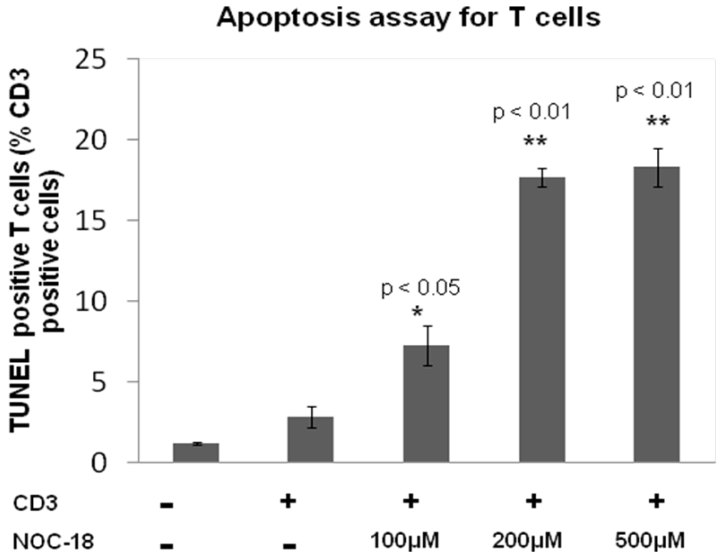
Apoptosis assay for T cells
TUNEL positive T cells (% CD3 positive cells)
25
20
15
10
5
0
p < 0.05
*
p < 0.01
**
p < 0.01
**
CD3 - + + + +
NOC-18 - - 100μM 200μM 500μM

Figure IV-4: NO has no significant effect on microglia proliferation.

BrdU-based cell proliferation assay was performed to assess the proliferation of T cells. n = 3.

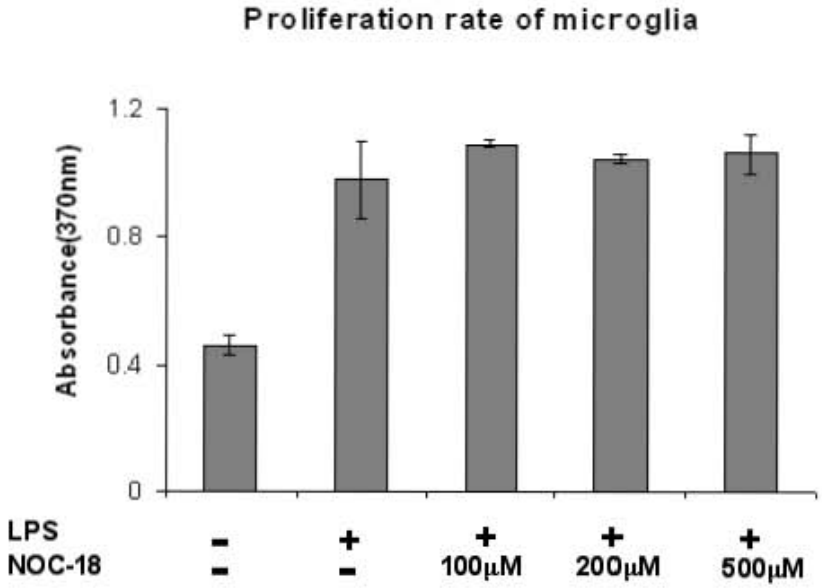
Proliferation rate of microglia
Absorbance(370nm)
1.2
0.8
0.4
0
LPS
NOC-18
-
-
+
-
+
100μM
+
200μM
+
500μM

Figure IV-5: The effect of NO on microglia cytokines production.

ELISA assay were performed to evaluate the proinflammatory cytokine TNFα (A), anti-inflammatory cytokine IL-10 (B) produced by microglia. n = 3.

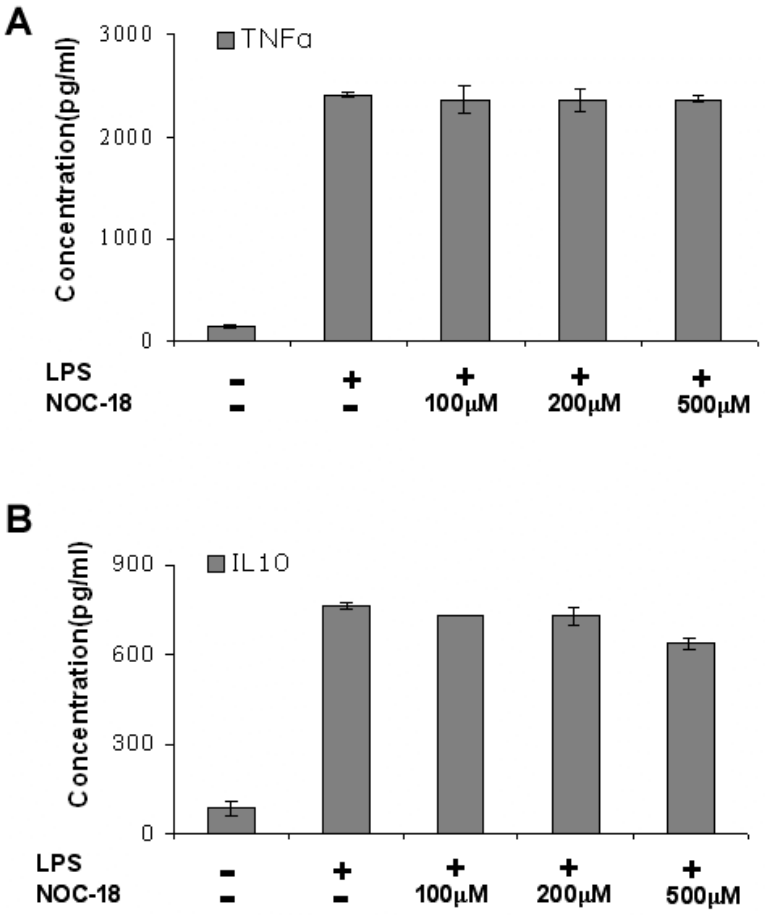
A
TNFa
Concentration(pg/ml)
3000
2000
1000
0
LPS
NOC-18
-
-
+
-
+
100μM
+
200μM
+
500μM
B
IL10
Concentration(pg/ml)
900
600
300
0
LPS
NOC-18
-
-
+
-
+
100μM
+
200μM
+
500μM

Chapter V

Tuftsin (TKPR) attenuates disease symptoms in Experimental Autoimmune Encephalomyelitis (EAE): a switch to anti-inflammatory responses

Introduction

T cells and microglia/macrophages contribute to the pathogenesis of MS/EAE by mediating inflammatory cascade. MS/EAE is a T helper 1 cell-mediated autoimmune disease, during which a lot of pro-inflammatory cytokines are generated, such as TNFα and IFNγ. Recovery in MS/EAE is normally promoted by T helper 2 cells and regulatory T cells, which produce anti-inflammatory cytokines, such as IL10 and TGFβ. The balance between the pro- and anti-inflammatory responses determines the outcome of disease.

Protective autoimmunity, a hypothesis formulated by Dr Michal Schwartz's group, suggests that in the CNS autoimmunity is not only an outcome of immune system malfunction, but rather it is the body's own protective mechanism against destructive self-compounds (Schwartz and Kipnis, 2005). Early activation of microglia could then ameliorate the disease by presenting antigen to T helper cells and subsequently coordinating the resulting adaptive immune response, thus inducing protective autoimmunity. Shaked et al. have shown in a model of optic nerve crush injury that earlier onset of phagocytic activity and antigen presentation by microglia results in resistance to injury and neuronal survival, and this is due to the fact that the early activation of microglia can modulate the adaptive immune response and thus promote the secretion of neurotrophic factors from T cells (Shaked et al., 2004).

Tuftsin is a naturally occurring tetrapeptide, which promotes phagocytic activity for cells of monocytic origin, such as neutrophils, macrophages and microglia, all of which

express tuftsin receptors. Subsequent reports indicated that tuftsin or tuftsin-like peptides exert multiple stimulatory effects on a subset of immunologic effector cells, including enhanced migration/chemotaxis, enhanced phagocytotic activity and antigen presentation (Siemion and Kluczyk, 1999). Additionally, tuftsin is reported to have effects on the nervous system, including induction of analgesia (Herman et al., 1981), and inhibition of axonal regeneration in a model of optic nerve transection (Thanos et al., 1993).

Previous work in our laboratory revealed that modification of the status of microglia affected the timing and symptoms of EAE (Bhasin et al., 2007). In particular, tuftsin decreased the severity of EAE symptoms and drastically improved recovery in wild-type mice. Real-time PCR showed that wild-type EAE mice exhibited a prevalent T-bet (transcription factor driving the expression of Th1 cytokines) presence, while tuftsin infusion resulted in a shift towards an increased GATA3 (transcription factor of Th2 cytokines) expression. I proposed that early activation of microglia with tuftsin ameliorated EAE by recruiting and interacting with the adaptive immune response, rather than worsening it, and by potentially inducing protective autoimmunity. In this chapter, I used both *in culture* and *in vivo* methods to investigate the mechanism by which tuftsin can modulate the immune response in the MOG-induced EAE model. The results showed that *in culture*, modulating microglia activity with tuftsin affected T cell responses by down-regulating the Th1 response and up-regulating anti-inflammatory cytokines. *In vivo*, tuftsin infusion promoted development of type II Th cells, and favored expansion of Tregs. Moreover, adoptive transfer of tuftsin-modulated T cells reversed clinical signs of disease in mice with established EAE.

Results

Modulating microglia activity with tuftsin switched T cell phenotypes *in culture*

Tuftsin-infused wild-type mice showed a shifted immune response towards an anti-inflammatory phenotype (Bhasin et al., 2007). I proposed that modulation of microglia activation with tuftsin can affect the immune system by modifying the T cell phenotypes. However, there is a possibility that tuftsin may exert a direct effect on T cells. I investigated these two hypotheses using primary cell cultures.

To test the direct effect of tuftsin on T cells, I cultured primary T cells isolated from wild-type mouse spleens, as described in Methods. MOG peptide was used to prime T cells, then a gradient of concentrations of tuftsin were added to the culture. After 72 hours incubation, supernatants from the T cell culture were collected, and ELISA assays were performed to determine the production of the Th1 cytokine TNFα, and the Th2 cytokine IL-10 (Fig. V-1). TNFα levels increased at the higher doses of tuftsin (Fig. V-1A), but there was no significant difference in IL-10 production (Fig. V-1B). Given that TNFα is a proinflammatory cytokine, these findings do not support our previous *in vivo* results, which indicated that tuftsin treatment yields increases in anti-inflammatory factors; I sought, therefore, to examine the indirect effect hypothesis.

To test such an indirect effect of tuftsin on T cells, we set up culture conditions to mimic the *in vivo* tuftsin infusion in the EAE model (Chart. V-1). Neuronal conditioned medium and tuftsin were added to primary microglia to modulate microglia activity. Neuronal conditioned medium (from neurons incubated with 25uM glutamate for 4 hrs)

was used to mimic the early excitotoxic events of EAE (Pitt et al., 2000). After 10 hours incubation, microglia medium was collected and added to primary T cells. 72 hours later the supernatants from the T cell culture were collected after 72 hours. ELISA assays were performed to measure the levels of the Th2 cytokine IL-10, and Th1 cytokine TNFα (Fig. V-2). Microglial medium treated with only neuronal conditioned medium or tuftsin had no significant effect on T cell cytokine production; however, the combined effect of neuronal conditioned medium and tuftsin modulated microglia activity, such that it had a significant effect on TNFα and IL10 levels produced by T cells. TNFα levels decreased with 50ug/ml, 100ug/ml and 150ug/ml tuftsin treatments; in contrast, a significant increase of IL10 production was observed. Microglia also secrete TNFα and IL10. Since microglial medium was added to T cell culture, the cytokines produced by microglia could be considered as factors affecting T cell cytokine levels. ELISA assays were performed on microglia medium after 82 hours (equal to the 10 hours of microglial exposure to NCM, plus 72 hours equal to the T cell exposure to microglial medium) incubation in culture. Both cytokine levels were low (data not shown), so the residual cytokine concentration in the conditioned microglia medium had insignificant effect on T cell cytokine levels.

These in culture experiments suggested that modulating microglia activity with tuftsin under glutamate-stimulation conditions affected T cell phenotype by down-regulating Th1 response while up-regulating Th2 response.

Identification of participating genes in T cells after tuftsin modulation.

To identify genes that are modulated in T cells under these conditions, mouse inflammatory cytokines and receptors arrays were performed on RNA samples isolated from T cells (Chart V-2). Several participating genes were identified (Table V-1). The expressions of the pro-inflammatory cytokine TNFα, and its receptor 1a and 1b were decreased after treatment with NCM plus tuftsin. Expression of several anti-inflammatory cytokines, such as the Th2 type cytokine IL 10 and its receptor alpha and beta, Interleukin 13 (IL13) and Interleukin 4 (IL4), were significantly up-regulated after treatment with NCM plus tuftsin. Transforming growth factor beta 1 (TGFβ1) functions as an anti-inflammatory cytokine; it is also a cytokine stimulus for Th17 and T regulatory cell generation. Our data showed a significant up-regulation of TGFβ1 expression after NCM and tuftsin treatment. The expression of CCR3, a chemokine receptor that has been reported to mediate the recruitment of Th2 cells, was also up-regulated. CCR5, which is reportedly expressed primarily by Th1 cells, was up-regulated as well after NCM plus tuftsin treatment. There was also an up-regulation of interferon γ (IFN γ), which has been regarded as a pro-inflammatory cytokine in EAE, but described with anti-inflammatory properties too, as IFN-γ knockout mice were susceptible to EAE (Ferber et al., 1996). Taken together, the PCR array results showed that modulating microglia activity with NCM and tuftsin effectively up-regulated Th2 response and also favored regulatory T cell formation.

Tuftsin infusion promoted the development of type II T cells.

STAT1 is a member of the Signal Transducers and Activators of Transcription family of transcription factors. STAT1 augments production of several pro-inflammatory cytokines (TNF and IL-12), while repressing production of anti-inflammatory cytokines (IL10). STAT1 phosphorylation (activation) is increased in EAE lesions. FoxP3, a regulatory T cell transcription factor, facilitates regulatory T cell lineage commitment by amplifying and stabilizing its own expression and by repressing alternative cell fates. In the presence of TGFβ, naïve T cells convert into FoxP3-expressing Tregs. I evaluated the levels of STAT1 phosphorylation and FoxP3 expression in wild-type mice subjected to MOG-induced EAE, and in mice infused with tuftsin. Mouse spinal cord homogenates were prepared at different time points after MOG immunization. Western blots were performed to examine protein expression. As shown in Fig. V-3, phospho-STAT1 expression increased on days 21 and 30 in PBS infused control mice, which is consistent with the literature that STAT1 phosphorylation (activation) is up-regulated in EAE lesions (Weber et al., 2007). Tuftsin infusion promoted development of type II T cells, characterized by increased secretion of IL10 and IL4. This shift towards the production of anti-inflammatory cytokines was associated with reduced STAT1 signaling in the tuftsin-infused mice. More interestingly, tuftsin infusion also presumably directed differentiation of regulatory T cells, by increasing the expression of the Treg transcriptional factor FoxP3 (Fig. V-3). Taken together, these results suggest that *in vivo*, tuftsin infusion promotes development of type II T cells, and favors expansion of Treg cells.

Tuftsin-modulated T cells reversed clinical symptoms following adoptive transfer in mice with established EAE.

To assess whether the protective effect of tuftsin in EAE was mediated by the tuftsin modulated T cells, I transferred tuftsin-treated T cells into wild-type EAE mice. 5 x 10^6 tuftsin-treated T cells were injected intravenously 14 days after the onset of disease into recipient C57BL/6 mice immunized with MOG. T cells treated with the NCM/tuftsin-modulated microglial medium decreased the clinical signs of EAE, and the disease course paralleled with that of tuftsin infused animals (Fig. V-4). However, T cells treated only with NCM or tuftsin modulated microglial medium resulted in a clinical course similar to that of PBS-infused control mice (Fig. V-4). The results were consistent with our *culture* data, indicating that modulating microglia activation using NCM and tuftsin affected the T cell fate and resulted in attenuated signs of EAE.

Attenuated demyelination pattern in EAE mice adoptively transferred with tuftsin-modulated T cells.

Inflammation and demyelination are two well-defined characteristics of EAE. Eriochrome cyanine (EC) staining was used to detect myelin profiles in mouse spinal cords. The timing of demyelination correlated with the clinical progression (Fig. V-5A). All three groups (PBS-infused wild-type mice, tuftsin-infused wild-type mice, and wild-type mice adoptively transferred with NCM/tuftsin-modulated T cells) showed minimal

demyelination on day 15. During the peak of disease (day 22), PBS-infused wild-type mice showed severe demyelination in spinal cord white matter, as characterized by large areas devoid of EC staining. EAE mice transferred with NCM/tuftsin T cells showed similar demyelination pattern as tuftsin-infused animals; both displayed less severe demyelination, and revealed almost complete remyelination by day 30, while there was still apparent demyelinated areas visible in PBS-infused mice.

Demyelination was also evaluated by FluoroMyelin, a fluorescent myelin stain, for which similar results were obtained (Fig. V-5B). Quantification of the fluorescence intensities (Fig. V-5C) revealed that the extent of demyelination in mice that received the NCM/tuftsin-T cells is comparable to that in tuftsin-infused mice; however, the extent of demyelination was significantly different between mice transferred with T cells alone and control animals.

Adoptive transfer of NCM/tuftsin-modulated T cells decreased microglia/macrophages infiltration and activation in EAE mice.

During EAE infiltrating T cells attack the endogenous myelin. Activated microglia are then recruited to the demyelinated areas and through their phagocytotic activity remove cellular debris (Benveniste, 1997; Diemel, 1998). I evaluated the levels of microglia/macrophage activation at different time-points (Day 15, 22, 30) during EAE, using an antibody against Iba1, which is expressed in resting microglia/macrophages and

becomes upregulated during activation (Fig. V-6A). Iba1 staining on day 15 revealed resting microglia/macrophages in all groups, as defined by the cells' ramified morphology with long thin cell bodies (arrows). On day 22, in PBS-infused wild-type animals high numbers of activated microglia/macrophages were visible in the white matter of spinal cord, with ameboid shape and extensive branches. On day 30, activated microglia/macrophages were still evident in these animals. In contrast, in tuftsin-infused mice and mice with adoptive transfer, microglia became activated on day 22, but cell density was less compared to PBS infused mice. On day 30, the number of Iba1-positive cells decreased with most of the cells re-assuming a resting morphology.

Spinal cord extracts were prepared at different time points during EAE and western blotting was performed to determine Iba1 expression, as a semi-quantitative measure of the extent of microglia/macrophage recruitment and activation (Fig. V-6B). All three groups expressed Iba1 at basal levels on day 15, and the level of Iba1 increased as disease progressed. PBS-infused animals showed a dramatic upregulation of Iba1 levels on day 22, while Iba 1 levels decreased but still remained higher on day30. In contrast, tuftsin-infused mice and mice with adoptive transfer showed lower extent of Iba1 upregulation on day 22, and the expression of Iba1 dropped to basal levels by day 30. These results correlate with the extent of microglia/macrophage activation described in panel A and with the clinical symptoms described earlier.

Neuropilin-1 (Nrp-1) expression is up-regulated after tuftsin infusion

In order to indentify the mechanism of immunomodulatory effect of tuftsin, it is important to determine the binding target/targets of tuftsin. It has been reported that cultured human aortic and umbilical vein endothelial cells express tuftsin receptors and that in these cells the binding target for tuftsin is Nrp-1 (von Wronski et al., 2006). Moreover, Nrp-1 has been found to be present on both microglia and T cells (Agudo et al., 2005; Majed et al., 2006; Tordjman et al., 2002). So I determined the expression of Nrp-1 in spinal cord protein samples after tuftsin infusion. Spinal cord homogenates were collected at multiple time points after EAE induction. Western blot was performed to evaluate Nrp-1 expression. Tuftsin-infused animals showed detectable Nrp-1 expression on day15, and much higher expression on day 22, followed by decreased expression on day 30. In contrast, PBS-infused animals only showed detectable Nrp-1 level on day 30 (Fig. V-7). Nrp-1 has been found to be surface marker of regulatory T cells, and Nrp-1 expression correlates with the expression of FoxP3 (Bruder et al., 2004). This is consistent with our previous results that increased FoxP3 expression was also observed in tuftsin-infused animals, particularly on day 22 (Fig. V-3). This result indicated an involvement of Nrp-1 in the tuftsin-modulated events.

Discussion

In this chapter, I found that *in culture* modulation of microglial activation with tuftsin under glutamate stimulation affected the phenotype of T cells by down-regulating the Th1 response and up-regulating the Th2 response. *In vivo*, tuftsin infusion promoted development of type II Th cells, and favored expansion of Tregs. Moreover, adoptive transfer of (NCM and) tuftsin-modulated T cells reversed clinical symptoms in mice with established EAE. The extent of demyelination and the infiltration and activation of microglia/macrophages were decreased in mice with NCM and tuftsin-modulated T cells adoptive transfer.

Since tuftsin was first identified by Najjar and Nishioka in 1970, it has been studied in the immune and nervous systems. Tuftsin primarily contributes to the function of the immune system. Tuftsin or tuftsin-like peptides exert multiple stimulatory effects on a subset of immunologic effector cells (Siemion and Kluczyk, 1999). Tuftsin deficiency, either hereditary or following splenectomy, results in increased susceptibility to infections. Tuftsin's broad activities on the phagocytotic cells, especially microglia and macrophages, make the peptide a potential candidate for immunotherapy. Tuftsin and its analogs have been chemically synthesized, and applied in clinical studies (Fridkin and Najjar, 1989). The normal tuftsin serum level is 250 – 500 ng/ml. It has been found that tuftsin can destroy several microorganisms at a high concentration of 60 μg/ml. The LD_{50} dose of tuftsin is 2.4 g/kg, which suggests that a serum level of 60 μg/ml is a suitable physiological concentration for applying tuftsin in therapeutic studies. Here we delivered

tuftsin through mini-osmotic pumps at a concentration of 500 μM, with an infusion rate of 0.25 μl/hour. In theory, an infusion of tuftsin with amount of 0.06 μg per hour will be diffused through the length of the whole spinal cord and surrounding tissues, which certainly brings it to a physiological concentration for the therapeutic effects without other untoward effects.

In our previous work, we found that early activation of microglia/macrophages by tuftsin attenuated clinical symptoms in EAE mice, and this correlated with a switch toward an increased expression of Th2 transcriptional factor. These findings led us to explore the concept of protective autoimmunity. In MS/EAE the balance between the proinflammatory Th1 response and the anti-inflammatory Th2 response, together with the beneficial effect of the regulatory T cells, is thought to determine the outcome of MS/EAE. Here I observed that after tuftsin treatment, there was development of type II T cells and expansion of Tregs. Our current studies confirmed the idea that early activation of microglia by tuftsin results in a coordination of the immune response, by favoring protective autoimmunity as opposed to autoimmune disease.

Many treatments for MS aim at the repression of the immune response. Some reagents work through the inhibition of activation of microglia and T cells, and cause a downregulation of the production of proinflammatory cytokines (Stanislaus et al., 2005). These treatments through their "anti-inflammatory effects" attenuate MS symptoms. Tuftsin, however, affects MS/EAE symptoms in a different manner, by inducing a protective autoimmunity response rather than attenuate the immune response itself. Tuftsin can modulate the T cell fates (promote Th2 and Tregs development), more than

just inhibiting Th1 response. So tuftsin works through the "modulation of the immune system".

Despite its 30-year history, the binding target and mechanism of action of tuftsin remain unknown. However, based on the broad range of action of tuftsin in both the immune and nervous systems, it's expected that the tuftsin receptor should be common in both systems. Recently a group identified that cultured human aortic and umbilical vein endothelial cells express tuftsin receptors and that in these cells the binding target for tuftsin is neuropilin-1 (von Wronski et al., 2006). Because neuropilin-1 plays a critical role in the immune, vascular, and nervous systems and interacts with a number of different ligands, cell surface receptors and adhesion proteins (Gavazzi, 2001; Tordjman et al., 2002; Wang et al., 2003), it is possible that some of the previously reported effects of tuftsin are mediated through neuropilin-1.

Neuropilin-1 (Nrp-1) binds to SEMA3A in the nervous system (Kolodkin et al., 1997), and vascular endothelial growth factor (VEGF) in cardiovascular development (Soker et al., 1998). Recent findings revealed important roles of Nrp-1 in immune system. Nrp-1 mediates interactions between DCs and T cells that are essential for the initiation of the primary immune response (Tordjman et al., 2002). Nrp-1 homotypic binding mediates prolonged interactions between Treg cells and immature DCs (iDCs) (Sarris et al., 2008). Nrp-1 is also expressed in microglia and its levels are increased during inflammatory conditions (Agudo et al., 2005; Majed et al., 2006). It is therefore possible that during inflammatory conditions, the binding of tuftsin to microglial Nrp-1 can initiate a series of events that would actually deliver tuftsin-modulated signals to regulatory T cells and

affect EAE outcomes. Our results showed up-regulation of Nrp-1 expression in tuftsin infused animals, which indicates an involvement of Nrp-1 in tuftsin-mediated protection. Future investigations should focus on the role of Nrp-1.

Figure V-1: The direct effect of tuftsin on T cells cytokines production.

ELISA assays were performed to evaluate the proinflammatory cytokine TNFα (A) and anti-inflammatory cytokine IL-10 (B) produced by T cells. n = 4, a two-tailed t-test was used for comparisons between experimental groups and MOG-primed untreated control. *, $p<0.05$; **, $p<0.01$; ***, $p<0.001$.

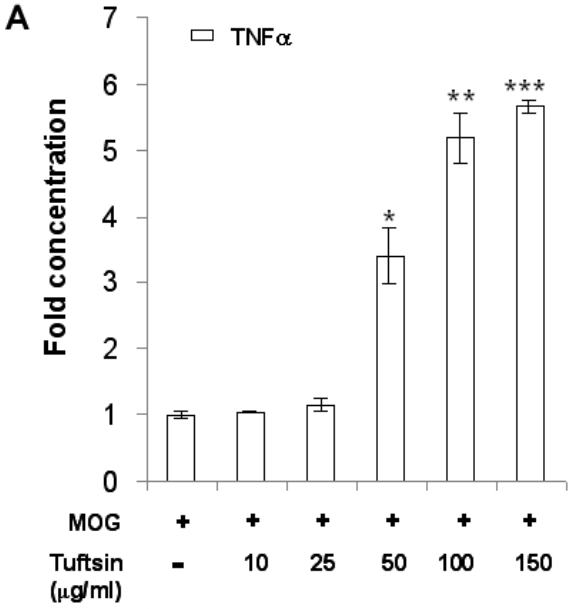
A
TNFα
Fold concentration
0
1
2
3
4
5
6
7
*
**
***
MOG + + + + + +
Tuftsin (μg/ml) - 10 25 50 100 150

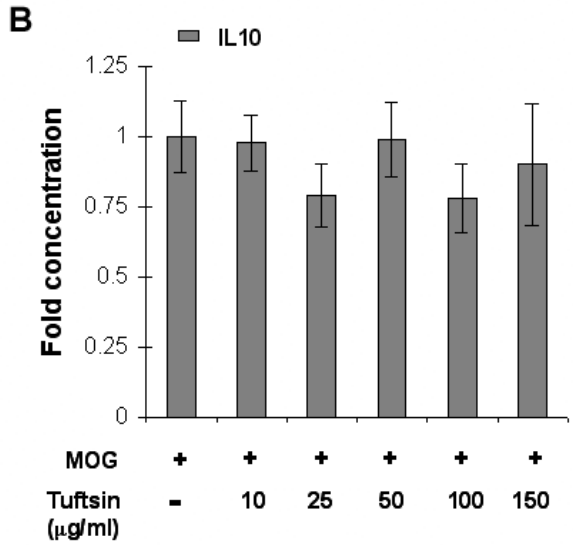
B
IL10
Fold concentration
0
0.25
0.5
0.75
1
1.25
MOG + + + + + +
Tuftsin (μg/ml) - 10 25 50 100 150

Figure V-2: Modulating microglia activity with tuftsin under excitotoxic conditions affected T cell cytokines production.

ELISA assays were performed to evaluate the proinflammatory cytokine TNFα (A) and anti-inflammatory cytokine IL-10 (B) produced by T cells. n = 4, a two-tailed t-test was used for comparisons between experimental groups and MOG-primed untreated control. *, $p<0.05$; **, $p<0.01$; ***, $p<0.001$.

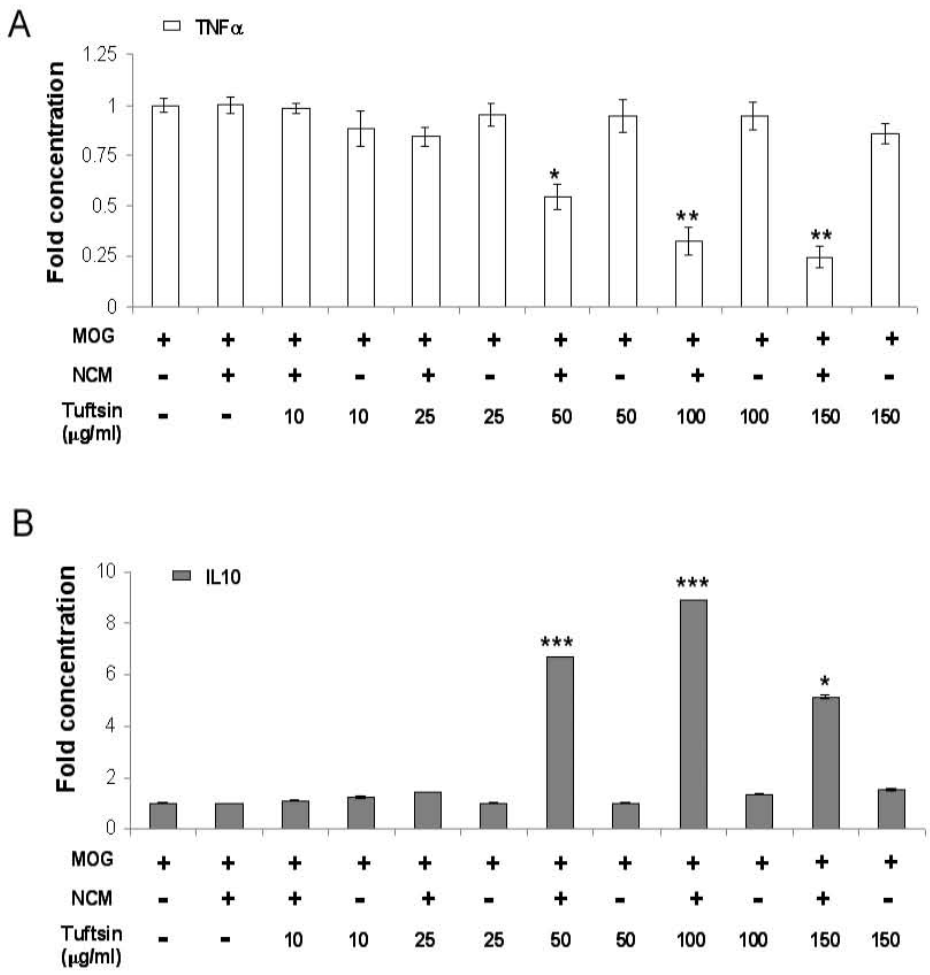
A
TNFα
Fold concentration
1.25
1
0.75
0.5
0.25
0
*
**
**
MOG + + + + + + + + + + + +
NCM - + + - + - + - + - + -
Tuftsin (μg/ml) - - 10 10 25 25 50 50 100 100 150 150
B
IL10
Fold concentration
10
8
6
4
2
0
***
***
*
MOG + + + + + + + + + + + +
NCM - + + - + - + - + - + -
Tuftsin (μg/ml) - - 10 10 25 25 50 50 100 100 150 150

Figure V-3: Tuftsin infusion induces type II T cells and Tregs.

Western blots were performed on mouse spinal cord extracts to examine protein expression. Phosphorylation of STAT1 is reduced in tuftsin infused EAE mice, anti-inflammatory cytokines IL10 and IL4 protein levels are up-regulated in tuftsin infused EAE mice. Treg transcriptional factor FoxP3 expression increases in tuftsin treated samples. Equal loading of protein was confirmed by pan-STAT1 blotting. (Western blot was repeated three times on mouse spinal cord samples from three separate EAE experiments.)

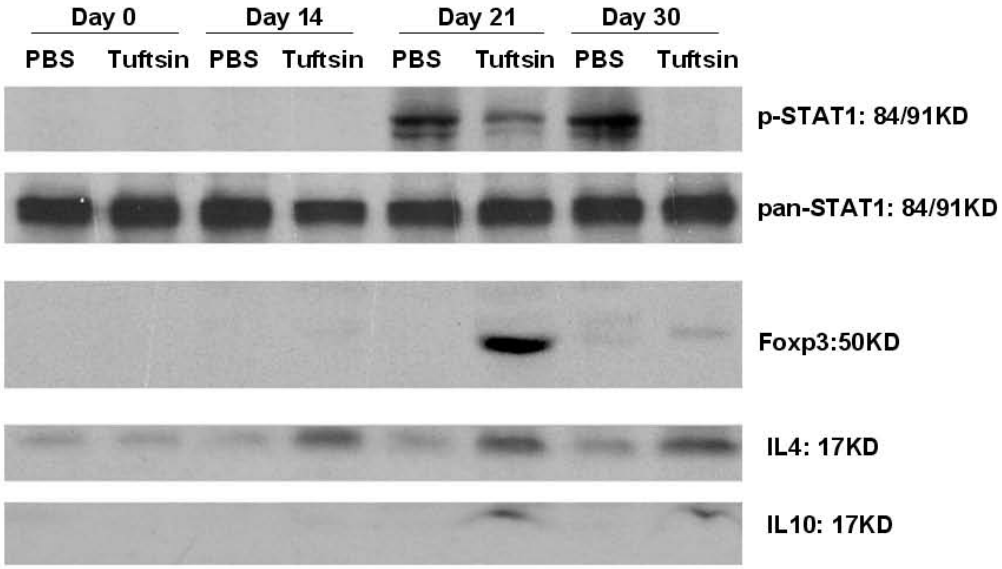
Day 0
Day 14
Day 21
Day 30
PBS
Tuftsin
PBS
Tuftsin
PBS
Tuftsin
PBS
Tuftsin
p-STAT1: 84/91KD
pan-STAT1: 84/91KD
Foxp3:50KD
IL4: 17KD
IL10: 17KD

Figure V-4: Adoptive transfer of tuftsin modulated T cells prevents and reverses established EAE.

Clinical course of EAE. Wild-type (WT) mice were injected with MOG_{35-55} peptide in CFA and pertussis toxin to induce EAE. Osmotic pumps filled with PBS or 500 μM tuftsin in PBS were implanted in the back of the mice on day 1 after MOG immunization. 5 x 10^6 tuftsin treated T cells (three conditions: tuftsin plus NCM treated T cells; tuftsin only treated T cells; NCM only treated T cells) were injected intravenously into recipient C57BL6 mice immunized with MOG on day 14, after the onset of disease (Arrow indicates timepoint when T cells transfer was performed). The disease severity was scored on a clinical scale from 0 to 5 as described in Methods. (Experiment has been repeated twice. Cumulative data was provided; total number of animals tested, n=12/PBS infused mice; n=12/tuftsin infused mice; n=12/mice adoptively transferred with tuftsin plus NCM modulated T cells; n=5/mice adoptively transferred with only tuftsin treated T cells; n=5/ mice adoptively transferred with only NCM treated T cells)

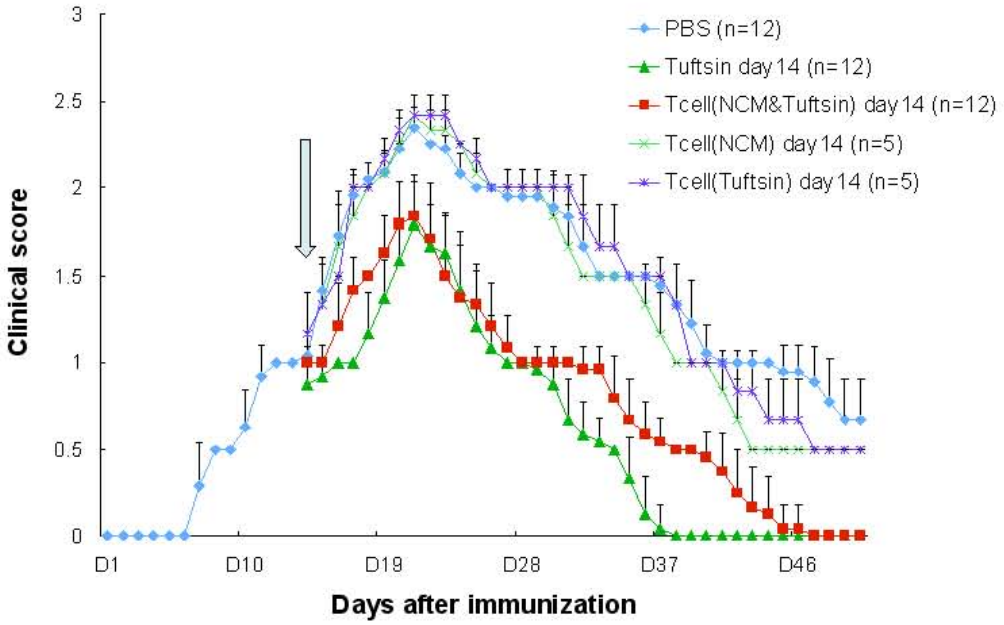
PBS (n=12)
Tuftsin day14 (n=12)
Tcell(NCM&Tuftsin) day14 (n=12)
Tcell(NCM) day14 (n=5)
Tcell(Tuftsin) day14 (n=5)
Clinical score
3
2.5
2
1.5
1
0.5
0
D1
D10
D19
D28
D37
D46
Days after immunization

Figure V-5A: Attenuated demyelination pattern in EAE mice adoptively transferred with tuftsin-modulated T cells.

(A). Frozen cross-sections of spinal cords were isolated at different time points during the EAE from PBS infused wild-type mice, Tuftsin infused wild-type mice and wild-type mice adoptively transferred with Tuftsin modulated T cells. spinal cord sections were stained with Eriochrome cyanine (EC), which visualizes myeline (blue). Sites of demyelination are indicated by asterisks (e.g. PBS infused wild-type mice at day 22).

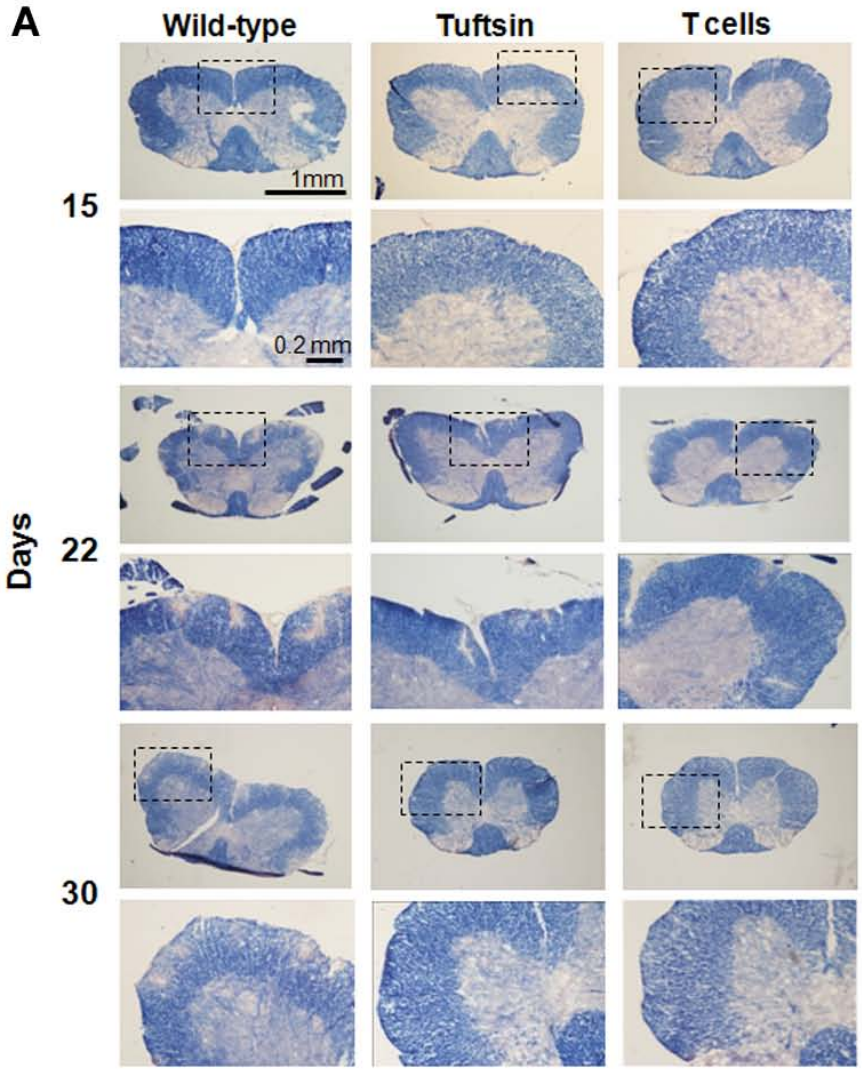
A
Wild-type
Tuftsin
T cells
1mm
0.2 mm
Days
15
22
30

Figure V-5B-C: Attenuated demyelination pattern in EAE mice adoptively transferred with tuftsin-modulated T cells.

(B). (C). Use of FluoroMyelin to fluorescently and quantitatively image myelin. (Quantifications were performed on five sections per mouse for three different mice in two separate EAE experiments; results are presented as an average with error bars indicating the standard error of the mean. A two-tailed t test was performed to analyze the significance of the difference of FluoroMyelin staining intensity across groups at each timepoint (*** $p<0.001$; **$p<0.01$).

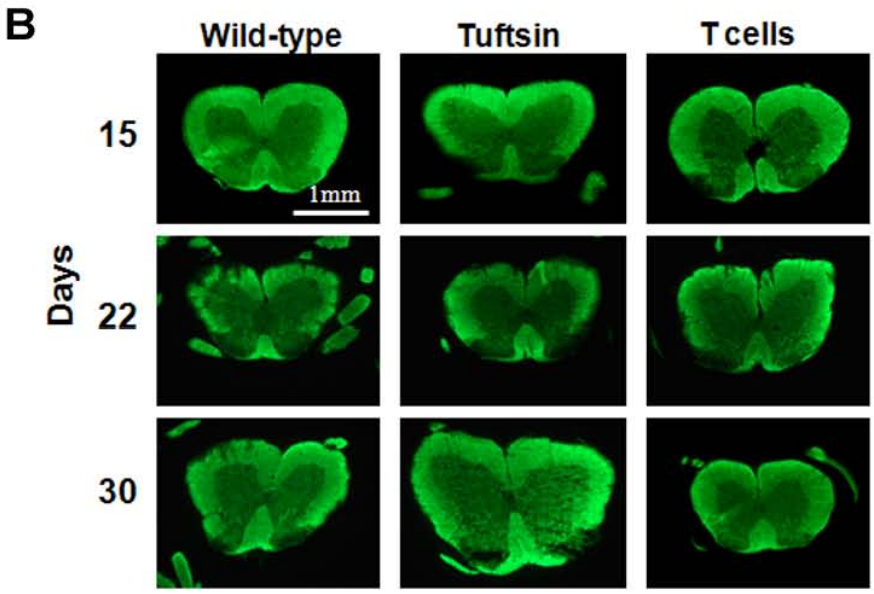
B
Wild-type
Tuftsin
T cells
15
22
30
Days
1mm

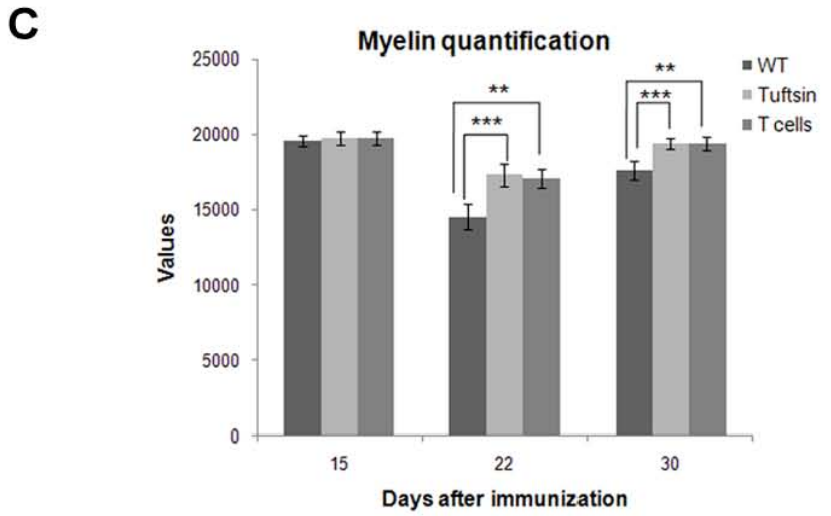
C
Myelin quantification
25000
20000
15000
10000
5000
0
Values
**
***
**
***
WT
Tuftsin
T cells
15
22
30
Days after immunization

Figure V-6: Reduced microglia/macrophage infiltration and activation in mice with adoptive tranfer.

(A). Frozen cross-sections of spinal cords from PBS, tuftsin infused and adoptively transferred mice at different time points in EAE were stained with anti-Iba1 to detect microglia. Iba1 is expressed on both resting and activated microglia, which can be distinguished by their morphological appearance. Arrowheads (e.g. as seen in Day 15 panel) indicate resting microglia, characterized by long, thin cell bodies. Arrowheads (e.g. as seen in Day 22 panel) indicate activated microglia that are characterized by thicker, rounded cell bodies and multi-branched cellular protrusions. (Experiment has been repeated three times. In total five mice were assessed for immunostaining each timepoint per genotype, representative data were provided. (B). Protein extracts from mice spinal cords were collected at different timepoints in EAE and analyzed using western blotting to quantitate levels of Iba1. Equal loading of protein was confirmed by anti-actin blotting. (Western blot was repeated three times on mouse spinal cord samples from two separate EAE experiments.)

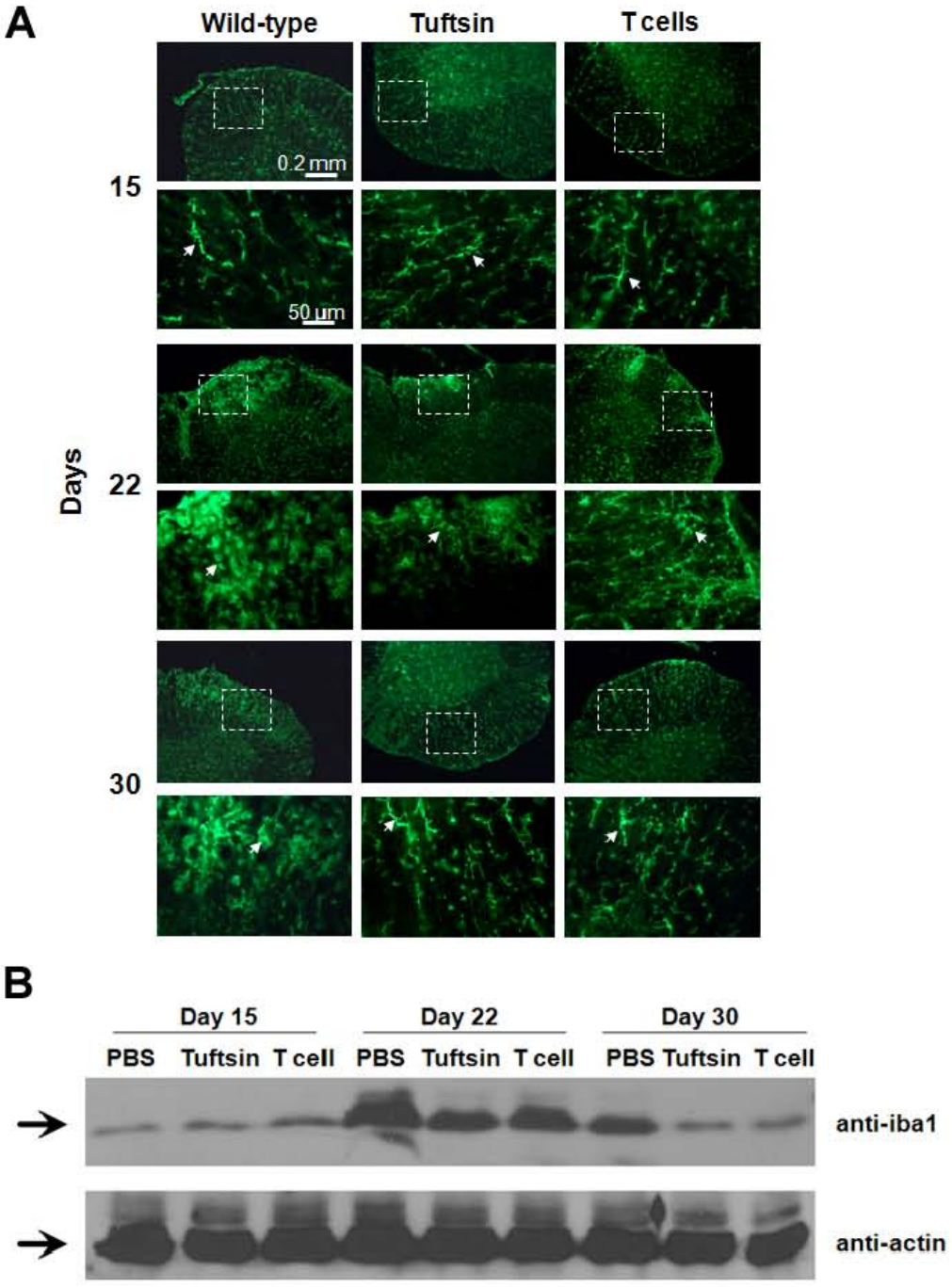
A
Wild-type
Tuftsin
T cells
0.2 mm
50 um
Days
15
22
30
B
Day 15
Day 22
Day 30
PBS
Tuftsin
T cell
PBS
Tuftsin
T cell
PBS
Tuftsin
T cell
anti-iba1
anti-actin

Figure V-7: Increased Nrp-1 expression in tuftsin infused animals.

Spinal cords protein extracts from WT mice infused with PBS or tuftsin were collected at different timepoints in EAE and analyzed using western blotting to quantitate levels of neuropilin-1. Equal loading of protein was confirmed by anti-actin blotting. (Western blot was repeated three times on mouse spinal cord samples from two separate EAE experiments.)

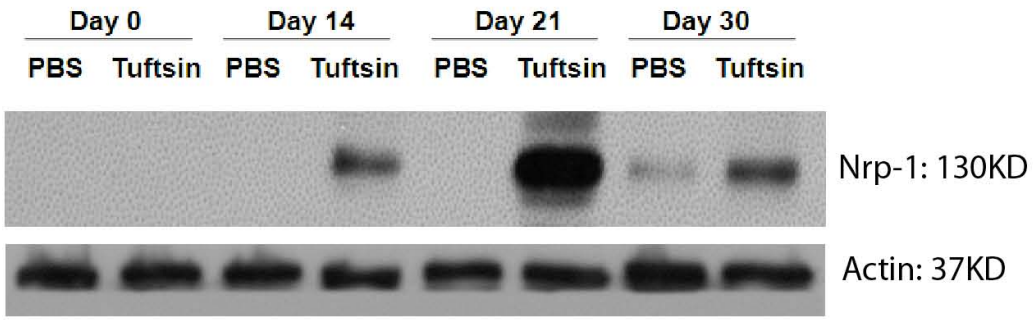
Day 0
Day 14
Day 21
Day 30
PBS
Tuftsin
PBS
Tuftsin
PBS
Tuftsin
PBS
Tuftsin
Nrp-1: 130KD
Actin: 37KD

Table V-1: PCR arrays on T cells reveal several responsible genes. n=2

	Fold Change (comparing to control group)		
Gene Symbol	Group 1 (NCM+Tuftsin)	Group 2 (Tuftsin)	Group 3 (NCM)
Tnf	0.1175	0.9979	1.3827
Tnfrsf1a	0.1183	0.7537	0.7717
Tnfrsf1b	0.0923	0.9618	1.2724
Bcl6	0.2016	0.8649	0.8938

	Fold Change (comparing to control group)		
Gene Symbol	Group 1 (NCM+Tuftsin)	Group 2 (Tuftsin)	Group 3 (NCM)
Il10	23.4176	1.0335	2.5401
Il10ra	19.4227	0.7006	0.8383
Il10rb	6.5925	1.1945	1.0885
Il13	12.7354	0.7719	1.0649
Il4	15.124	0.7938	1.6686
Tgfb1	27.6091	1.2373	1.3031
Ccr3	36.8303	0.841	0.9663
Ccr5	86.9654	31.0864	0.9342
Ifng	7.6099	0.839	1.1929

Chart V-1: An *in culture* model to mimic the tuftsin infused EAE model *in vivo*.

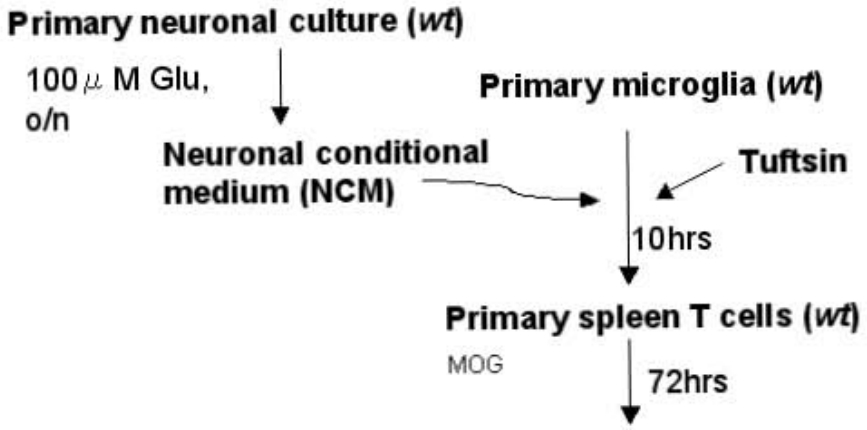
Primary neuronal culture (*wt*)
100 μ M Glu,
o/n
Neuronal conditional
medium (NCM)
Primary microglia (*wt*)
Tuftsin
10hrs
Primary spleen T cells (*wt*)
MOG
72hrs

Chart V-2: Diagram of PCR array samples preparation.

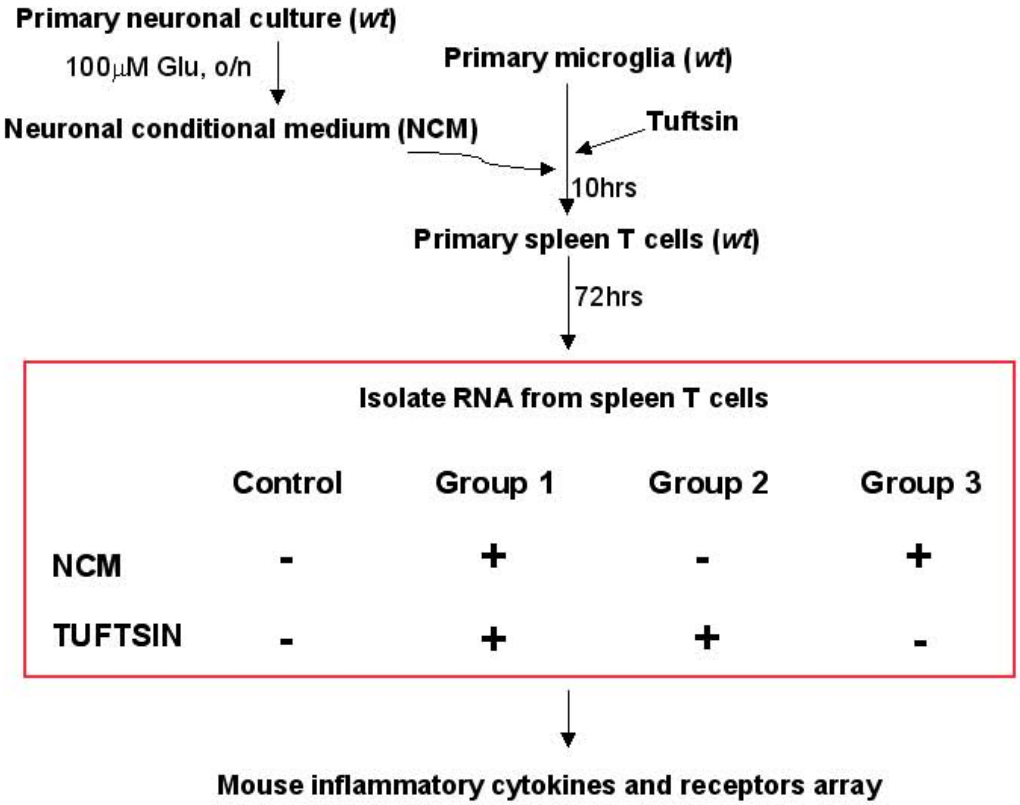
Primary neuronal culture (*wt*)
100μM Glu, o/n
Neuronal conditional medium (NCM)
Primary microglia (*wt*)
Tuftsin
10hrs
Primary spleen T cells (*wt*)
72hrs
Isolate RNA from spleen T cells
Control
Group 1
Group 2
Group 3
NCM
- + - +
TUFTSIN
- + + -
Mouse inflammatory cytokines and receptors array

Chapter VI

General Conclusions, Discussion and Future Directions

NO and MS/EAE

A major part of this dissertation concerns the investigation of the role of NO, and the elucidation of the contributions of different NOS isoforms during EAE. We concluded that the cellular-independent production of NO had protective roles during the recovery period of EAE, while different NOS isoform-derived NO participated during the early onset and progress of disease. NO is not stable in the tissue, it can be converted to a lot of metabolites, one of which is peroxynitrite ($ONOO^-$). Peroxynitrite has many toxic effects. It has been reported that peroxynitrite can induce myelin damage and cause loss of oligodendrocytes. It always remains a question: is the toxic effect of NO caused by peroxynitrite? To address this question, we can infuse peroxynitrite scavengers FeTMPyP and FeTPPS into wild-type mice, and monitor if the clinical symptoms will be ameliorated; or we can provide peroxynitrite into wild-type mice, to see if the symptoms become severe. Pathological markers, such as demyelination and oligodendrocytes loss, can also be evaluated. Providing or scavenging peroxynitrite during different phases of EAE could generate a timeline for the functions of peroxynitrite.

The blood brain barrier

Initial BBB breakdown is crucial for the induction of MS/EAE. It has been reported that NO can disturb BBB permeability in both *in vivo* and *in vitro* settings, however, the precise mechanism is poorly understood. One major part of this dissertation focused on the determination of the responsible sources that contribute to BBB disruption. In chapter

III, we identified that eNOS$^{-/-}$ mice showed delayed BBB breakdown, which can not be restored by infusion of general NO donor, suggesting that eNOS-derived NO contributes to BBB breakdown. This is in agreement with previous findings that showed that eNOS displays protective effects in ischemia by increasing cerebral blood flow and blocking platelet aggregation (Samadani et al., 1997). It has been reported that eNOS expression is up-regulated in endothelial cells during EAE (Zhao et al. 1996). In addition, astrocytes and neurons also are cellular sources of eNOS. It will be important to determine the cellular sources of eNOS during MS/EAE. To address this question, we can examine the expression of eNOS in these cell types both qualitatively and quantitatively during MS/EAE, and also evaluate whether its expression correlates with the timeline of BBB breakdown.

Another interesting result we obtained is that the nNOS$^{-/-}$ mice also showed delayed (and even more delayed than eNOS$^{-/-}$ mice) BBB breakdown. Previous work in our lab showed that nNOS was a mediator of neurodegeneration and nNOS$^{-/-}$ mice resisted excitotoxicity (Parathath et al. 2006). Is the delayed BBB breakdown in these mice a consequence of the resistance to excitotoxicity due to nNOS deficiency? Or nNOS may mediate BBB permeability independently from eNOS through indirect signaling events from neurons to the BBB? All these questions need to be further addressed.

Both eNOS and nNOS derived NO participate in BBB disruption, however, blocking global NO production using NMMA has no effect on BBB breakdown as showed that these mice had normal disease onset. One explanation may be that the concentration of NMMA infused in the wild-type mice was not sufficient to block all NOS activity.

Another possibility is that NO may only partly contribute to the BBB breakdown, and there are other factors that mediate BBB disruption during NMMA infusion.

Peroxynitrite (ONOO-), a NO metabolite product has been found to be critical for BBB breakdown in CNS pathologies involving chronic inflammation, such as MS. A question may arise: whether it is NO or $ONOO^-$ that directly influence BBB permeability? To answer this question, we can infuse $ONOO^-$ scavengers FeTMPyP and FeTPPS into wild-type mice before induction of EAE, then monitor the onset of disease and measure the breakdown of BBB. Elucidating the roles of NO versus $ONOO^-$ will help us target the cure for MS/EAE more specifically.

Activated T cells infiltrate the CNS once the BBB is compromised. It is of great interest to assess the extent of T cell infiltration during disease progression both temporally and quantitatively. To investigate this, we can prepare MOG-specific GFP-labeled T cell clones isolated from β-actin GFP transgenic mice, and adoptively transfer these T cells into wild-type and NOS deficient mice. The extent of T cell infiltration could then be determined by imaging GFP-positive T cells in mouse spinal cord sections at multiple timepoints during EAE progression. Flow cytometry could be used to quantitatively evaluate T cell infiltration.

Excitotoxicity and MS/EAE

MS/EAE has been recognized as a demyelinating, autoimmune disease, which is associated with T cell-mediated inflammation. Accumulating evidence also indicates that MS/EAE is generally linked with excitotoxicity. In the CSF of MS patients, high levels of glutamate correlated with disease severity and progression (Barkhatova et al. 1998). Moreover, in MS/EAE lesions, excitotoxicity-induced oligodendrocyte loss contributes to axonal damage (Matute et al. 2001). Our results with the nNOS-/- mice also suggest a correlation between nNOS-mediated excitotoxicity and pathological features of EAE. One explanation of the delayed pathological events observed in $nNOS^{-/-}$ mice could be that due to the resistance to excitotoxicity, all the events that would be required to trigger BBB breakdown were inhibited, so BBB breakdown slowly occurred and disease onset was delayed. A new question may arise: whether other pathological markers, such as those for axonal and oligodendrocytes loss, would also be attenuated due to nNOS deficiency? Although it has been reported that in KA-induced excitotoxicity $nNOS^{-/-}$ mice were protected from BBB breakdown and neurodegeneration as well (Parathath et al. 2007), we showed here in EAE, $nNOS^{-/-}$ mice do show delayed BBB breakdown, but with increased disease severity, severe demyelination and extensive infiltration and activation of microglia/macrophages. One may wonder whether the resistance to excitotoxicity mediated by nNOS deficiency is not sufficient to protect against EAE. Or, whether this protective effect of nNOS deficiency is restricted within certain time frame (i.e. early disease onset). To address these questions, we could induce EAE in wild-type mice, and provide nNOS-specific inhibitors during different phases of disease to

determine the effective time frame of nNOS inhibition. One possible explanation would be that in MS/EAE, more factors in addition to excitotoxic mechanisms contribute to disease progression: T cell, microglia/macrophages-mediated inflammation may be minimally affected by preventing excitotoxicity.

Protective autoimmunity and MS/EAE

Autoimmune diseases are usually recognized as the mal-functioning of the immune system. An autoimmune response is the body's own mechanism to deal with the CNS damage, however, when it goes out of control, it elicits immune attacks on itself. So in other words, if well controlled, the effect of protective autoimmunity will be beneficial. Protective autoimmunity has been observed during a lot of diseases. In type 1 diabetes (T1D) and EAE, microbial agents, such as Bacille Calmette-Guérin (BCG) or Freund's adjuvant (CFA), induce a regulatory Th17 response, which are protective. The induction of innate immunity by these microbial products alters the balance in the cytokine microenvironment and may be responsible for modulation of the inflammation (Nikoopour et al. 2008). In cancer, naturally occurring antibodies act as the first line of defense against malignant cells invasion. Natural protective autoantibodies against tumor-antigens isolated from cancer patients reflect the development of naturally occurring B-cell responses during the process of cancer evolvement. Autoimmunity and malignancy always coexist and they may share etiological and pathological mechanisms.

The concept of protective autoimmunity provides therapeutic perspectives to treat CNS diseases. For treatment of CNS diseases which are not due to the mal-function of immune response, one can boost the autoimmune response; for treatment of autoimmune diseases, one can modulate the immune response by maximizing the beneficial component while minimizing the destructive part, rather than suppressing the entire immune response.

Numerous molecules and approved drugs alleviate MS/EAE by inducing protective autoimmunity. Matrix metalloproteinase 12 (MMP 12) has been found to be highly up-regulated in EAE spinal cord, which was associated with protection, as MMP-12 null mice had significantly worse symptoms. Moreover, spleen T cells isolated from MMP-12 null mice had significantly higher Th1 to Th2 cytokine ratio, and increased T-bet expression (Weaver et al. 2005). Glatiramer acetate (GA), an administered immunomodulatory agent approved for MS treatment, and statins exhibit immunomodulatory properties. Combination therapy using both agents prevented development of EAE, with decreased secretion of Th1 cytokines and increased Th2 cytokine production (Weber et al., 2007). Recently, it has been reported that type I IFNs exhibits protective function during autoimmune inflammation of the CNS. Interferon alpha receptor 1 deficient mice ($Ifnar1^{-/-}$ mice) showed enhanced disease severity with increased Th1, Th17 immune response (Guo et al. 2008).

Here, as described in chapter V, I identified that tuftsin may induce a protective effect in EAE in the same manner: early activation of microglia by tuftsin results in a coordination of the immune response by favoring protective autoimmunity as opposed to

autoimmune disease. Working through the "modulation of the immune system", tuftsin modulate the T cell fates (promote Th2 and Tregs development) more than just inhibiting Th1 response. It will be intriguing to examine the effect of tuftsin on CD8+ T lymphocytes, which are important for protection against chronic (latent) CNS viral infections. We hypothesize that if tuftsin shows no suppression on CD8+ T lymphocyte function or even promotes their differentiation, it could be considered a possibly safe, therapeutic target in MS.

In chapter III, I showed that NO appears to play both aggravating and protective roles in EAE. Blocking NO production by NMMA in wild-type mice, or using NOS deficient mice, I found a significantly worse disease course in these mice. In chapter IV, *in vitro* analysis showed that NO modulates T cell cytokine profiles: NO has no significant effect on Th1 cytokine TNFα, however low concentrations of NO increase Th2 cytokines IL4 and IL10 production. These results suggest a protective effect of NO on the T cell immune response, which is beneficial for disease development. Based on these data, further investigation could focus on the mechanism of NO mediated protection, identifying gene changes and differentiation pattern of T cells.

Neuropilin-1 and tuftsin

In chapter V, I showed the immunomodulatory effect of tuftsin during EAE. Future investigation could focus on the underlying mechanisms. One important question is: what

is/are the binding target/targets of tuftsin? As I mentioned before, we proposed that neuropilin-1 is a potential candidate as a receptor for tuftsin. Up-regulated levels of Nrp-1 expression in tuftsin infused animals indicate an involvement of Nrp-1 (Fig. V-7). Both *in vivo* and in culturing results showed that the direct effect of tuftsin on T cells is to promote the pro-inflammatory response. The protective effect of tuftsin observed *in vivo* represents a more complicated scenario, during which both microglia and T cells are involved. We hypothesized that it is the factors present in the microglial conditioned medium after treatment that modulate T cell properties. However, microglial conditioned medium treated with only tuftsin or only NCM has no effect on T cells, suggesting that both components are necessary for triggering changes in microglia. NCM mimics the excitotoxicity which occurs in EAE *in vivo*. This *in culture* model mimics the in vivo model most efficiently.

Nrp-1 is expressed in microglia and its levels are increased during inflammatory conditions (Agudo et al. 2005; Majed et al. 2006). Nrp-1 mediates interactions between DCs and T (Tordjman et al. 2002), and it's also constitutively expressed on regulatory T cells. Nrp-1 can form homotypic bindings. Based on these, I proposed that, during EAE, microglia express high levels of Nrp-1 under excitotoxic conditions. Tuftsin activates microglia and further up-regulates Nrp-1 expression. Thus microglia could be able to interact with Treg cells through homotypic bonds, and have prolonged interactions with Treg cells. On the other hand, tuftsin also suppresses the interaction between microglia and T helper cells, particularly Th1, Th17 cells, and inhibits the pro-inflammatory response during EAE. To investigate this hypothesis, we can first examine the expression

of Nrp-1 on microglia and T cells both *in vivo* and *in culture*, and evaluate the changes of Nrp-1 expression after tuftsin plus NCM treatment. Both of the excitotoxic signals and tuftsin treatment are required, which may be explained by a threshold of Nrp-1 expression on microglia in order to form more efficient contact with T cells. The expression pattern after treatment of tuftsin or NCM alone may be a control to determine the threshold. Another possibility for this combined requirement could be that both the excitotoxic signals and tuftsin treatment are needed to trigger signaling events downstream. It has been shown that Nrp-1 can form a receptor complex with plexin-A1 which functions as a signal transducer in the targeted cells.

It would be intriguing to determine the interaction of the homotypic bindings of Nrp-1 between microglia and T cells. A detailed confocal microscopic analysis could be used to construct a 3-dimentional image. One may ask whether Nrp-1 homotypic interactions functionally contribute to this tuftsin mediated protection. A straightforward experiment would be adding Nrp-1 blocking antibody to microglia and T cells respectively in culture to see if the beneficial phenomenon is abrogated.

Reference

Abbott NJ, Ronnback L, Hansson E (2006) Astrocyte-endothelial interactions at the blood-brain barrier. Nat Rev Neurosci 7:41-53.

Adachi M, Roussel MF, Havenith K, Sherr CJ (1997) Features of macrophage differentiation induced by p19INK4d, a specific inhibitor of cyclin D-dependent kinases. Blood 90:126-137.

Agudo M, Robinson M, Cafferty W, Bradbury EJ, Kilkenny C, Hunt SP, McMahon SB (2005) Regulation of neuropilin 1 by spinal cord injury in adult rats. Molecular and cellular neurosciences 28:475-484.

Ahern GP, Hsu SF, Klyachko VA, Jackson MB (2000) Induction of persistent sodium current by exogenous and endogenous nitric oxide. J Biol Chem 275:28810-28815.

Albina JE, Henry WL, Jr. (1991) Suppression of lymphocyte proliferation through the nitric oxide synthesizing pathway. J Surg Res 50:403-409.

Alderton W, Cooper C, Knowles R (2001) Nitric oxide synthases: structure, function and inhibition. Biochem J 357:593-615.

Arnett HA, Hellendall RP, Matsushima GK, Suzuki K, Laubach VE, Sherman P, Ting JP. 2002. The protective role of nitric oxide in a neurotoxicant-induced demyelinating model. J Immunol 168(1):427-33.

Ayata C, Ayata G, Hara H, Matthews RT, Beal MF, Ferrante RJ, Endres M, Kim A, Christie RH, Waeber C, Huang PL, Hyman BT, Moskowitz MA (1997) Mechanisms of reduced striatal NMDA excitotoxicity in type I nitric oxide synthase knock-out mice. J Neurosci 17:6908-6917.

Balabanov R, Dore-Duffy P (1998) Role of the CNS microvascular pericyte in the blood-brain barrier. Journal of neuroscience research 53:637-644.

Bal-Price A, Brown GC (2001) Inflammatory neurodegeneration mediated by nitric oxide from activated glia-inhibiting neuronal respiration, causing glutamate release and excitotoxicity. J Neurosci 21:6480-6491.

Bamforth SD, Kniesel U, Wolburg H, Engelhardt B, Risau W (1999) A dominant mutant of occludin disrupts tight junction structure and function. J Cell Sci 112 (Pt 12):1879-1888.

Barkhatova VP, Zavalishin IA, Askarova L, Shavratskii V, Demina EG. (1998) Changes in neurotransmitters in multiple sclerosis. Neurosci Behav Physiol 28(4):341-4.

Baumann N, Pham-Dinh D (2001) Biology of oligodendrocyte and myelin in the mammalian central nervous system. Physiol Rev 81:871-927.

Bechmann I, Galea I, Perry VH (2007) What is the blood-brain barrier (not)? Trends Immunol 28:5-11.

Beckman JS, Chen J, Ischiropoulos H, Crow JP (1994) Oxidative chemistry of peroxynitrite. Methods Enzymol 233:229-240.

Beckman JS, Koppenol WH (1996) Nitric oxide, superoxide, and peroxynitrite: the good, the bad, and ugly. Am J Physiol 271:C1424-1437.

Benveniste EN (1997) Role of macrophages/microglia in multiple sclerosis and experimental allergic encephalomyelitis. J Mol Med 75:165-173.

Bernard CC, Johns TG, Slavin A, Ichikawa M, Ewing C, Liu J, Bettadapura J (1997) Myelin oligodendrocyte glycoprotein: a novel candidate autoantigen in multiple sclerosis. J Mol Med 75:77-88.

Bhasin M, Wu M, Tsirka SE (2007) Modulation of microglial/macrophage activation by macrophage inhibitory factor (TKP) or tuftsin (TKPR) attenuates the disease course of experimental autoimmune encephalomyelitis. BMC immunology 8:10.

Boje KM, Lakhman SS (2000) Nitric oxide redox species exert differential permeability effects on the blood-brain barrier. J Pharmacol Exp Ther 293:545-550.

Brenman, J. E., D. S. Chao, et al. (1996). "Interaction of nitric oxide synthase with the postsynaptic density protein PSD-95 and alpha1-syntrophin mediated by PDZ domains." Cell 84(5): 757-67.

Brian JE, Jr., Faraci FM, Heistad DD (1996) Recent insights into the regulation of cerebral circulation. Clin Exp Pharmacol Physiol 23:449-457.

Brown G, Bal-Price A. 2003. Inflammatory neurodegeneration mediated by nitric oxide, glutamate and mitochondria. Mol Neurobio 27:325-355.

Bruder D, Probst-Kepper M, Westendorf AM, Geffers R, Beissert S, Loser K, von Boehmer H, Buer J, Hansen W (2004) Neuropilin-1: a surface marker of regulatory T cells. Eur J Immunol 34:623-630.

Calabrese V, Scapagnini G, Ravagna A, Bella R, Foresti R, Bates TE, Giuffrida Stella AM, Pennisi G (2002) Nitric oxide synthase is present in the cerebrospinal fluid of patients with active multiple sclerosis and is associated with increases in cerebrospinal fluid protein nitrotyrosine and S-nitrosothiols and with changes in glutathione levels. Journal of neuroscience research 70:580-587.

Cannella B, Raine CS (1995) The adhesion molecule and cytokine profile of multiple sclerosis lesions. Ann Neurol 37:424-435.

Carson MJ (2002) Microglia as liaisons between the immune and central nervous systems: functional implications for multiple sclerosis. Glia 40:218-231.

Chao CC, Hu S, Molitor TW, Shaskan EG, Peterson PK (1992) Activated microglia mediate neuronal cell injury via a nitric oxide mechanism. J Immunol 149:2736-2741.

Compston A (1997) Genetic epidemiology of multiple sclerosis. J Neurol Neurosurg Psychiatry 62:553-561.

Cowden WB, Cullen FA, Staykova MA, Willenborg DO (1998) Nitric oxide is a potential down-regulating molecule in autoimmune disease: inhibition of nitric oxide production renders PVG rats highly susceptible to EAE. J Neuroimmunol 88:1-8.

Cross AH, Manning PT, Stern MK, Misko TP (1997) Evidence for the production of peroxynitrite in inflammatory CNS demyelination. J Neuroimmunol 80:121-130.

Crow JP, Beckman JS (1996) The importance of superoxide in nitric oxide-dependent toxicity: evidence for peroxynitrite-mediated injury. Advances in experimental medicine and biology 387:147-161.

Dalton D, Wittmer S. 2005. Nitric-oxide-dependent and independent mechanisms of protection from CNS inflammation during Th1-mediated autoimmunity: evidence from EAE in iNOS KO mice. J Neuroimmunol 160(1-2):110-121.

Dawson VL, Dawson TM, London ED, Bredt DS, Snyder SH (1991) Nitric oxide mediates glutamate neurotoxicity in primary cortical cultures. Proc Natl Acad Sci U S A 88:6368-6371.

Diemel LT, Copelman CA, Cuzner ML (1998) Macrophages in CNS remyelination: friend or foe? Neurochem Res 23:341-347.

Dinter H, Stock G, Perez HD (1997) Multiple sclerosis: pathogenesis and models. J Mol Med 75:164.

Dore-Duffy P, Washington R, Dragovic L (1993) Expression of endothelial cell activation antigens in microvessels from patients with multiple sclerosis. Advances in experimental medicine and biology 331:243-248.

Ebers GC, Sadovnick AD, Risch NJ (1995) A genetic basis for familial aggregation in multiple sclerosis. Canadian Collaborative Study Group. Nature 377:150-151.

Eikelenboom P, Hoogendijk WJ, Jonker C, van Tilburg W (2002) Immunological mechanisms and the spectrum of psychiatric syndromes in Alzheimer's disease. J Psychiatr Res 36:269-280.

Elovaara I, Lalla M, Spare E, Lehtimaki T, Dastidar P (1998) Methylprednisolone reduces adhesion molecules in blood and cerebrospinal fluid in patients with MS. Neurology 51:1703-1708.

Endoh M, Mainese K, Wagner J (1994) Expression of the inducible form of nitric oxide synthase by reactive astrocytes after transient global ischemia. Brain Res 651:92-100.

Farias AS, de la Hoz C, Castro FR, Oliveira EC, Ribeiro dos Reis JR, Silva JS, Langone F, Santos LM (2007) Nitric oxide and TNFalpha effects in experimental autoimmune encephalomyelitis demyelination. Neuroimmunomodulation 14:32-38.

Fenyk-Melody JE, Garrison AE, Brunnert SR, Weidner JR, Shen F, Shelton BA, Mudgett JS (1998) Experimental autoimmune encephalomyelitis is exacerbated in mice lacking the NOS2 gene. J Immunol 160:2940-2946.

Floris S, Blezer EL, Schreibelt G, Dopp E, van der Pol SM, Schadee-Eestermans IL, Nicolay K, Dijkstra CD, de Vries HE (2004) Blood-brain barrier permeability and monocyte infiltration in experimental allergic encephalomyelitis: a quantitative MRI study. Brain 127:616-627.

Franklin R (2002) Why does remyelination fail in multiple sclerosis? Nature Reviews Neuroscience 3:705-714.

Fridkin M, Najjar VA (1989) Tuftsin: its chemistry, biology, and clinical potential. Critical reviews in biochemistry and molecular biology 24:1-40.

Gaillard PJ, van der Sandt IC, Voorwinden LH, Vu D, Nielsen JL, de Boer AG, Breimer DD (2000) Astrocytes increase the functional expression of P-glycoprotein in an in vitro model of the blood-brain barrier. Pharm Res 17:1198-1205.

Gale CR, Martyn CN (1995) Migrant studies in multiple sclerosis. Prog Neurobiol 47:425-448.

Garden GA (2002) Microglia in human immunodeficiency virus-associated neurodegeneration. Glia 40:240-251.

Gavazzi I (2001) Semaphorin-neuropilin-1 interactions in plasticity and regeneration of adult neurons. Cell and tissue research 305:275-284.

Ghafourifar P, Cadenas E (2005) Mitochondrial nitric oxide synthase. Trends in Pharmacological Sciences 26:190-195.

Giovannoni G, Lai M, Thorpe J, Kidd D, Chamoun V, Thompson AJ, Miller DH, Feldmann M, Thompson EJ (1997) Longitudinal study of soluble adhesion molecules in multiple sclerosis: correlation with gadolinium enhanced magnetic resonance imaging. Neurology 48:1557-1565.

Giovannoni G (1998) Cerebrospinal fluid and serum nitric oxide metabolites in patients with multiple sclerosis. Mult Scler 4:27-30.

Guo B, Chang EY, Cheng G. (2008) The type I IFN induction pathway constrains Th17-mediated autoimmune inflammation in mice. J Clin Invest 118(5):1680-90.

Hafler DA, Compston A, Sawcer S, Lander ES, Daly MJ, De Jager PL, de Bakker PI, Gabriel SB, Mirel DB, Ivinson AJ, Pericak-Vance MA, Gregory SG, Rioux JD, McCauley JL, Haines JL, Barcellos LF, Cree B, Oksenberg JR, Hauser SL (2007) Risk alleles for multiple sclerosis identified by a genomewide study. N Engl J Med 357:851-862.

Hanisch UK (2002) Microglia as a source and target of cytokines. Glia 40:140-155.

Hartung HP, Reiners K, Archelos JJ, Michels M, Seeldrayers P, Heidenreich F, Pflughaupt KW, Toyka KV (1995) Circulating adhesion molecules and tumor necrosis factor receptor in multiple sclerosis: correlation with magnetic resonance imaging. Ann Neurol 38:186-193.

Hawkins BT, Davis TP (2005) The blood-brain barrier/neurovascular unit in health and disease. Pharmacological reviews 57:173-185.

Hayashi Y, Nomura M, Yamagishi S, Harada S, Yamashita J, Yamamoto H (1997) Induction of various blood-brain barrier properties in non-neural endothelial cells by close apposition to co-cultured astrocytes. Glia 19:13-26.

Hemmer B, Nessler S, Zhou D, Kieseier B, Hartung HP (2006) Immunopathogenesis and immunotherapy of multiple sclerosis. Nat Clin Pract Neurol 2:201-211.

Herman ZS, Stachura Z, Opielka L, Siemion IZ, Nawrocka E (1981) Tuftsin and D-Arg3-tuftsin possess analgesic action. Experientia 37:76-77.

Hickey WF (1991) Migration of hematogenous cells through the blood-brain barrier and the initiation of CNS inflammation. Brain Pathol 1:97-105.

Hirase T, Staddon JM, Saitou M, Ando-Akatsuka Y, Itoh M, Furuse M, Fujimoto K, Tsukita S, Rubin LL (1997) Occludin as a possible determinant of tight junction permeability in endothelial cells. J Cell Sci 110 (Pt 14):1603-1613.

Hjelmstrom P, Penzotti JE, Henne RM, Lybrand TP (1998) A molecular model of myelin oligodendrocyte glycoprotein. J Neurochem 71:1742-1749.

Hooper DC, Scott GS, Zborek A, Mikheeva T, Kean RB, Koprowski H, Spitsin SV (2000) Uric acid, a peroxynitrite scavenger, inhibits CNS inflammation, blood-CNS barrier permeability changes, and tissue damage in a mouse model of multiple sclerosis. Faseb J 14:691-698.

Huang, P. L., T. M. Dawson, et al. (1993). "Targeted disruption of the neuronal nitric oxide synthase gene." Cell 75(7): 1273-86.

Hurst RD, Fritz IB (1996) Nitric oxide-induced perturbations in a cell culture model of the blood-brain barrier. J Cell Physiol 167:89-94.

Ilzecka J (1996) The structure and function of blood-brain barrier in ischaemic brain stroke process. Ann Univ Mariae Curie Sklodowska [Med] 51:123-127.

Janzer RC, Raff MC (1987) Astrocytes induce blood-brain barrier properties in endothelial cells. Nature 325:253-257.

Jessen KR (2004) Glial cells. Int J Biochem Cell Biol 36:1861-1867.

Kahl KG, Zielasek J, Uttenthal LO, Rodrigo J, Toyka KV, Schmidt HH. 2003. Protective role of the cytokine-inducible isoform of nitric oxide synthase induction and nitrosative stress in experimental autoimmune encephalomyelitis of the DA rat. J Neurosci Res 73(2):198-205.

Kahl K, Schmidt H, Jung S, Sherman P, Toyka K, Zielasek J. 2004. Experimental autoimmune encephalomyelitis in mice with a targeted deletion of the inducible nitric oxide synthase gene: increased T-helper 1 response. Neurosci Lett 358(1):58-62.

Kirk J, Plumb J, Mirakhur M, McQuaid S (2003) Tight junctional abnormality in multiple sclerosis white matter affects all calibres of vessel and is associated with blood-brain barrier leakage and active demyelination. J Pathol 201:319-327.

Kobzik L, Stringer B, Balligand J, Reid M, Stamler J (1995) Endothelial type nitric oxide synthase in skeletal muscle fibers:mitochondrial relationships. Biochemical and biophysical research communications 211:375-381.

Kohm AP, Carpentier PA, Anger HA, Miller SD (2002) Cutting edge: CD4+CD25+ regulatory T cells suppress antigen-specific autoreactive immune responses and central nervous system inflammation during active experimental autoimmune encephalomyelitis. J Immunol 169:4712-4716.

Kolodkin AL, Levengood DV, Rowe EG, Tai YT, Giger RJ, Ginty DD (1997) Neuropilin is a semaphorin III receptor. Cell 90:753-762.

Koprowski H, Zheng YM, Heber-Katz E, Fraser N, Rorke L, Fu ZF, Hanlon C, Dietzschold B (1993) In vivo expression of inducible nitric oxide synthase in experimentally induced neurologic diseases. Proc Natl Acad Sci U S A 90:3024-3027.

Kreutzberg GW (1996) Microglia: a sensor for pathological events in the CNS. Trends in neurosciences 19:312-318.

Kroncke K-D, Fehsel K, Suschek C, Kolb-Bachofen V. 2001. Inducible nitric oxide synthase-derived nitric oxide in gene regulation, cell death and cell survival. International Immunopharmacology 1(8):1407-1420.

Kubes P, Suzuki M, Granger DN (1991) Nitric oxide: an endogenous modulator of leukocyte adhesion. Proc Natl Acad Sci U S A 88:4651-4655.

Kurenny DE, Moroz LL, Turner RW, Sharkey KA, Barnes S (1994) Modulation of ion channels in rod photoreceptors by nitric oxide. Neuron 13:315-324.

Lamas S, Marsden PA, Li GK, Tempst P, Michel T (1992) Endothelial nitric oxide synthase: molecular cloning and characterization of a distinct constitutive enzyme isoform. Proc Natl Acad Sci U S A 89:6348-6352.

Langrish CL, Chen Y, Blumenschein WM, Mattson J, Basham B, Sedgwick JD, McClanahan T, Kastelein RA, Cua DJ (2005) IL-23 drives a pathogenic T cell population that induces autoimmune inflammation. The Journal of experimental medicine 201:233-240.

Laubach, V. E., E. G. Shesely, et al. (1995). "Mice lacking inducible nitric oxide synthase are not resistant to lipopolysaccharide-induced death." Proc Natl Acad Sci U S A 92(23): 10688-92.

Lee SW, Kim WJ, Choi YK, Song HS, Son MJ, Gelman IH, Kim YJ, Kim KW (2003) SSeCKS regulates angiogenesis and tight junction formation in blood-brain barrier. Nat Med 9:900-906.

Lewandowsky M (1900). Zur Lehre der Zerebrospinalflussigkeit. Z Klin Med 40: 480-484.

Linares D, Taconis M, Mana P, Correcha M, Fordham S, Staykova M, Willenborg DO. 2006. Neuronal nitric oxide synthase plays a key role in CNS demyelination. J Neurosci 26(49):12672-81.

Lin L, Taktakishvili O, Talman W. (2007). Identification and localization of cell types that express endothelial and neuronal nitric oxide synthase in the rat nucleus tractus solitarii. Brain Res 1171:42-51.

Liu Y, Teige I, Birnir B, Issazadeh-Navikas S (2006) Neuron-mediated generation of regulatory T cells from encephalitogenic T cells suppresses EAE. Nature medicine 12:518-525.

Lock C, Hermans G, Pedotti R, Brendolan A, Schadt E, Garren H, Langer-Gould A, Strober S, Cannella B, Allard J, Klonowski P, Austin A, Lad N, Kaminski N, Galli SJ, Oksenberg JR, Raine CS, Heller R, Steinman L (2002) Gene-microarray analysis of multiple sclerosis lesions yields new targets validated in autoimmune encephalomyelitis. Nature medicine 8:500-508.

Lohr J, Knoechel B, Wang JJ, Villarino AV, Abbas AK (2006) Role of IL-17 and regulatory T lymphocytes in a systemic autoimmune disease. The Journal of experimental medicine 203:2785-2791.

Losy J, Niezgoda A, Wender M (1999) Increased serum levels of soluble PECAM-1 in multiple sclerosis patients with brain gadolinium-enhancing lesions. J Neuroimmunol 99:169-172.

Losy J, Michalowska-Wender G, Wender M (2002) Interleukin 12 and interleukin 10 are affected differentially by treatment of multiple sclerosis with glatiramer acetate (Copaxone). Folia Neuropathol 40:173-175.

Lu W, Bhasin M, Tsirka SE (2002) Involvement of tissue plasminogen activator in onset and effector phases of experimental allergic encephalomyelitis. J Neurosci 22:10781-10789.

Majed HH, Chandran S, Niclou SP, Nicholas RS, Wilkins A, Wing MG, Rhodes KE, Spillantini MG, Compston A (2006) A novel role for Sema3A in neuroprotection from injury mediated by activated microglia. J Neurosci 26:1730-1738.

Marques CP, Cheeran MC, Palmquist JM, Hu S, Lokensgard JR (2008) Microglia are the major cellular source of inducible nitric oxide synthase during experimental herpes encephalitis. Journal of neurovirology 14:229-238.

Matute C, Alberdi E, Domercq M, Perez-Cerda F, Perez-Samartin A, Sanchez-Gomez MV. (2001) The link between excitotoxic oligodendroglial death and demyelinating diseases. Trends Neurosci 24(4):224-30.

Mayhan WG (1995) Role of nitric oxide in disruption of the blood-brain barrier during acute hypertension. Brain research 686:99-103.

Mayhan WG, Didion SP (1996) Glutamate-induced disruption of the blood-brain barrier in rats. Role of nitric oxide. Stroke; a journal of cerebral circulation 27:965-969; discussion 970.

McGeachy MJ, Stephens LA, Anderton SM (2005) Natural recovery and protection from autoimmune encephalomyelitis: contribution of CD4+CD25+ regulatory cells within the central nervous system. J Immunol 175:3025-3032.

Mitrovic B, Ignarro LJ, Montestruque S, Smoll A, Merrill JE (1994) Nitric oxide as a potential pathological mechanism in demyelination: its differential effects on primary glial cells in vitro. Neuroscience 61:575-585.

Montecot C, Borredon J, Seylaz J, Pinard E (1997) Nitric oxide of neuronal origin is involved in cerebral blood flow increase during seizures induced by kainate. J Cereb Blood Flow Metab 17:94-99.

Morgan L, Shah B, Rivers LE, Barden L, Groom AJ, Chung R, Higazi D, Desmond H, Smith T, Staddon JM (2007) Inflammation and dephosphorylation of the tight junction protein occludin in an experimental model of multiple sclerosis. Neuroscience 147:664-673.

Morganti-Kossmann MC, Hans VH, Lenzlinger PM, Dubs R, Ludwig E, Trentz O, Kossmann T (1999) TGF-beta is elevated in the CSF of patients with severe traumatic brain injuries and parallels blood-brain barrier function. J Neurotrauma 16:617-628.

Mosmann TR, Coffman RL (1989) TH1 and TH2 cells: different patterns of lymphokine secretion lead to different functional properties. Annual review of immunology 7:145-173.

Murphy S (2000) Production of nitric oxide by glial cells. Glia 29:1-14.

Murata M, Kojima T, Yamamoto T, Go M, Takano K, Osanai M, Chiba H, Sawada N (2005) Down-regulation of survival signaling through MAPK and Akt in occludin-deficient mouse hepatocytes in vitro. Exp Cell Res 310:140-151.

Najjar VA, Nishioka K (1970) "Tuftsin": a natural phagocytosis stimulating peptide. Nature 228:672-673.

Nathan C, Xie Q (1994) Regulation of biosynthesis of nitric oxide. J Biol Chem 269:13725-13728.

Nikoopour E, Schwartz JA, Singh B. (2008) Therapeutic benefits of regulating inflammation in autoimmunity. Inflamm Allergy Drug Targets 7(3):203-10.

Nitta T, Hata M, Gotoh S, Seo Y, Sasaki H, Hashimoto N, Furuse M, Tsukita S (2003) Size-selective loosening of the blood-brain barrier in claudin-5-deficient mice. The Journal of cell biology 161:653-660.

Nomura Y, Kitamura Y (1993) Inducible nitric oxide synthase in glial cells. Neurosci Res 18:103-107.

O'Brien NC, Charlton B, Cowden WB, Willenborg DO (1999) Nitric oxide plays a critical role in the recovery of Lewis rats from experimental autoimmune encephalomyelitis and the maintenance of resistance to reinduction. J Immunol 163:6841-6847.

Okuda Y, Sakoda S, Fujimura H, Yanagihara T (1997) Nitric oxide via an inducible isoform of nitric oxide synthase is a possible factor to eliminate inflammatory cells from the central nervous system of mice with experimental allergic encephalomyelitis. J Neuroimmunol 73:107-116.

Okuda Y, Sakoda S, Fujimura H, Yanagihara T (1998) Aminoguanidine, a selective inhibitor of the inducible nitric oxide synthase, has different effects on

experimental allergic encephalomyelitis in the induction and progression phase. J Neuroimmunol 81:201-210.

Olerup O, Hillert J (1991) HLA class II-associated genetic susceptibility in multiple sclerosis: a critical evaluation. Tissue Antigens 38:1-15.

Olivares-Villagomez D, Wang Y, Lafaille JJ (1998) Regulatory CD4(+) T cells expressing endogenous T cell receptor chains protect myelin basic protein-specific transgenic mice from spontaneous autoimmune encephalomyelitis. The Journal of experimental medicine 188:1883-1894.

Parathath SR, Parathath S, Tsirka SE (2006) Nitric oxide mediates neurodegeneration and breakdown of the blood-brain barrier in tPA-dependent excitotoxic injury in mice. J Cell Sci 119:339-349.

Parathath SR, Gravanis I, Tsirka SE (2007) Nitric oxide synthase isoforms undertake unique roles during excitotoxicity. Stroke; a journal of cerebral circulation 38:1938-1945.

Pardridge WM (2007) Blood-brain barrier delivery. Drug Discov Today 12:54-61.

Pluchino S, Quattrini A, Brambilla E, Gritti A, Salani G, Dina G, Galli R, Del Carro U, Amadio S, Bergami A, Furlan R, Comi G, Vescovi AL, Martino G (2003) Injection of adult neurospheres induces recovery in a chronic model of multiple sclerosis. Nature 422:688-694.

Raivich G, Banati R (2004) Brain microglia and blood-derived macrophages: molecular profiles and functional roles in multiple sclerosis and animal models of autoimmune demyelinating disease. Brain research 46:261-281.

Reese TS, Karnovsky MJ (1967) Fine structural localization of a blood-brain barrier to exogenous peroxidase. The Journal of cell biology 34:207-217.

Rieckmann P, Martin S, Weichselbraun I, Albrecht M, Kitze B, Weber T, Tumani H, Broocks A, Luer W, Helwig A, et al. (1994) Serial analysis of circulating adhesion molecules and TNF receptor in serum from patients with multiple sclerosis: cICAM-1 is an indicator for relapse. Neurology 44:2367-2372.

Rieckmann P, Altenhofen B, Riegel A, Baudewig J, Felgenhauer K (1997) Soluble adhesion molecules (sVCAM-1 and sICAM-1) in cerebrospinal fluid and serum correlate with MRI activity in multiple sclerosis. Ann Neurol 41:326-333.

Rogove, A. and S. Tsirka (1998). "Neurotoxic responses by microglia elicited by excitotoxic injury in the mouse hippocampus." Curr. Biol. 8: 19-25.

Rott O, Fleischer B, Cash E (1994) Interleukin-10 prevents experimental allergic encephalomyelitis in rats. European journal of immunology 24:1434-1440.

Samadani AF, Dawson TM, Dawson VL (1997) Nitric oxide synthase in models of focal ischemia. Stroke; a journal of cerebral circulation 28:1283-1288.

Sarris M, Andersen KG, Randow F, Mayr L, Betz AG (2008) Neuropilin-1 expression on regulatory T cells enhances their interactions with dendritic cells during antigen recognition. Immunity 28:402-413.

Sattler, R. and M. Tymianski (2000). "Molecular mechanisms of calcium-dependent excitotoxicity." J Mol Med 78: 3-13.

Schulzke JD, Gitter AH, Mankertz J, Spiegel S, Seidler U, Amasheh S, Saitou M, Tsukita S, Fromm M (2005) Epithelial transport and barrier function in occludin-deficient mice. Biochim Biophys Acta 1669:34-42.

Schwartz M, Kipnis J (2005) Protective autoimmunity and neuroprotection in inflammatory and noninflammatory neurodegenerative diseases. Journal of the neurological sciences 233:163-166.

Shaked I, Porat Z, Gersner R, Kipnis J, Schwartz M (2004) Early activation of microglia as antigen-presenting cells correlates with T cell-mediated protection and repair of the injured central nervous system. J Neuroimmunol 146:84-93.

Shepro D, Morel NM (1993) Pericyte physiology. Faseb J 7:1031-1038.

Shesely, E. G., N. Maeda, et al. (1996). "Elevated blood pressures in mice lacking endothelial nitric oxide synthase." Proc Natl Acad Sci U S A 93(23): 13176-81.

Shin T, Kim S, Moon C, Wie M, Kim H (2000) Aminoguanidine-induced amelioration of autoimmune encephalomyelitis is mediated by reduced expression of inducible nitric oxide synthase in the spinal cord. Immunological investigations 29:233-241.

Shukla A, Dikshit M, Srimal RC (1996) Nitric oxide-dependent blood-brain barrier permeability alteration in the rat brain. Experientia 52:136-140.

Siao, C.-J. and S. E. Tsirka (2002). "Tissue Plasminogen Activator Mediates Microglial Activation via Its Finger Domain through Annexin II." J. Neurosci. 22(9): 3352-3358.

Sibley WA, Bamford CR, Clark K (1985) Clinical viral infections and multiple sclerosis. Lancet 1:1313-1315.

Siemion IZ, Kluczyk A (1999) Tuftsin: on the 30-year anniversary of Victor Najjar's discovery. Peptides 20:645-674.

Smith KJ, Lassmann H (2002) The role of nitric oxide in multiple sclerosis. Lancet neurology 1:232-241.

Soker S, Takashima S, Miao HQ, Neufeld G, Klagsbrun M (1998) Neuropilin-1 is expressed by endothelial and tumor cells as an isoform-specific receptor for vascular endothelial growth factor. Cell 92:735-745.

Stanislaus R, Gilg AG, Singh AK, Singh I (2005) N-acetyl-L-cysteine ameliorates the inflammatory disease process in experimental autoimmune encephalomyelitis in Lewis rats. Journal of autoimmune diseases 2:4.

Steinman L (1996) Multiple sclerosis: a coordinated immunological attack against myelin in the central nervous system. Cell 85:299-302.

Steinman L (2001) Multiple sclerosis: a two-stage disease. Nat Immunol 2:762-764.

Steinman L (2003) Medicine: Collateral damage repaired. Nature 422:671-672.

Stevens DB, Gould KE, Swanborg RH (1994) Transforming growth factor-beta 1 inhibits tumor necrosis factor-alpha/lymphotoxin production and adoptive transfer of disease by effector cells of autoimmune encephalomyelitis. J Neuroimmunol 51:77-83.

Stuehr DJ, Gross SS, Sakuma I, Levi R, Nathan CF (1989) Activated murine macrophages secrete a metabolite of arginine with the bioactivity of endothelium-derived relaxing factor and the chemical reactivity of nitric oxide. The Journal of experimental medicine 169:1011-1020.

Swanborg RH (1995) Experimental autoimmune encephalomyelitis in rodents as a model for human demyelinating disease. Clinical immunology and immunopathology 77:4-13.

Tao-Cheng JH, Nagy Z, Brightman MW (1987) Tight junctions of brain endothelium in vitro are enhanced by astroglia. J Neurosci 7:3293-3299.

Teixeira SA, Castro GM, Papes F, Martins ML, Rogerio F, Langone F, Santos LM, Arruda P, de Nucci G, Muscara MN (2002) Expression and activity of nitric oxide

synthase isoforms in rat brain during the development of experimental allergic encephalomyelitis. Brain research 99:17-25.

Thanos S, Mey J, Wild M (1993) Treatment of the adult retina with microglia-suppressing factors retards axotomy-induced neuronal degradation and enhances axonal regeneration in vivo and in vitro. J Neurosci 13:455-466.

Thiel VE, Audus KL (2001) Nitric oxide and blood-brain barrier integrity. Antioxidants & redox signaling 3:273-278.

Tordjman R, Lepelletier Y, Lemarchandel V, Cambot M, Gaulard P, Hermine O, Romeo PH (2002) A neuronal receptor, neuropilin-1, is essential for the initiation of the primary immune response. Nature immunology 3:477-482.

Tran EH, Hardin-Pouzet H, Verge G, Owens T (1997) Astrocytes and microglia express inducible nitric oxide synthase in mice with experimental allergic encephalomyelitis. J Neuroimmunol 74:121-129.

Van Dam AM, Bauer J, Man AHWK, Marquette C, Tilders FJ, Berkenbosch F (1995) Appearance of inducible nitric oxide synthase in the rat central nervous system after rabies virus infection and during experimental allergic encephalomyelitis but not after peripheral administration of endotoxin. Journal of neuroscience research 40:251-260.

van Rossum D, Hanisch UK. (2004). Microglia. Metab Brain Dis 19(3-4):393-411.

Verkhratsky A, Toescu EC (2006) Neuronal-glial networks as substrate for CNS integration. J Cell Mol Med 10:826-836.

von Wronski MA, Raju N, Pillai R, Bogdan NJ, Marinelli ER, Nanjappan P, Ramalingam K, Arunachalam T, Eaton S, Linder KE, Yan F, Pochon S, Tweedle MF, Nunn AD (2006) Tuftsin binds neuropilin-1 through a sequence similar to that encoded by exon 8 of vascular endothelial growth factor. The Journal of biological chemistry 281:5702-5710.

Wang L, Zeng H, Wang P, Soker S, Mukhopadhyay D (2003) Neuropilin-1-mediated vascular permeability factor/vascular endothelial growth factor-dependent endothelial cell migration. The Journal of biological chemistry 278:48848-48860.

Wardlaw JM, Sandercock PA, Dennis MS, Starr J (2003) Is breakdown of the blood-brain barrier responsible for lacunar stroke, leukoaraiosis, and dementia? Stroke 34:806-812.

Weaver A, Goncalves da Silva A, Nuttall RK, Edwards DR, Shapiro SD, Rivest S, Yong VW. 2005. An elevated matrix metalloproteinase (MMP) in an animal model of multiple sclerosis is protective by affecting Th1/Th2 polarization. FASEB J 19(12):1668-70.

Weber MS, Prod'homme T, Youssef S, Dunn SE, Rundle CD, Lee L, Patarroyo JC, Stuve O, Sobel RA, Steinman L, Zamvil SS (2007) Type II monocytes modulate T cell-mediated central nervous system autoimmune disease. Nat Med 13:935-943.

Wilson NJ, Boniface K, Chan JR, McKenzie BS, Blumenschein WM, Mattson JD, Basham B, Smith K, Chen T, Morel F, Lecron JC, Kastelein RA, Cua DJ, McClanahan TK, Bowman EP, de Waal Malefyt R (2007) Development, cytokine profile and function of human interleukin 17-producing helper T cells. Nature immunology 8:950-957.

Yednock TA, Cannon C, Fritz LC, Sanchez-Madrid F, Steinman L, Karin N (1992) Prevention of experimental autoimmune encephalomyelitis by antibodies against alpha 4 beta 1 integrin. Nature 356:63-66.

Yepes M, Sandkvist M, Moore EG, Bugge TH, Strickland DK, Lawrence DA (2003) Tissue-type plasminogen activator induces opening of the blood-brain barrier via the LDL receptor-related protein. The Journal of clinical investigation 112:1533-1540.

Zehntner S, Bourbonniere L, Hassan-Zahraee M, Tran E, Owens T. 2004. Bone marrow-derived versus parenchymal sources of inducible nitric oxide synthase in experimental autoimmune encephalomyelitis. J Neuroimmunol 150(1-2):70-79.

Zettl UK, Mix E, Zielasek J, Stangel M, Hartung HP, Gold R (1997) Apoptosis of myelin-reactive T cells induced by reactive oxygen and nitrogen intermediates in vitro. Cellular immunology 178:1-8.

Zhang Z, Chopp M, Bailey F, Malinski T (1995) Nitric oxide changes in the rat brain after transient middle cerebral artery occlusion. J Neurol Sci 128:22-27.

Zhao W, Tilton RG, Corbett JA, McDaniel ML, Misko TP, Williamson JR, Cross AH, Hickey WF (1996) Experimental allergic encephalomyelitis in the rat is inhibited by aminoguanidine, an inhibitor of nitric oxide synthase. J Neuroimmunol 64:123-133.